2015

Effect of cryomilling on zinc sulfide effectiveness as antibacterial substance for burn wound healing

Jianqiang Li
Iowa State University

Effect of cryomilling on zinc sulfide effectiveness as antibacterial substance for burn wound healing

by

Jianqiang Li

A thesis submitted to the graduate faculty

in partial fulfillment of the requirements for the degree of

MASTER OF SCIENCE

Major: Industrial Engineering

Program of Study Committee:
Iris V. Rivero, Major Professor
Matt Frank
Max Morris
Kaitlin Bratlie

Iowa State University

Ames, Iowa

2015

TABLE OF CONTENTS

LIST OF FIGURES

Page

LIST OF TABLES

Page

LIST OF NOMENCLATURE

Ag	Silver
ANOVA	Analysis of Variance
ATP	Adenosine Triphosphate
CaCl2·2H2O	Calcium Chloride Dihydrate
CFU	Colony Forming Unit
CLSM	Confocal Laser Scanning Microscopy
Comp A	Compound A: Zinc sulfide particles produced by sulfate reducing bacteria
Comp B	Compound B: Cryomilled biosynthesized zinc sulfide particles
Comp C	Compound C: Zinc sulfide particles produced by one-pot colloidal synthesis
Comp D	Compound D: Cryomilled chemically synthesized zinc sulfide particles
CPS	Counts per Second
Cu	Copper
DDAB	Didodecyldimethylammonium Bromide
df	Degree of Freedom
DMF	Dimethyl Formamide
DNA	Deoxyribonucleic Acid
EGF	Epidermal Growth Factor
EPS	Extracellular Polysaccharide Matrix
E. Coli	*Escherichia coli*
FGF	Fibroblast Growth Factor
GFP	Green Fluorescence Protein
H_2S	Hydrogen Sulfide

i.i.d.	Identical and Independently Distributed
LB	Luria Bertani
ME	Mercapto Ethanol
$MgCl_2 \cdot 6H_2O$	Magnesium Chloride Hexahydrate
MRSA	Methicillin-resistant *Staphylococcus aureus*
NaCl	Sodium Chloride
$NaHCO_3$	Sodium Bicarbonate
NaI	Sodium Iodine
Na_2S	Sodium Sulfide
$NH_4 \cdot Cl$	Ammonium Chloride
OD	Optical Density
PBS	Phosphate Buffer Saline
PDGF	Platelet-derived Growth Factor
PEG	Polyethylene Glycol
PVP	Poly(*N*-vinyl-2-pyrrolidone)
P. aeruginosa	*Pseudomonas aeruginosa*
ROS	Reactive Oxygen Species
RNA	Ribonucleic Acid
SEM	Scanning Electron Microscopy
SRB	Sulfate Reducing Bacteria
S. aureus	*Staphylococcus aureus*
TAA	Thioacetamide
TGF	Transforming Growth Factor

TOPO	Trioctylphosphine Oxide
XRD	X-ray Diffraction
Zn	Zinc
$ZnCl_2$	Zinc Chloride
ZnO	Zinc Oxide
ZnS	Zinc Sulfide
$ZnSO_4$	Zinc Sulfate
$Zn(Ac)_2$	Zinc Acetate
$Zn(No_3)_2$	Zinc Nitrate
ZOI	Zone of Inhibition

ACKNOWLEDGEMENTS

I feel very thankful, as this thesis could not be completed without help from many people, and I'd like to take this opportunity to express my gratitude. First of all, Dr. Iris Rivero has the most influence on this thesis and on my academic development, it is because of her professionalism and firm grasp of principles that this project could be done successfully, and I've learnt tremendously under her advisory for two years, which I feel very thankful for. I'd also like to thank Dr. Abdul Hamood and Dr. Phat Tran from Texas Tech University for their great support for the biological tests, without which this project could only be theoretical. Dr. Ilia Ivanov has also played an important role in terms of biological synthesis of materials, without whom the availability of materials would be a big problem. This is a cooperated project, and I feel the strong sense of spirit of cooperation in every email, every conference call and every shipment, which is an enlightening experience that can be helpful in my future career development. Also, I'd like to thank my committee members Dr. Matt Frank, Dr. Max Morris and Dr. Kaitlin Bratlie for their generosity and kindness when helping me go through the hardship and problems during the project. Last but definitely not the least, my gratitude goes to my family, who stand firmly behind me and support me whenever I need them! This is not the end, this is just a new start of my life to come, and everything I've learnt during this project will be of great benefit and I truly appreciate that!

ABSTRACT

This study aims to investigate the effect of the manufacturing process cryomilling on the antibacterial effectiveness of a novel antibacterial agent ZnS. ZnS nanoparticles are getting attention for their potential antibacterial properties due to the fact that release of Zn ions has demonstrated promising preliminary effects when applied on skin wounds. Particle size is essential to achieve bacteria inhibition and elimination since it has been shown that antibacterial activity can be increased with reduced particle size, which results in higher surface to volume ratio. In this study, ZnS nanoparticles were synthesized using one-pot colloidal synthesis as well as using biological Sulfate Reducing Bacteria synthesis under anaerobic environment with proper media. Both types of ZnS were further processed through cryomilling after synthesis to reduce the particle size. Scanning electron microscopy and X-ray diffraction techniques were used to characterize the morphology and crystallinity of the ZnS nanoparticles. To assess bacteria inhibition and elimination, *in vitro* ZOI studies consisting of inoculating cellulose disks on agar plates with *Staphylococcus aureus* (*S. aureus*) followed by incubation for 24 hours were performed. *In vitro* biofilm models consisting of inoculating cellulose disks on well-developed *S. aureus* biofilm on agar plates followed by 24-hour incubation were also conducted. CLSM was employed to qualitatively observe the antibacterial effectiveness; statistical analysis was also performed to quantitatively study the effectiveness of ZnS as antibacterial agents by counting the residual CFU left on the cellular disks. Results showed that the ZnS nanoparticles possess very good antibacterial properties against *S. aureus*, and incorporating cryomilling enhances ZnS antibacterial effectiveness.

THESIS ORGANIZATION

In this thesis, Chapter 1 presents the general introduction and information of this research. Chapter 2 gives a thorough literature review of the current studies on related fields including wound healing process, antibacterial agents on burn wound healing and common manufacturing processes for synthesis of ZnS, which provides the knowledge basis for the development of this research. Chapter 3 describes a pilot evaluation of the effectiveness of chemically synthesized ZnS as an antibacterial agent, which provides the rationale for choosing the alternative method of manufacturing for ZnS. Chapter 4 illustrates the detailed experiment design and implementation, together with results analysis and conclusions about the study of ZnS antibacterial effectiveness for healing burn wounds. Chapter 5 provides the general conclusions and the future research direction of this project.

CHAPTER 1.

GENERAL INTRODUCTION

Burn wounds are one of the most commonly encountered damages to the skin, due to the thermal damage from burn, the immune systems surrounding the wounds can be destroyed, thus causing a higher possibility of bacterial infection than other wounds [1-3]. There are many different types of bacteria that can colonize on the burn wound site, however, *S. aureus* and *P. aeruginosa* are the major infections sources [4]. As delay in bacteria clearance on the wound site can result in delay of wound healing or even transition from acute wound to chronic wound [5], many different types of antibacterial agents were applied in order to treat burn wound and reduce the time frame of wound healing. Other than infection itself, the formation of biofilm poses an even more serious problem as biofilm is even harder for antibiotics to completely eradicate than common bacterial infection [6].

Antibiotics used to play a major role for burn infection treatment, however, over the past decades, the emerging problem of antibiotic resistance has become a serious issue due to the overuse of antibiotics [7, 8]. In recent years, metallic compounds are starting to gain popularity in terms of their broad spectrum of antibacterial effectiveness, among them, Ag and ZnO are two extensively studied examples. However, studies have shown that bacteria are gaining resistance against Ag [9, 10], thus new drugs are always in need in order to counter the bacteria mutation. ZnS is a novel antibacterial substance that recently started to attract attention, however, available studies basically utilized environmentally unfriendly chemical synthesis to produce ZnS [11], and limited to very few types of bacteria, which did not include one of the most common burn wound infection source *S. aureus* [12-14]. As an alternative, we used SRB to biologically synthesize ZnS to test its effectiveness on *S. aureus*.

An important factor that contributes to the antibacterial properties is the particle size of the material. Smaller sized particles have larger surface to volume ration, resulting in larger surface in direct contact with the exterior environment under same amount of antibacterial agents, thus it is expected that the smaller the particle size of the drugs, the higher antibacterial properties they will possess [15]. In order to test the effect of size reduction on antibacterial properties, cryomilling was used as a manufacturing process to reduce the particle size, and the ZnS with two different particle sizes were used to compare the antibacterial properties.

This study aims at investigating the antibacterial effectiveness of ZnS on *S. aureus* infection. In order to compare the effectiveness of cryomilling as well as different manufacturing methods for ZnS synthesis, four types of ZnS were synthesized. The Comp A was the original ZnS produced using SRB as described in previous study [16], and Comp B was produced using cryomilling as a manufacturing process over the original biosynthesized ZnS Comp A. In conjunction with this study, the conventional chemical synthesis was also employed to produce ZnS, and the antibacterial effectiveness was evaluated accordingly. Comp C was the chemically synthesized ZnS particles, and Comp D was the chemical synthesized ZnS which was further processed using cryomilling. Evaluation results showed that, although cryomilled Comp D showed very good antibacterial properties, the chemical synthesized ZnS Comp C did not show antibacterial properties. Based on the evaluation results and the other drawbacks related to production such as environmental hazard and high temperature requirement, we chose biosynthesis as the source for ZnS in this study.

The characterization methods used included SEM analysis and XRD analysis. The results showed that the produced particles are ZnS with sphalerite crystal structures, and the particle size has been dramatically decreased by cryomilling.

In order to test the antibacterial effectiveness, several tests were conducted including ZOI assay, followed by *in vitro* biofilm study. In biofilm study, the residual biofilm after being treated with ZnS was first observed using CLSM to qualitatively observe biofilms development, and later it was quantitatively counted to determine the effectiveness of the ZnS as antibacterial agent. The results showed that the Comp A and Comp B ZnS are both effective against *S. aureus*, and reached the desired level of effectiveness. In the meantime cryomilling as a post-synthesis process has played a positive role in increasing the antibacterial effectiveness of ZnS.

CHAPTER 2.

LITERATURE REVIEW

This review of literature is divided into 8 parts: 1) Types of wounds, 2) Wound healing process, 3) Bacteria and impact on wound healing, 4) Antibacterial mechanisms, 5) Topical antibacterial drugs for burn wound treatment, 6) Synthesis of ZnS, 7) Cryomilling, 8) Summary of literature.

2.1 Types of Wounds

Wounds are common around the world, and there are many different ways of categorizing wounds. Sections 2.1.1 to 2.1.4 illustrate 4 major criteria by which the wounds can be classified. As the major type of wound that this study focused on, burn wounds are explained specifically in Section. 2.1.5.

2.1.1 Causes of Wounds

Based on the causes of the wounds, they can be categorized into traumatic, iatrogenic and burn wounds. Traumatic wounds are severe break or injury in the soft tissue of the skin, which may include trauma from sharp or blunt object [17, 18]. Iatrogenic wounds are wounds caused by medical practices such as radiotherapy burns, surgical wound dehiscence, chemotherapy-induced skin necrosis and Foley catheter-induced hypospadias, this is more common to see in cancer patients [19]. Burn wounds are the type of wounds caused by burns, which include thermal, electrical and chemical burns [17]. In this study, burn wounds are the major focus, more literature review is provided for burn wounds in section 2.1.5.

2.1.2 Length of Time Since Formation of Wounds

Based on length of time since formation, the wounds can be categorized into acute wounds and chronic wounds [20]. Acute wounds are usually referred as wounds that can heal in 6 weeks or shorter period [17, 21]. Without effective bacteria clearance, an acute wound can progress into a chronic wound [5]. Chronic wounds are wounds that don't heal within 6 weeks period [17]. In section 2.2, more detailed description of chronic wounds is provided.

2.1.3 Injury Mode of Wounds

Based on the mode of injury, they can be categorized into the following types: abrasion, ulceration, incision, lacerations and degloving injury [17]. An abrasion is the wound that only involves the outer layer of the skin, a ulceration refers to the discontinuity or break in a bodily membranes that impedes the organs of which that membrane is a part from continuing its normal functions [22], if the wound occurs on the skin, it causes defect in epithelial lining [17]. Incisions are wounds caused by sharp objects such as needle. Lacerations are wounds caused by blunt objects such as stone. Degloving injury refers to a type of avulsion in which an extensive section of skin is completely torn off the underlying tissue [23].

2.1.4 Contamination and Risk of Postoperative Infection

Based on the contamination and risk of postoperative infection, the wounds can be categorized into: clean wound, clean/contaminated wound, contaminated wound and dirty wound [17]. Clean wound refers to the wound with no infection, only microflora can potentially contaminate the wound and no hollow viscus is contaminated with bacteria. Clean/contaminated

wounds indicate the wounds which hollow viscus such as respiratory, alimentary or genitourinary tracts with indigenous bacterial flora is opened under controlled circumstances. Contaminated wounds refer to open accident wounds encountered early after injury, with extensive introduction of bacteria into a normally sterile area of the body. Dirty wound refers to the traumatic wounds in which a significant delay in treatment has occurred and necrotic issue is present [17].

There are some other wounds categorization methods such as depth, site and complexity. Based on depth, the wounds can be categorized into superficial and deep wounds. Based on site, the wounds can be classified into midline laparotomy, suprapubic and thoracotomy and so on. Based on complexity, the wounds can be categorized into simple, complex and complicated wounds [17].

2.1.5 Burn Wounds Introduction

Burn wound is the major focus of this study, it is one of the most common and devastating forms of trauma, even though the surface of a wound is sterile immediately after injury, the site will eventually be colonized with bacteria [24], and infections on burn wounds pose serious possibility of complications that can occur in the acute period following injury [25] as thermal destruction caused by burn has impact on the skin barrier system and accompanying local and systemic immune response, thus compromising the integrity of the skin and the immune system, which plays key roles in contributing to infections for patients with severe burns [1-3]. There are various microorganisms that can accumulate on the burn wound sites, among them, gram-positive bacteria *S. aureus* and gram-negative bacteria *P. aeruginosa* are still

the major infection sources [4]. The wound site is a protein rich environment which provides an excellent environment for bacteria colonization and proliferation [24, 26, 27].

Same way as regular wounds, burn wounds are also subject to biofilm formation [28, 29], persister cells within the biofilms can temporarily disable the inherent mechanism of cell deaths on the biofilm which is resistant to the antibiotic treatments and thus lead to failure to eradicate the biofilms [6, 30, 31]. Animal studies on cutaneous burn wounds show that mature biofilms can be formed in 48 to 70 hours, and biofilms formed by *P. aeruginosa* on human burn wounds can be achieved in 10 hours [32]. Inhibition of biofilm formation or removing the existing biofilm developed on the wound site is the key issue in order to facilitate the wound healing process.

2.2 Wound Healing Process

In a typical wound healing process, there are five different phases: Injury, coagulation, inflammation, tissue formation and tissue remodeling [33-35]. Some papers would define the phases as hemostasis, inflammation, migration, proliferation and maturation [5, 36-39]. Each of these phases lasts a specific length of time, they are both interdependent and overlapping, together with various cellular and matrix components involved to act on the wound healing process in order to restore the damaged tissues [40, 41].

Injury can be caused by various reasons, examples include trauma, surgery, burn, infections, the injured cells will release cytokines such as PDGF [42-44], TGF-β [35, 45-48] and TGF-α [49, 50] to initiate subsequent wound healing phases. Immediately after the injury, the second phase of wound healing: coagulation or hemostasis would occur, with platelets accumulating at the wound site and fibrin clot forming [33, 38]. This process is accompanied

with the release of PDGF, TGF-β, EGF and TGF-α, as well as adhesive glycoproteins such as fibronectin [33] which help attract the fibrin clots to the wound sites. Inflammation is the third phase that usually occurs 1-5 days after injury, with neutrophils predominating in the first few hours of inflammation, and the phagocytosis of neutrophils sterilize bacteria and foreign bodies present at the wound site [33]. Later in the process, macrophages, which are the most important inflammatory cells [51], will outnumber the neutrophils. Still through phagocytosis, macrophages decontaminate the wound sites, along with various growth factors such as PDGF, TGF-β, FGF [52, 53], the existence of macrophages signals the transition from inflammatory phase to tissue repair phase. In this phase, there will be re-epithelialization and granulation involved. Re-epithelialization is served as reestablishment of epidermal barriers to protect the internal organs, while granulation is formed by macrophages. Fibroblasts and endothelial cells move into the wound site, with fibroblasts constructing new extracellular matrix to support cell growth [33]. Following this is the phase of tissue remodeling, with attempt to return the damaged tissue to its original condition prior to injury.

If acute wounds are not treated properly and are colonized by bacteria, they may progress into chronic wounds. Chronic wounds are wounds that do not heal in an orderly set of stages and in predictable amount of the time as most wounds do. Wounds that do not heal within three months are often considered as chronic wounds [54]. Most chronic wounds can be classified into three major types: pressure ulcers, venous ulcers, and diabetic ulcers, and the causative factors can be categorized into four types: local tissue hypoxia, bacterial colonization, repetitive ischemia reperfusion injury, and for elderly patients, an altered cellular and systemic stress response can also be the cause for chronic wound [55]. All chronic wounds have measurable

bacteria counts [56], and critical colonization is by itself sufficient to result in a chronic wound [57], thus clearance of bacteria on the wound sites is critical.

2.3 Bacteria and Impact on Wound Healing

2.3.1 Bacteria Infection

The healing process as stated in Section 2.2 is expected to occur in a chronological order without disruption or delay, any discrepancies or prolongation of this process may result in delayed wound healing. There are a number of factors that impact the wound healing process, which can be basically categorized into local and systemic [5]. The local factors examples include oxygenation, infection, foreign body, venous sufficiency, while the systemic factors include age and gender, sex hormones, stress, ischemia, diseases like diabetes, obesity, medications, alcoholism and smoking.

Bacteria however, play an important part in delaying wound healing, and evidence showed that bacteria infected patients have higher rate of mortality [58]. Once the skin is injured, microorganisms will obtain access to the tissues beneath the skin. There are different states of infection based on the severity of replication, these include: contamination, colonization, local infection, critical infection and spreading invasive infection [5], each condition is more serious than the last. Contamination is merely the presence of non-replicating microorganisms. Colonization refers to the presence of replicating microorganisms on the wound site without damage of the tissue. Local infection and critical infection mean the replication of organisms and the following tissue responses. Invasive infection is the presence of replicating organisms with actual host injury [59]. During the normal inflammatory process, the removal of invading microorganisms is crucial, the incomplete microbial clearance will result in prolonged

inflammatory phase, if this continues, the wound may enter a chronic state with inability to heal by itself. Prolonged inflammation can also lead to extracellular matrix degradation and growth factor degradation [5, 59].

There are two major categories of bacteria that cause infection, Gram-positive and Gram-negative bacteria. The two categories show structural differences in their cell walls. Gram-positive bacteria have a thick layer of peptidoglycan while gram-negative bacteria do not. However, gram-negative bacteria are more resistant against antibodies because of their impenetrable cell walls [60].

2.3.2 Biofilms

Another important element that inhibits wound healing is the biofilm formed by bacteria colonies. Biofilms are of complex composition made up by accumulated bacteria in a self-secreted EPS [59]. A mature biofilm will develop a protective mechanism which is more resistant to regular antibiotic treatments, it is a result of natural tendency of microorganisms to attach to wet surfaces, and to multiply and embed themselves in a slimy matrix [61]. Among all the microorganisms, *S. aureus* and *P. aeruginosa* are the most commonly found bacteria in infected wound sites according to the studies [4, 62].

Biofilms formation can be used to explain the ineffectiveness of antibiotics as treatment to chronic wounds due to its self-protection mechanism, however, the mechanism is not fully understood yet, but there are studies that proposed several models to explain the mechanism, including physical or chemical diffusion barriers to antimicrobial penetration, biofilm slow growth, activation of the biofilm general stress response and so on [63]. The protection mechanism can also differ depending on the bacterial complement of the biofilm and the agent

used to treat it. In the meantime, the environmental heterogeneity within the biofilm can promote the formation of a heterogeneous population of cells, thus different levels of resistance can be expressed throughout the biofilm community, which altogether contribute to the antibacterial mechanism to regular antibiotics [64, 65].

Ideally, biofilm should be prevented instead of being treated, however, the currently there is no known existing technology that can successfully prevent or control the formation of unwanted biofilms without causing side effects [61]. The main strategy used to prevent the formation of biofilm is to clean and disinfect the wounded area before biofilm develops and firmly attaches to the surface [66, 67]. Biofilm detectors were already developed to monitor the surface colonization by bacteria and allow control of biofilm formation in early stages [68, 69].

Antibiotics are relatively ineffective for eradicating biofilm infections, and very high doses are required to reduce biofilm presence [70]. Mupirocin irrigation, gentian violet, and thiamphenicol glycinate acetylcysteine can effectively eradicate biofilms [71-73]. Physical disruptions, surfactants and probiotics are also reported to be able to eradicate biofilms [74]. Metal compounds such as Ag and ZnO are also very effective against biofilm eradication [75, 76]. However, there are no studies that researched on effectiveness of ZnS on eradicating *S. aureus* biofilms.

2.3.3 Drug Resistant Bacteria

The threat of infection is made worse by drug resistant bacteria. With high rates of nucleotide substitution and poor mutation error-correction ability, the bacteria have high capacity to adapt to new hosts including human [7, 77, 78]. One example of these types of bacteria is MRSA [79], which has become an increasingly serious issue. MRSA was first isolated in the

early 1960s [80], it is the strain of *S. aureus* that acquired the mecA gene which expresses the methicillin resistance [81], but it is also resistant to many antibiotics including penicillin [82]. MRSA infection resulted in mortality rates of 22% in 2000 [83], and mortality rates have been dramatically increasing from 1993 to 2002 period [84]. In another study, invasive MRSA resulted in death rates of 19% in 2007 in United States [85].

2.4 Antibacterial Mechanisms

2.4.1 Cell Death Induced by Oxygen

Although the human body has self-healing functions, acceleration of wound healing is still preferable. By controlling infection, effective topical antibacterial therapy can decrease the conversion of partial thickness to full thickness wounds [4]. Topical antibacterial agents are applied directly to the wound sites, major mechanisms of antibacterial actions include: inhibition of cell wall synthesis, inhibition of protein synthesis, inhibition of nucleic acid synthesis, inhibition of metabolic pathways and interference with cell membrane integrity [86-90].

In the natural process of wound healing, oxygen plays an important role [35, 91-93], besides providing oxygen needed for metabolism which generates energy during the wound healing process, some oxygen is used to convert into highly reactive ions as well as ROS, including superoxide ions and hydrogen peroxide, which are essential for infection prevention in the inflammatory phase. ROS like H_2O_2 and O^{2-} can be produced by neutrophils and macrophages during the wound healing process [35], which can cause DNA damage, lipid peroxidation, protein damage, and oxidation of important enzymes [94]. Also, generation of ROS can cause disruption of ATP production of the cells [95]. All these effects are able to kill the

colonized bacteria at the wound site. ROS generated by other substances like Ag nanoparticles and Zn ions are also proven to have antibacterial properties [95-98].

2.4.2 Cell Death Induced by Membrane Damage

Membranes are important components for the cells, they separate the interior of cells from the outside environment [99], they maintain the structure of cells, and they are selectively permeable to ions and organic molecules, and control the movement of substances in and out of cells. Membranes are also important to transport nutrients and wastes, which involve active transportation. Signaling and marking are also important functions for membranes in order to identify cells from each other and process signals received from the extracellular environment [100]. Overall, membranes play crucial roles to support lives of cells, destruction of cell membranes can cause leakage of cellular proteins which will stop cell functioning and eventually kill the cells, and many studies showed that the antibacterial properties stemmed from particles deposition on the membranes which stopped cell functioning [101-103].

2.5 Topical Antibacterial Drugs for the Treatment of Burn Wounds

2.5.1 Antibiotics

There are many different types of antibacterial agents, selection of topical drugs should be based on the ability to inhibit microorganisms growth [4]. The typical and most commonly used are antibiotics.

Antibiotics have been used for wound treatment for a very long time. Penicillin, for example, has been used as an antibacterial agent since 1929 [104]. Penicillin served as a very effective method to eliminate mortality of burn wound patients [105, 106]. Many other types of

antibiotics were also used such as methicillin [107], gentamicin [108, 109], erythromycin [110], and neomycin [110, 111]. However, development of antibiotic resistance has become an emerging problem [79, 112, 113], especially after widespread use of antibiotics in recent decades [8, 114]. One of the most representative examples is MRSA which was previously mentioned in Section 2.3.3, it is not only resistant to methicillin, but is multi-resistant to many different antibiotics [115]. Studies have already proven a clear association between the overuse of antibiotics and MRSA isolation [116]. Thus antibiotic treatment continuously relies on the development of new antibiotics, as for example, daptomycin [115]. The mechanisms of how antibiotics kill bacteria is still not clearly determined, however, the following two models were proposed to explain the possible antibacterial mechanisms: inhibition of DNA replication, protein translation and ATP generation, induction of ROS formation, inhibition of cell walls formation [104].

2.5.2 Ag Containing Agents

One commonly studied family of topical antibacterial agents is Ag and Ag containing compounds, this family includes Ag simple substances, Ag proteins, Ag salts and Ag compounds [117]. Ag has long been used as an antimicrobial agent since the 1800s [118, 119], but the interest of using Ag as an antibacterial agent declined since the discovery of antibiotics. However, the trend of using Ag has regained popularity in the past two decades due to the emerging problem of antibiotics resistant bacteria [119]. Ag simple substances, especially Ag nanoparticles, possess a broad spectrum of antimicrobial properties, including being active against MRSA [120-123]. Since the commencement of nanotechnology, Ag nanoparticles have drawn special attention for its high surface area to volume ratio and unique chemical and

physical properties [124, 125]. Ag protein refers to small proteins attached with Ag or Ag nanoparticles suspended in protein binder, with the purpose of enhancing solubility in solution. Although they possessed antibacterial properties, they are much less effective than ionic Ag or metallic Ag compounds, thus were replaced by Ag salts in the 1960s [117]. There are many more types of Ag salts that are applied for wound healing, since the Ag ions are highly bactericidal [117]. Typical examples of Ag salts include: silver nitrate, silver sulfate, silver chloride [126]. The effective antibacterial properties are due to their high solubility. However, the solutions are usually unstable when exposed to light, as they produce black stains. Also, nitrate is toxic to wounds and cells and seem to decrease the healing which is believed to offset the benefits of the antibacterial effect of Ag ions. The reduction from nitrate to nitride may cause oxidant induced cell damage, which is likely responsible for impaired re-epithelialization [117].

A typical example of a Ag compound is silver sulfadiazine, which was introduced in the 1970s [127]. Ag is combined with propyleneglycol, stearyl alcohol and isopropyl myrislate and mixed with the antibiotic sulfadiazine in order to produce a combined formulation [117]. Among many Ag burn wound agents with combinations of sulfur, silver sulfadiazine appeared to display the most effectiveness in vitro tests [128]. However, there are also reports claiming that the silver sulfadiazine has poor usefulness on burns [129] and overuse of silver sulfadiazine may cause potential risk of silver toxicity [130].

Although the antibacterial mechanism on infection has not been clearly identified, there are reports that document how Ag plays a role in wound healing. Ag is biologically active when it is in soluble form, either as Ag^{+} or as Ag^{0} clusters, Ag^{+} is found in Ag proteins, salts and other ionic compounds like silver sulfadiazine. Ag^{0} on the other hand, is found in metallic Ag like Ag nanoparticles [119]. Free Ag ions can destroy microorganisms immediately by blocking cellular

respiration, stopping ATP production and disrupting the function of cell membranes, especially when they are bound to the tissue proteins, thus causing the structure of the cell membrane to change and eventually kill the bacteria. Also, Ag ions are able to bind and denature the cell DNA and RNA, which also hinder cell replication [95, 131-133]. Ag nanoparticles, due to their small dimensions of 100 nm or less, possess unique properties like catalytic capabilities and ability of generating ROS [134], smaller sized Ag nanoparticles with 10nm in diameter or less may pass through or directly deposit on the cell membrane and accumulate on the intracellular nanoparticles thus leading to cell malfunctioning [95, 126]. Overall, the major components that contribute to the antibacterial properties for wound healing are Ag ions and metallic Ag nanoparticles. Although Ag is proven to possess antibacterial properties against a wide spectrum of bacteria, there has been reports about the development of Ag resistant bacteria due to overuse of Ag as wound care, which poses danger to current burn wound management [9, 10]. And in actuality, bacteria are able to gradually develop resistance over many different toxic metal ions [135].

2.5.3 Zn Containing Agents

Another family of metallic compounds used for wound healing are Zn ionic compounds with typical examples being zinc oxide [136], zinc sulfate [137], zinc chloride [138], zinc sulfadiazine [139] zinc sulfide [12]. ZnO is a common therapy for various skin disorders as it is protective, astringent and antibacterial [140], and it is effective on both Gram-positive and Gram-negative infections. ZnO, when produced in nanoscale, will exhibit excellent antibacterial properties, and the effectiveness is inversely proportional to the size of the ZnO particles, this finding is applicable for sizes changed by either synthesis methods or mechanical methods [15,

141, 142]. $ZnSO_4$ has been proven to be able to assist wound healing by taking it orally as it provides necessary nutrients for protein synthesis [143, 144]. However, although it is not widely used as an antibacterial agent for burn wound healing, $ZnSO_4$ has been listed by pharmacopoeias as a local astringent and antiseptic [145]. $ZnCl_2$ is used as an escharotic after burn injury, as it is soluble in water, it results in higher Zn ions concentration on the wound sites [137]. Zinc sulfadiazine, as suggested by the name, contains the antibacterial compounds sulfadiazine, and exhibit antibacterial properties to common burn wound infection bacteria like *P. aeruginosa* [139, 146]. This compound is more economical than its Ag counterpart silver sulfadiazine [146]. ZnS, which this review will discuss in more in detail in the later paragraphs, has also been reported by very few studies in relation to its antibacterial properties [12-14]. However, its application has not been extensively studied.

In terms of antibacterial mechanism, similar to Ag, there are also two major contributors for the antibacterial properties, the Zn ions and nanoparticles themselves. The production of increased levels of ROS caused by Zn ions [147, 148], such as hydroxyl radicals and singlet oxygen, and the deposition of nanoparticles on the surface of bacteria which cause disruption and disorganization of membranes are the main reasons that cause the bacteria cell death [141]. Similar to Ag, smaller sized nanoparticles show better antibacterial properties, it is particularly interesting that mechanically grinded ZnO shows better antibacterial properties due to the decrease of lattice distance as a result of mechanical grinding, which induces more formation of H_2O_2 on the particle surface [15, 149], and thus are more capable of killing bacteria. Although bacteria are capable to develop metal ion resistance, there have not been reports on Zn resistant bacteria for burn wound infection. Zn is relatively harmless by comparison to Ag, only exposure to high doses has toxic effects, making acute Zn intoxication a rare event [150].

2.5.4 Other Antibacterial Agents

Besides the antibacterial agents mentioned in the previous sections, there are also many other types of agents for burn wound infection control. Nystatin has been reported to possess antifungal properties [151], povidone iodine is also believed to help wound healing [152], however, its effectiveness is also questioned and even criticized for impairing wound healing and reducing wound strength [152, 153]. Pexiganan is a 22-amino acid peptide isolated from the skin of frogs and is drawing interests on wound healing aspect, it is also effective on *S. aureus* and *P. aeruginosa*. However, its antibacterial mechanism and application studies are still underway [154]. Other examples include nitrofurazone [155], nitrofurantoin [156], chlorhexidine [157], sodium hypochloride [110, 158].

2.5.5 Zinc Sulfide

As mentioned in the previous sections, very few studies have been conducted on ZnS antibacterial properties. In these studies, ZnS particles were chemically synthesized. In the following study, TAA was used as precursor for sulfur and $Zn(Ac)_2$ as precursor for Zn [12], during the reaction, the surfactant Fc-loaded DDAB were dissolved to acquire more uniform distributed particle sizes. The solution was then heated at 80 °C in a water bath and maintained for 6 hours with magnetic stirring, and the white precipitates were acquired using centrifugation and dried in vacuum. The ZnS particles as synthesized were tested on *E. Coli*, a typical gram-negative bacteria on agar plate assay. The result of this study has shown that the viable colonies on the plates were reduced significantly as the concentration of ZnS particles increased, the experiment also showed that by comparison to more commonly used antibacterial agent ZnO,

ZnS has more efficient antibacterial properties. The ZnS nanoparticles have also been proven to be able to deposit on the surface of bacteria and inhibit the regular bacteria functions thus killing the bacteria [13]. However, other studies demonstrated that ZnS possesses better antibacterial properties after oxidation which resulted in formation of ZnO [159]. Another study on the chemical precipitation method uses $ZnCl_2$ and Na_2S as precursors for the reactions to create ZnS nanoparticles [14], the particles had an average diameter of 2-4 nm. In order to assess the antibacterial properties, disk bacteriological tests on *P. aeruginosa*, *Actinomycete* and *Salmonella typhi* were conducted. The result concluded that ZnS showed different antibacterial effectiveness against different bacteria, it also has different effectiveness when applied with different concentrations. The general trend is the higher the concentration, the larger the ZOI area. Based on this study, the ZnS is most effective on *Salmonella typhi*. In another relevant study, ZnS also showed antibacterial activity over *B. subtilis* and *K. planticola* [16].

Overall, many different types of topical antibacterial agents have been reported, antibiotics and typical metallic compounds like Ag and ZnO have been reported extensively. However, very few studies have been done on antibacterial effectiveness of ZnS particles. Based on the information provided in the previous sections, the bacteria used for the study of ZnS antibacterial effectiveness did not include the most commonly seen burn wound infection bacteria strain *S. aureus*. Further investigation is needed to validate the antibacterial effectiveness of ZnS on this particular type of bacteria strain.

2.6 Synthesis of ZnS

2.6.1 Chemical Synthesis of ZnS

There are two major ways to synthesize ZnS [12, 16], one is chemical precipitation method, and the other is biological synthesis. The chemical synthesis requires precursors of Zn and sulfur, and the reaction takes place in a solution based environment, usually requiring heating under different temperatures. In order to control the size of the precipitates, different parameters are involved, and many of them usually require stabilizing agents that control the shape of the precipitates. Typical precursors for Zn include: zinc chloride [14, 160], zinc acetate dihydrate [12, 161-164], zinc nitrate hexahydrate [165, 166], zinc sulfate [167]. And typical precursors for sulfur include: 1-thioglycerol [161], TAA [162, 165, 166], thiourea [163, 164], sodium sulfide [14]. The basic reaction mechanism is shown below in Equation (2.1):

$$Zn^{2+} + S^{2-} \rightarrow ZnS \quad (2.1)$$

G. R. Amiri and his group used $ZnCl_2$ as Zn precursor and Na_2S as sulfur precursor, and ME or starch was used as surfactants. The reaction took place in distilled water. $ZnCl_2$ was added first followed by adding of ME or starch, Na_2S was added at last under vigorous stirring. The experiment was done under room temperature. After the reaction, the ZnS precipitates were centrifuged and dried [14].

Gaiping Li and his group used precursor of $Zn(Ac)_2$ and TAA for ZnS production. DDAB was used as surfactant. In the study, DDAB solution was prepared by dissolving DDAB into water, and $Zn(Ac)_2$ and TAA were dissolved in the DDAB solution under stirring until all chemicals were completely dissolved. The crude solution was then heated to 80 °C for 6 hours. After the reaction, the ZnS precipitates were centrifuged and dried [12].

J. Nanda and his group used $Zn(Ac)_2$ as Zn precursor and Na_2S as sulfur precursor, however, 1-thioglycerol was used as capping agent to control the particle size [161]. $Zn(Ac)_2$ and Na_2S were dissolved in DMF, then the solution was stirred under argon atmosphere. 1-thioglycerol was added in the solution, the solution was stirred for 8-10 hours, and then the ZnS precipitates were centrifuged and dried.

Jin Joo and his group studied the generalized and facile synthesis of metal sulfide nanocrystals in which the synthesis of ZnS was also studied [160]. This study also used $ZnCl_2$ as precursor for Zn, but used sulfur simple substance as precursor for sulfur. The reaction took place in oleylamine solution with presence of TOPO as surfactant. Zinc-oleylamine-TOPO solution was prepared by heating up to 170 °C for 1 hour, sulfur was later added. After that, the solution was heated to 320 °C and aged for 1 hour. After the reaction, the ZnS particles were centrifuged and dried.

Subhendu K. Panda and his group studied the optical properties of ZnS nanospheres [166]. In this study, they used the one-pot colloidal synthesis. Precursor used for Zn was $Zn(NO_3)_2$ and the precursor for sulfur was TAA. PVP was used as stabilizer for spherical structures. First PVP was dissolved in water followed by $Zn(NO_3)_2$ under vigorous stirring. After that, TAA was added and the solution was heated at 80 °C for 2 hours. Later the ZnS precipitates were centrifuged and dried.

In order to create different shapes of ZnS particles, the use of different agents or methods is involved. For photonic applications, spheres with ZnS as shell and silica as core were developed. The reaction took place with silica spheres in the solution under sonication, and the ZnS grew onto the silica particles [165]. In order to create spherical ZnS particles, PVP was used

as stabilizer to aggregate the ZnS particles to create a spherical structure [166]. By changing the reaction environment, we can also get hollow ZnS spheres [164].

With regards to controlling the size of ZnS particles, changing the precursor composition will have an impact [161]. Some other parameters during the reaction are also reported to have impact on the final particle sizes of ZnS, such as reaction time and temperature [164, 166]. Generally, the longer the reaction time, the larger the particle size, and the higher the temperature, the larger the particle size [164, 166].

2.6.2 Biological Synthesis of ZnS

The traditional chemical production methods have some problems, including poor reproducibility, some require high temperature, or high pressure to initiate the reaction, some methods may use or produce toxic matters such as H_2S in the process [11]. So recently, the biosynthesis methods, which are generally considered as more eco-friendly, cleaner, more economical and more reproducible [16], have attracted much attention. Biological synthesis usually requires SRB or metal reducing bacteria in an anaerobic environment, the end products of SRB metabolism under an anaerobic environment, sulfide, can react with metal ions and create insoluble metal sulfide [168]. Different pH values in the environment will result in different forms of sulfide (S^{2-}, HS^- or H_2S) [169], thus controlling pH plays an important role in ZnS production in the biosynthesis. Besides the requirement of the medium and environment as described in the previous section, incubation time, temperature, supplement nutrients and their amounts, bacterial species and precursor types can all have impact on the particle size of ZnS [16].

Studies showed that the biosynthesized ZnS nanoparticles are usually bound to proteins, these proteins can not only facilitate keeping the nano dimension of ZnS particles, but also increase aggregation, which can prevent redissolving of ZnS nanoparticles into the solution and incidental uptake by sulfate reducing bacteria which may in turn kill the cells [16, 170]. There are two major pathways for the proteins to bind on ZnS: first, proteins, peptides or amino acids could be released after sulfate reducing bacteria cell death and then captured by hydrophobic ZnS surfaces, and alternatively, bacteria can generate toxic metal-binding proteins themselves and bind to ZnS [170]. This is likely due to the bacterial resistance mechanism to heavy metals and metalloids [171].

Another important characteristic that biosynthesis possesses is the scale-up potential and the reduced cost based on larger scale production. The exponential growth of bacteria is currently of great economic importance in terms of the production of a wide variety of microbial products [172]. For laboratory scale cultivation, certain costly media components might be needed, but for industrial purposes, they should be economical and readily available [173]. Among various fermentation methods, the in vitro Liquid State Fermentation (LSF) will have large positive effect of economy of scale-up production [174]. Using this method, the biosynthesis study of ZnS particles have demonstrated that even with scalability factor of 2400 of medium scale, the production remains stable and the quality of the ZnS nanoparticles showed no significant difference in comparison to small scale production [16]. Thus biosynthesis of ZnS particles can be more economical to scale up and produce in bulk.

In the meantime, studies showed that in the laboratory environment, the productivity of ZnS particles is still relatively low comparing to chemical production, the daily average ZnS production rate of 1 L medium is about 0.5 g, while study showed that chemical production can

produce around 30 g every 3 hours using 1 L solution [16, 166]. However, as the biosynthesis of ZnS has not yet been commercialized, the costs for bulk synthesis cannot be evaluated at this time.

2.7 Cryomilling

Cryomilling is the mechanical attrition of powders under a cryogenic environment. It is often used as a method of strengthening materials through grain size refinement and dispersion of fine, nanoscale particles, mostly for metallic application. It involves the transformation of plasticity-induced dislocation structures into high angle grain boundaries in metallic powders under liquid nitrogen environment [175]. Other than grain size refinement, it is usually used to decrease particle sizes [176]. Cryomilling combines both the environment of cryogenic temperatures and conventional mechanical milling. The extremely low temperature suppresses recovery and recrystallization of the materials, which in turn leads to finer grain structures and more rapid grain refinement [177], so that the desired nanostructures can be reached in shorter time in comparison to conventional mechanical ball milling [178]. A study showed that direct ball milling of Zn under regular environment results in ZnO particles [179], which indicates that rapid oxidation takes place during regular ball billing process. However, as cryomilling operates under a cryogenic environment, a high rate of oxidation is avoided which can only be achieved when materials are sealed in inert gas environment for regular ball milling [178, 180].

As particle size has been decreased through cryomilling, the surface to volume ratio is increased accordingly. Researchers have found that in nanoparticles, small dimension results in large surface to volume ratio, yielding to increase of the chemical activity [181]. Although few papers have reported the effect of cryomilling on antibacterial properties, studies have been

conducted on the effect of ball milling on antibacterial properties. Generally, the longer the milling period, the smaller the particle size and the better antibacterial effectiveness the particles possess [15, 182]. The relationship between milling time and antibacterial activity as mentioned in the previous sentence applies to typical metallic antibacterial agents such as ZnO and Ag nanoparticles [183] and are thus expected to have the same effect on other antibacterial nanoparticles, and this is what this study is interested.

2.8 Summary of Literature

This literature review summarizes the key areas related to this study, which describe the following aspects: 1) Different types of wounds and their classifications, 2) burn wound healing process and common infections indicating the necessity of antibacterial agents during burn wound healing, 3) emerging problems of drug resistance and biofilm development which implies the importance of new drug development and 4) the necessity of using biosynthesis methods for fabrication of antibacterial substances. This literature review serves as fundamental knowledge basis for the development of this research.

CHAPTER 3.

CHEMICALLY SYNTHESIZED ZNS ANTIBACTERIAL ACTIVITY EVALUATION

This Chapter is dedicated to demonstrate the pilot evaluations of the traditional methods of ZnS synthesis and its antibacterial effectiveness, which provided the rationale for the research developed for this thesis. This chapter contains four different sections: 1) Synthesis Method Selection; 2) Materials and Methods; 3) Evaluation Results; 4) Discussions.

3.1 Synthesis Method Selection

Chemical synthesis is by far the most popular method for ZnS production, Section 2.6.1 has numerated different synthesis methods, and there are also many other chemical synthesis methods [167]. However, in terms of feasibility, the one-pot colloidal synthesis was the most favorable. $Zn(NO_3)_2$ and TAA were more economically available by comparison to other precursors. In the meantime, this synthesis method requires relatively low reaction temperature and shorter reaction time without special requirement for atmosphere. The reaction can be easily achieved in a regular laboratory environment.

3.2 Materials and Methods

3.2.1 ZnS Preparation

PVP was purchased from Sigma Aldrich with average molecular weight of 40,000, TAA was purchased through Sigma Aldrich with > 99.0% purity, $Zn(NO_3)_2 \cdot 6H_2O$ was purchased from Fisher Scientific. All chemicals were used without further purification.

In the preparation process, 3 g of PVP was dissolved in 90 ml of distilled water, then 0.03 Mole, or 8.92 g of $Zn(NO_3)_2 \cdot 6H_2O$ was added to the solution. After 1 hour of stirring, 0.03 Mole, or 1.50 g of TAA was added in the solution. Then the solution was stirred under 80 °C for 2 hours. This process was conducted in fume hood, as H_2S generated through the chemical reaction is hazardous. The solution was then cooled down to room temperature, the ZnS precipitates were then centrifuged, washed using distilled water and ethanol, and later dried in the vacuum oven overnight before ZnS particles were collected.

The prepared ZnS nanoparticles were then cryomilled using freezer mill 6870 (SPEX, Metuchen, NJ, USA), which was operated under cryogenic environment of -196°C. 5 g of synthesized ZnS nanoparticles were used for cryomilling, and the parameters used were: 5 min precool, 8 cycles, 7 min run time for each cycle, 2 min cool time in between each two cycles and 15 CPS for grinding. The total time period for grinding is 56 min [15]. The original as-synthesized ZnS sample was labeled as Comp C and cryomilled sample was labeled as Comp D.

3.2.2 SEM Analysis

The morphology of ZnS particles were imaged using JEOL JCM-6000 NeoScope Benchtop SEM. In order to clearly observe the morphology of the samples, the image was taken under 15 kV accelerating voltage, high vacuum, and magnification of 10000× and 5000×, using secondary imaging mode. The image was analyzed using JCM-6000 software version 1.1.

3.2.3 XRD Analysis

The ZnS particles were analyzed using Rigaku MiniFlex 600 X-ray Diffractometer (Rigaku Inc, Woodlands, TX, USA) to determine the particles composition and the corresponding crystal structures. The voltage and current X-ray generator applied were 40 kV and 15 mA, with Cu as the source of X-ray, the detector used was NaI scintillator. The XRD profiles were analyzed using the Rigaku powder X-ray diffraction software PDXL version 2.1.3.4.

3.2.4 Bacterial Strains and Media

As previously mentioned in Chapter 1, no study has been conducted on antibacterial properties of ZnS on common burn wound infection *S. aureus*. In this evaluation, evaluation was done on *S. aureus* and all the organisms will be stored at -80 °C until use. Bacteria were grown in either LB Broth or on LB Agar plates at 37 °C. The strain used was *S. aureus* AH133 which carries plasmid pCM11 which contains the gene that codes for the GFP [184].

3.2.5 ZOI Assay

The bacteria were grown in LB broth, until the media were visibly turbid, and then the suspension was diluted until turbidity at OD600 of 0.5 was reached. The turbidity was measured using spectrophotometer. At this OD600 level, there are approximately 10^8 CFU per ml. Normal PBS (pH = 7.4) was used to adjust the desired optical density. The LB agar plates were inoculated within 15 min after the inoculums suspension has been adjusted. A sterile cotton swab was dipped into the bacterial suspension, and a confluent lawn of bacteria was made on each plate using the dipped cotton swab. Within 15 min after the plates were inoculated, 50 mg of ZnS

powders were distributed at three spots onto the LB Agar surface, with at least 24 mm (center to center) between them [185]. The plates were incubated at 37 °C for 24 hours before results were read. The diameters of the zones of complete inhibition, including the diameter of the disk, were measured to the nearest second decimal place.

3.3 Evaluation Results

3.3.1 Morphology

Figures 3.1 and 3.2 showed the morphologies of Comp C and Comp D. The Comp C showed very uniform size distribution, with mean diameter of each individual nanosphere of 356 nm with 21 nm of standard deviation. However, although it is expected that cryomilling decreases the particle size, due to agglomeration effect, Comp D actually showed an increase of mean diameter which is 1.068 μm and standard deviation of 1.052 μm. Also, due to cryomilling, the morphology of ZnS particles has turned from sphere to arbitrary shapes with sharp edges. This is possibly due to aggregation effect that holds small individual particles into a larger bulk [16].

Cryomilling in this case has introduced agglomeration to the particles, as the technology can mill the particles into submicron in size, and they have the tendency to agglomerate and form the conglomeration with size as big as 50 μm or larger due to the presence of electrostatic, steric and van der Waals forces between particles [186-188]. Agglomeration is different from aggregation. Agglomerates are an assembly of primary particles, and the total surface area does not differ appreciably from the sum of specific surface areas of primary particles [189]. Thus even though the particle size of Comp D seemed larger than the non-cryomilled samples Comp C,

the agglomeration effect does not impact the amount of surface area in contact with PEG, and surface area to volume ratio was still expected to increase comparing to non-cryomilled Comp C.

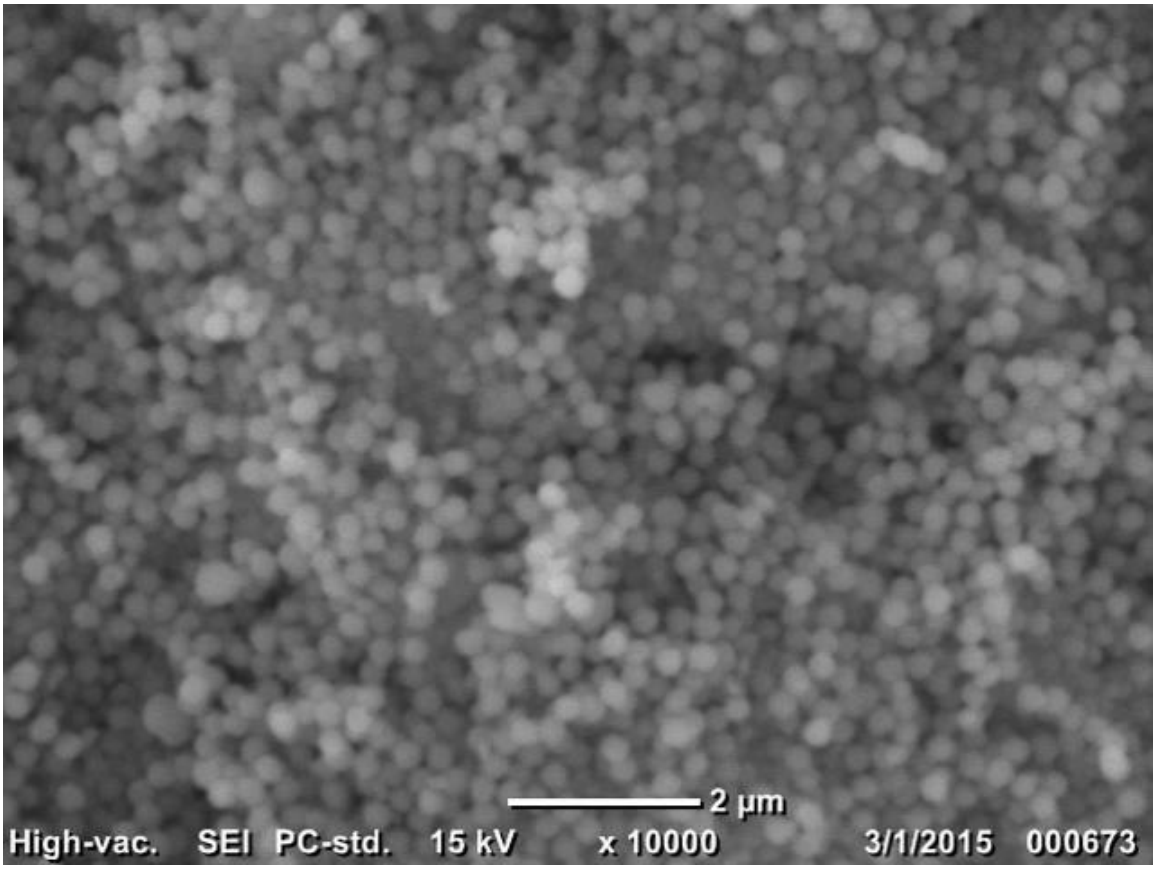

Figure 3.1: SEM image of Comp C

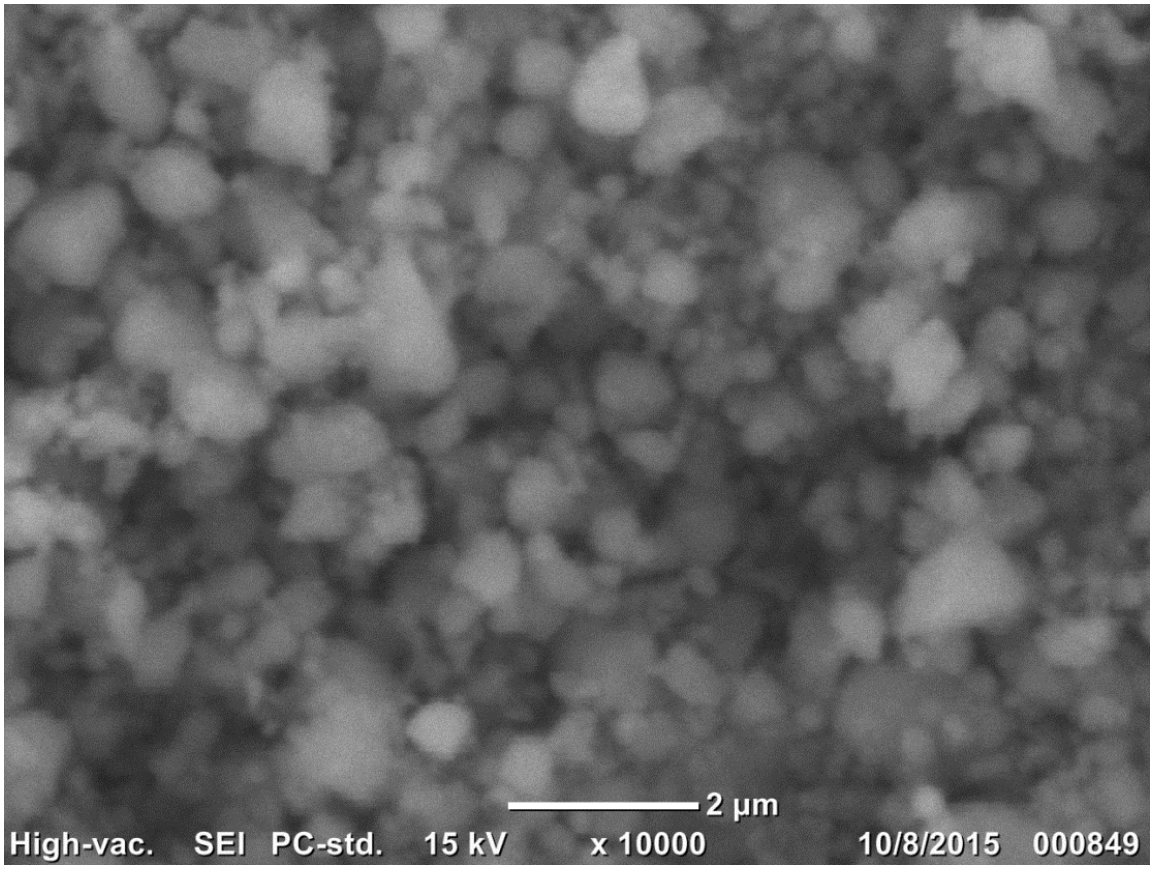

Figure 3.2: SEM image of Comp D

3.3.2 XRD Analysis

Figure 3.3 showed the XRD profile of the particles synthesized. The three major diffraction peaks corresponded to the (111), (220), (311) planes of crystalline ZnS, which matched with XRD profile of ZnS sphalerite. The result showed that ZnS sphalerite has a cubic crystal structure with 5.408620 Å in unit cell dimension.

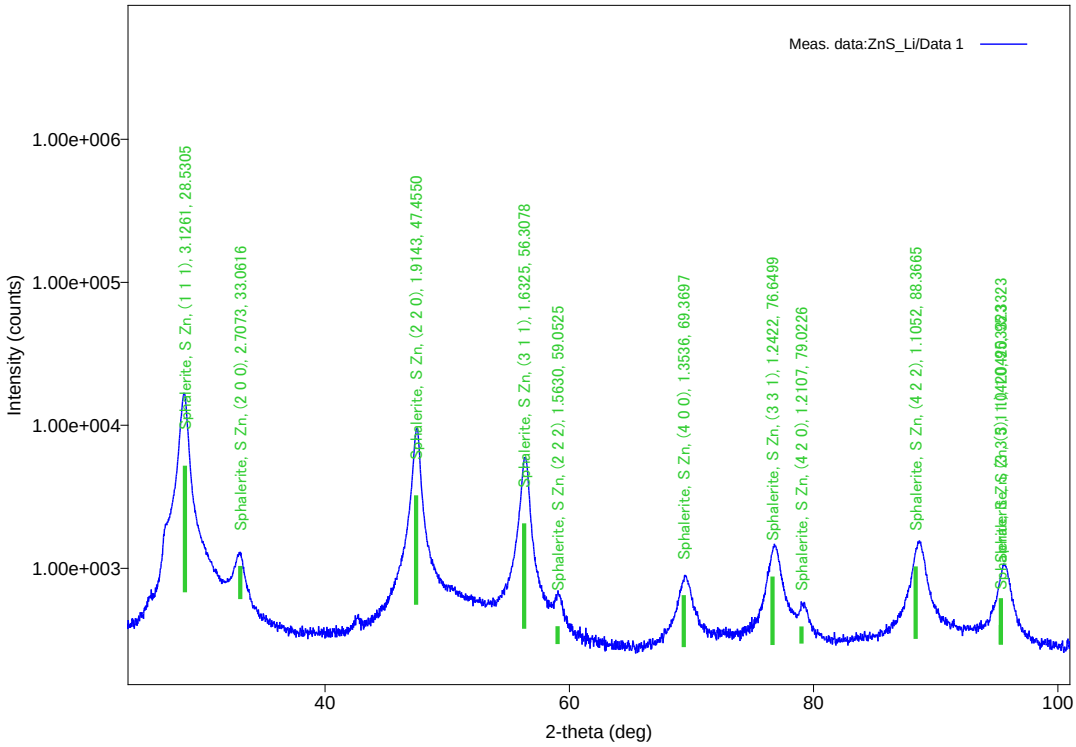

Figure 3.3: XRD profile of the as-synthesized Comp C

3.3.3 ZOI Assay

Figure 3.4 showed the ZOI assay results for Comp C and Figure 3.5 showed the ZOI assay results for Comp D. Based on the ZOI assays, Comp C showed no antibacterial properties as there were no clear inhibition zones with 50 mg ZnS Comp A treatment at 3 different locations, while Comp D showed ZOI of average of diameter of 20.22 mm with standard deviation of 0.83 mm.

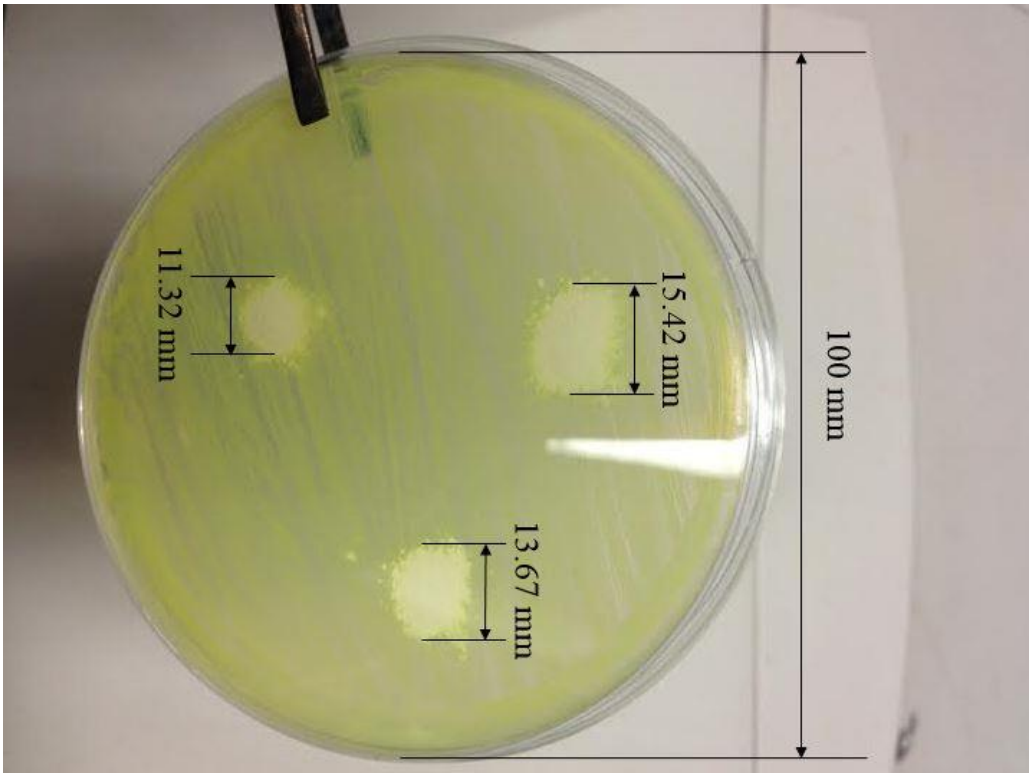

Figure 3.4: ZOI assay result for Comp C

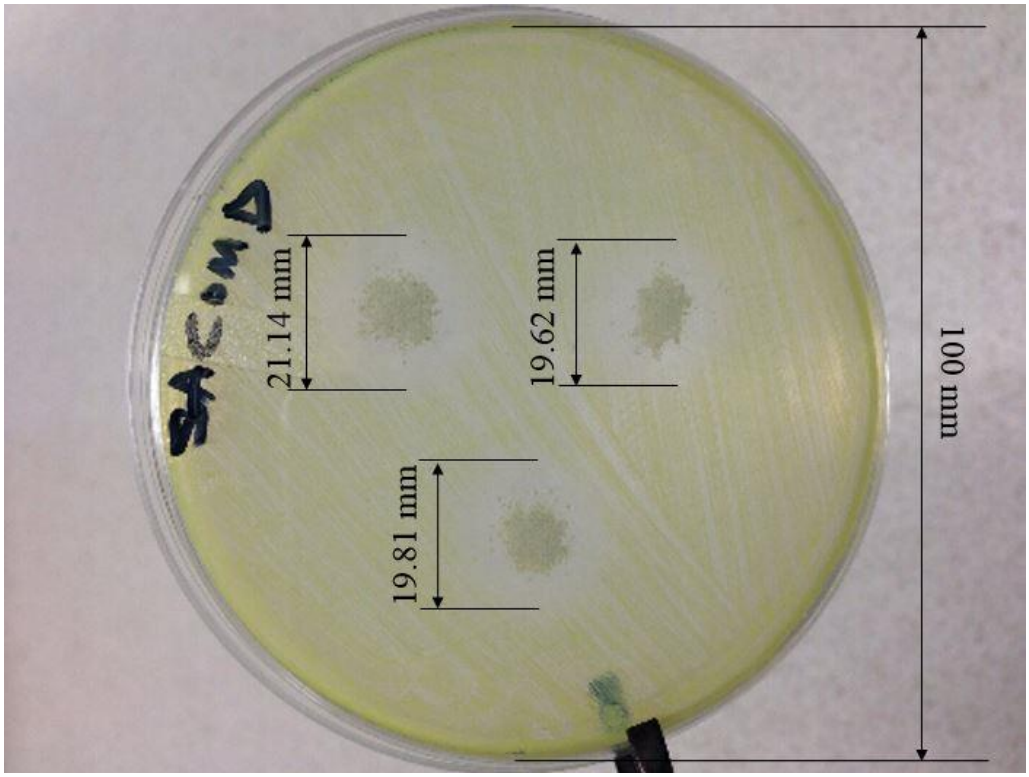

Figure 3.5: ZOI assay result for Comp D

3.4 Discussion

This evaluation has provided basic information of chemical synthesis of ZnS and its antibacterial properties. Based on the morphological SEM results, one-pot colloidal synthesis successfully produced monodispersed ZnS nanoparticles with mean diameter of 356 nm with 21 nm of standard deviation, but cryomilling has dramatically changed the morphologies of the particles, making the particle size larger and with larger standard deviation. However, this may be due to the aggregation effect [188]. According to the XRD profile, the synthesized particles were ZnS sphalerite.

The ZOI results showed different results for Comp C and Comp D. Comp C basically showed no antibacterial properties against *S. aureus*. Although there are studies that showed as-synthesized ZnS has antibacterial properties against certain bacteria [12, 14], this study showed that the as-synthetized ZnS did not have a broad spectrum of antibacterial properties, and specifically might not have antibacterial properties against *S. aureus*. However, in this evaluation, Comp D showed very clear inhibition zones, which indicated that cryomilling has positive effect on antibacterial properties.

Study showed that under certain PVP/Zn^{2+} ratio, PVP could encapsulate the ZnS nanoparticles, so that the ZnS would be passivated [190], thus the Zn^{2+} might be unable to be released to act upon the bacteria to inhibit the bacteria growth. In the meantime, PVP is basically non-toxic [191] and will not impact bacteria growth, this might explain why Comp C, which could be passivated by PVP, did not show antibacterial properties. However, based on the SEM analysis, cryomilling deformed the particles morphologies and could destroy the encapsulation on the outside layer, so that the Zn^{2+} would be easier to be released to act on bacteria. The

reasons above could possibly explain the fact that Comp D showed good antibacterial properties while Comp C did not.

Therefore, based on the following reasons, the major part of this study will focus on understanding and further improving via cryomilling the antibacterial properties of biological synthesis of ZnS: 1) chemically synthesized ZnS did not show antibacterial effectiveness against common burn wound *S. aureus* infections; 2) the chemical production usually requires special conditions including high temperature, inert gas environment as described in section 1 of this chapter; 3) the chemical process usually involves H_2S production which is hazardous for human beings and the environment; 4) biological synthesis is usually more biocompatible, and biosafe as mentioned in the literature review.

As cryomilling proved to have positive effect on antibacterial properties over the as-synthesized ZnS, this study will continue to use cryomilling as a material refining process in expectation to enhance the antibacterial effectiveness.

CHAPTER 4.

EFFECT OF CRYOMILLING ON ZINC SULFIDE EFFECTIVENESS AS ANTIBACTERIAL SUBSTANCE FOR BURN WOUND HEALING

Manuscript to be submitted to *Burns*

Jianqiang Li[1a], Phat Tran[3a], Ilia Ivanov[2], Abdul Hamood[4], Iris Rivero[1*]

4.1 Abstract

This study introduced a novel antibacterial agent, zinc sulfide nanoparticles, for burn wound treatment against common infectious bacteria *Staphylococcus aureus*. Zinc sulfide nanoparticles were synthesized using Sulfate Reducing Bacteria under anaerobic environment, and the synthesized nanoparticles were further processed through cryomilling. Scanning electron

---

[1] Department of Industrial and Manufacturing Systems Engineering, Iowa State University, Ames, Iowa, USA;

[2] Center for Nanophase Materials Sciences, Oak Ridge National Laboratory, Oak Ridge, Tennessee, USA;

[3] Department of Ophthalmology and Visual Sciences, Texas Tech University Health Sciences Center, School of Medicine, Lubbock, Texas, USA;

[4] Department of Molecular Microbiology and Immunology, Texas Tech University Health Sciences Center, Lubbock, Texas, USA.

[a] These two authors contributed equally to this work

[*] Corresponding Author. Email: rivero@iastate.edu

microscopy and X-ray diffraction techniques were used to characterize the morphology and crystal structure of the zinc sulfide nanoparticles. To assess bacteria inhibition and elimination, in vitro zone of inhibition studies consisting of inoculating cellulose disks on agar plates with Staphylococcus aureus followed by incubation for 24 hours were performed. In vitro biofilm models consisting of inoculating cellulose disks on well-developed Staphylococcus aureus biofilm on agar plates followed by 24-hour incubation were also conducted. Confocal laser scanning microscopy was employed to qualitatively observe the antibacterial effectiveness of zinc sulfide as antibacterial agent and statistical analysis was performed to quantitatively study the effectiveness by counting the residual colony forming units on the cellular disks. Results showed that the zinc sulfide nanoparticles show antibacterial properties, and cryomilling showed a positive effect on the antibacterial properties of zinc sulfide

Key words: Zinc sulfide, Antibacterial, Staphylococcus aureus, Cryomilling

4.2 Introduction

Burn wounds are one of the most common and devastating forms of trauma, and series of complications can occur as thermal destruction on the skin barrier system and accompanying local and systemic immune system can be critical contributor for the infections for burn patients [1-3]. Evidence showed that bacteria infected patients usually have a higher rate of mortality [4]. Removal of invading infections is crucial and the incomplete microbial clearance will result in prolonged inflammatory phase which can lead to transition from acute into chronic wound [5, 6], thus hindering the healing process. Various types of microorganisms are able to colonize the wound sites, and gram-positive bacteria usually dominate the microorganisms population

immediately after the burn [7, 8]. Among them a typical example is the gram-positive bacteria *Staphylococcus aureus* [9].

The development of biofilm can be a serious problem on the wound sites [10]. Biofilms are complex compositions made up by accumulated bacteria in a self-secreted extracellular polysaccharide matrix (EPS) [6]. A mature biofilm is able to develop a self-protective mechanism which is more resistant to regular antibiotic treatments than regular bacteria [11]. Burn wounds are also subjected to biofilm formation [12], persister cells within biofilms can temporarily disable the inherent mechanism of cell death, which in turn is resistant to antibiotic treatment and lead to failure of eradication of biofilm [13, 14]. *Staphylococcus aureus* is among those commonly isolated bacteria that can develop biofilms [12].

With the overuse of antibiotics and antibacterial agents, drug resistance has become an emerging problem threatening the world [15], and the resistance can be against both antibiotics [16, 17] and metallic compounds such as silver [18]. Bacteria have high rates of nucleotide substitution and poor ability of mutation error-correction, in general the genetically mutated bacteria have high capability to adapt to new hosts including human [19-21]. The biofilm developed by these bacteria pose even higher risk for human beings, thus the identification of alternative antibacterial substances is always necessary.

Previous studies indicated that Zinc Sulfide (ZnS) possesses antibacterial properties against several types of bacteria, including *E. Coli* [22], *P. aeruginosa*, *Actinomycete*, *S. typhi* [23], *B. subtilis* and *K. planticola* [24]. However, no test has been carried out on *Staphylococcus aureus*. ZnS in this study was biosynthesized, which was more eco-friendly, reproducible and economical than chemical synthesis. Cryomilling is the mechanical attrition of powders under cryogenic condition [25], and it was applied as a post-synthesis fabrication process to decrease

particle size of as-synthesized ZnS. Smaller sized ZnS particles are expected to possess better antibacterial properties than larger sized particles [26].

4.3 Materials and Methods

4.3.1 ZnS Preparation

ZnS nanoparticles were extracellular synthesized using the fast-growing metal reducing thermophilic bacterial, *Thermoanaerobacter*, X513 [27]. Media used were modified from TOR-39 medium, which contained the following ingredients: $NaHCO_3$, $CaCl_2 \cdot 2H_2O$, $NH_4 \cdot Cl$, $MgCl_2 \cdot 6H_2O$, NaCl, hydroxyethylpiperazine-N'-2-ethanesulfonic acid (HEPES) buffer, yeast extract and resazurin, with Oak Ridge National Laboratory (ORNL) trace minerals which include selenium, molybdate, vitamin mixture solutions and Phosphate Buffer Saline (PBS) [28]. No exogenous electron carrier substance or reducing agent was added to the anaerobic medium. The dissolved basal medium was boiled with N_2 gas purging and cooled with continuous N_2 purging. Incubation was initiated with inoculation of glucose, sulfur source such as thiosulfate or sulfite. After cell growth and development of S^{2-}, aliquots of zinc chloride were ($ZnCl_2$, reagent grade > 98%) dosed. The precipitate of ZnS nanoparticles was recovered by centrifugation and washed four times with deionized water and stored as wet condensed samples or freeze-dried solid samples. The original ZnS particles were labeled as Comp A.

The prepared ZnS nanoparticles were then cryomilled using a freezer mill 6870 (SPEX, Metuchen, NJ, USA), which was operated under a cryogenic environment of -196°C. 5 g of synthesized ZnS nanoparticles were used for cryomilling, and the parameters used were: 5 min precool, 8 cycles, 7 min run time for each cycle, 2 min cool time in between two cycles and 15

counts per second (CPS) for grinding. The total time period for grinding was 56 min [26]. Sample acquired using this method was labeled as Comp B.

4.3.2 Scanning Electron Microscopy (SEM) Analysis

The morphology of ZnS particles were imaged using JEOL JCM-6000 NeoScope Benchtop SEM. In order to clearly observe the morphology of the samples, images were taken under 15 kV accelerating voltage, high vacuum, and magnification of 5000×, using secondary imaging mode. The image was analyzed using JCM-6000 software version 1.1.

4.3.3 X-ray Diffraction (XRD) Analysis

The ZnS particles were analyzed using Rigaku MiniFlex 600 X-ray Diffractometer (Rigaku Inc, Woodlands, TX, USA) to determine the particles composition and the corresponding crystal structures. The voltage and current X-ray generator applied were 40 kV and 15 mA, with Cu as the source of X-ray, the detector used was NaI scintillator. The XRD profiles were analyzed using the Rigaku powder X-ray diffraction analysis software PDXL version 2.1.3.4.

4.3.4 Bacterial Strains and Media

All the organisms were stored before use at -80 °C to ensure low cell activity [29]. Bacteria were grown in Luria Bertani (LB) Broth at 37 °C. The strains used were *Staphylococcus aureus* AH133. This type of strain carries plasmid pCM11 which contains the gene that codes for the green fluorescent protein [30]. To maintain the plasmid, erythromycin was incorporated in the growth medium at a concentration of 1 µg/ml.

4.3.5 Zone of Inhibition (ZOI) Assays

Bacteria were grown in LB broth, until the media were visibly turbid, and then the suspension was diluted until an OD_{600} of 0.5 was achieved. The turbidity was measured by spectrophotometer. At 0.5 OD_{600} level, there are approximately 10^8 Colony Forming Unit (CFU) per ml [31]. PBS (pH = 7.4) was used to adjust the desired optical density. The LB agar plates were inoculated within 15 min after the inoculums suspension has been adjusted. A sterile cotton swab was dipped into the bacterial suspension, and a confluent lawn of bacteria was made on each plate using the dipped cotton swab. Within 15 min after the plates were inoculated, ZnS powders were distributed at three spots onto the LB Agar surface. Each spot contained 50 mg ZnS particles with at least 24 mm (center to center) between two spots [32]. The plates were incubated at 37 °C for 24 hours before results were read. The diameters of the zones of complete inhibition, including the diameter of the disk, were measured and rounded to the second decimal place. The diameter of the zone is related to the susceptibility of the isolate and to the diffusion rate of the drugs, but the larger the inhibition zone, the better the antibacterial properties.

4.3.6 *In vitro* Biofilm Model CFU Analysis

The biofilm assay was performed as previously described with some modifications [33]. Briefly, *S. aureus* Green Fluorescence Protein (GFP) bacteria were grown overnight, washed once with PBS (pH 7.4), re-suspended in PBS (pH 7.4) to an optical density (OD_{600}) of 0.5 (10^8 CFU/ml), and serially diluted (10-fold). Three sterile cellulose disks with diameter of 6 mm were placed on the surface of freshly prepared LB agar with at least 24 mm (center to center) between them, and 10 µl containing 10^2-10^3 CFU of tested strain was inoculated onto each disk.

The disks were then treated with ZnS particles mixed in 100 mg PEG (PEG Ointment Base, B1300, Spectrum, Gardena, CA, USA) in order to cover the whole disk. Due to the strong antibacterial properties exhibited by ZOI assay using 50 mg, the starting amount of ZnS used for biofilm study was also 50 mg. The quantity was gradually decreased until biofilm can no longer be completely eradicated. In this study, 25 mg, 15 mg and 10 mg were used. The plates were then incubated at 37 °C for 24 hours. Following incubation, the disks were rinsed lightly to remove any unattached bacteria, and the disks were examined by Confocal Laser Scanning Microscopy (CLSM) and CFU assay. In CFU assay, the disks were transferred to a 1.5 ml microfuge tube in 1 ml of PBS and sonicated for 10 minutes. The tubes were then vortexed for 1 minute to disrupt and disperse the biofilm. Bacterial suspensions were serially diluted 10-fold in PBS, and 10 µl aliquots of each dilution and undiluted suspension were plated on LB agar. The plates were air dried and they were then incubated at 37^{o}C for 24 hours before the results are read. The number of CFU/disk was determined as described above, using the formula CFU/disk = (CFU counted × dilution factor) × 100. All experiments were done in triplicate, and dilutions were also plated in triplicate.

4.3.7 CLSM Analysis

For *in vitro* studies, disks were treated with *S. aureus* GFP AH133 bacteria as described above for the in vitro biofilm model. After 24 hours of incubation, three control disks under PEG and three treated disks under ZnS in PEG were examined for the presence of *S. aureus* GFP AH133 biofilm by a CLSM. Visualization of the *S. aureus* AH133 biofilms was accomplished by using a Nikon A1+/AIR+ Confocal Microscope (Nikon Inc., Melville, NY, USA) with images acquired at 2 µm intervals through the biofilms. Two and/or three-dimensional images were

acquired using the Nis Elements Imaging software v. 4.20. Several image stacks of each biofilm were examined by CLSM, and the images were analyzed as previously described [34]. Experiments were done in triplicate.

4.3.8 Statistical Analysis

Results of the CFU assays were plotted with Prism® version 4.03 (GraphPad Software, San Diego, CA, USA) with 95% confidence intervals (CI) of the difference. Linear mixed effect model was used to model the experiment data in order to account for repeated measurements [35, 36]. Shapiro-Wilk W test was used to determine the normality of the data due to its higher power based on small sample size comparing to other normality tests [37]. Levene's test was used to test equal variance between treatment groups as it can be used to compare variances between two or more groups. One-way ANOVA was performed to check the difference in means between two or more treatment groups. One-tailed and Two-tailed Student's *t*-tests were used to determine if the means between two groups are different [38]. Type I error rate is the possibility of incorrect rejection of a true null hypothesis, and a null hypothesis is the hypothesis that sample observations result purely from chance. Bonferroni correction was used to control the overall familywise Type I error rate during multiple comparisons as they will result in increase in Type I error rate [39]. The statistical analyses were performed using JMP® software (SAS, Cary, NC, USA). All tests were conducted with generally accepted designated Type I error rate of 0.05, implying that it is acceptable to have a 5% probability of incorrectly rejecting the null hypothesis [40, 41].

4.4 Results and Analysis

4.4.1 ZnS Morphologies:

Figures 4.1 and 4.2 showed the morphologies of synthesized (Comp A) and cryomilled ZnS particles (Comp B). Due to aggregation effect of smaller sized particles, the original ZnS particles synthesized have an average diameter of 2.836 mm with standard deviation of 1.499mm, while the cryomilled ZnS particles have an average diameter of 0.801 μm with standard deviation of 0.407 μm. Meanwhile, the shape of the particles has been altered from arbitrary shapes with sharp edges to more spherical shapes. Due to the decrease in size of the particles, the surface area to volume ratio has been increased.

Based on the previous study of biosynthesis of ZnS, the average crystallite size (ACS) is around 6.5 to 10 nm. However, nanoparticles in aqueous solution have higher surface energy than bulk materials [42], and the resulting particles often become cemented together into aggregates. Because particles dispersed in liquid media are in constant thermal or Brownian motion, they exhibit a strong affinity for nanoparticles as they move through medium and collide [43], and the surface characteristics affect aggregation in dispersion [44]. In this case we saw very large original Comp A particles even though the ACS was produced in nanoscale.

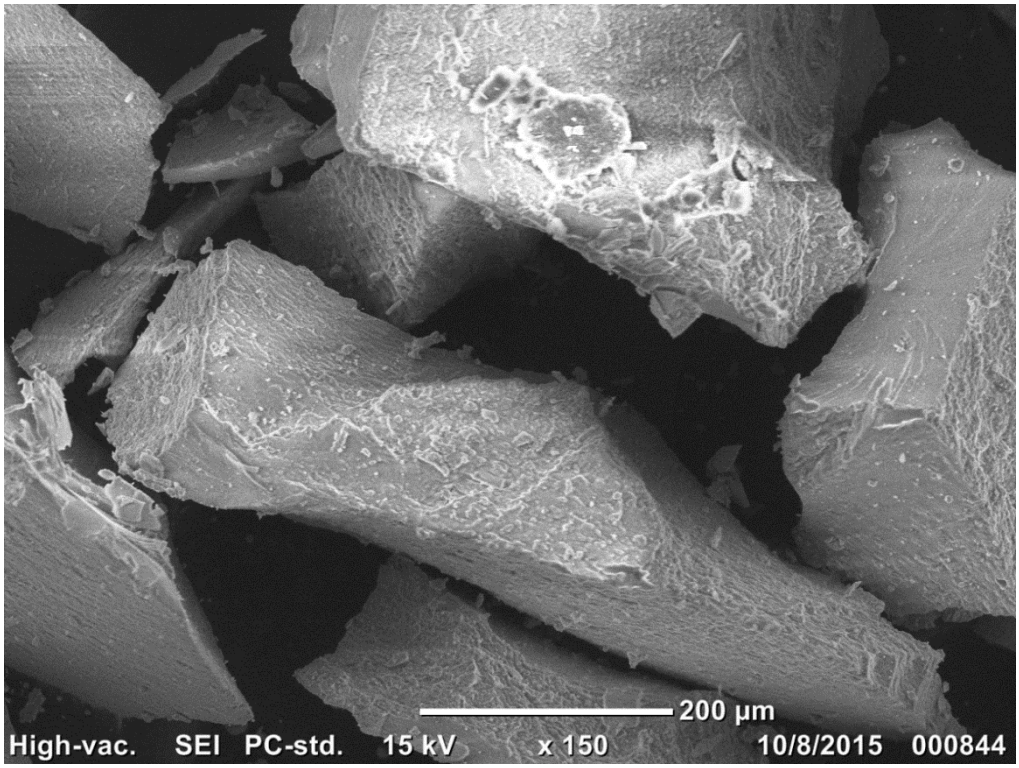

Figure 4.6: SEM image of Original ZnS particles (Comp A)

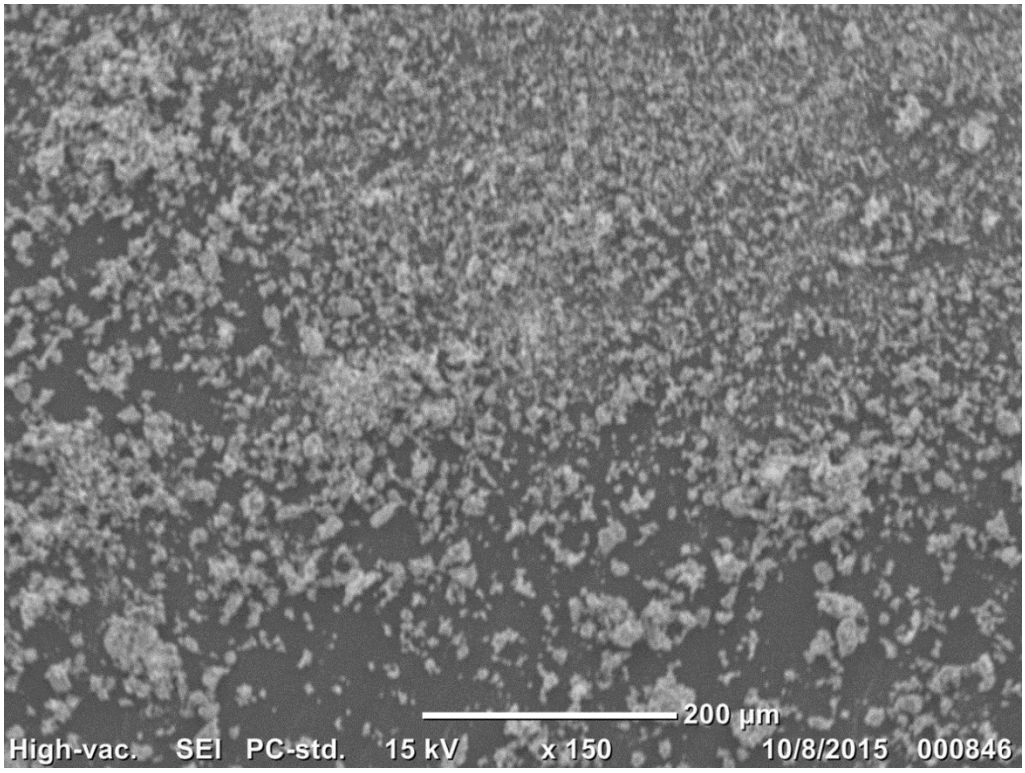

Figure 4.7: SEM image of Cryomilled ZnS particles (Comp B)

4.4.2 XRD Analysis

Figure 4.3 shows the XRD profile of the particles synthesized for wound dressing and the reference profile for ZnS sphalerite structure. The three major diffraction peaks corresponded to the (111), (220), (311) planes of crystalline ZnS, which matched the XRD profile of ZnS sphalerite. The result showed that ZnS sphalerite has a cubic crystal structure with 5.394493 Å in unit cell dimension.

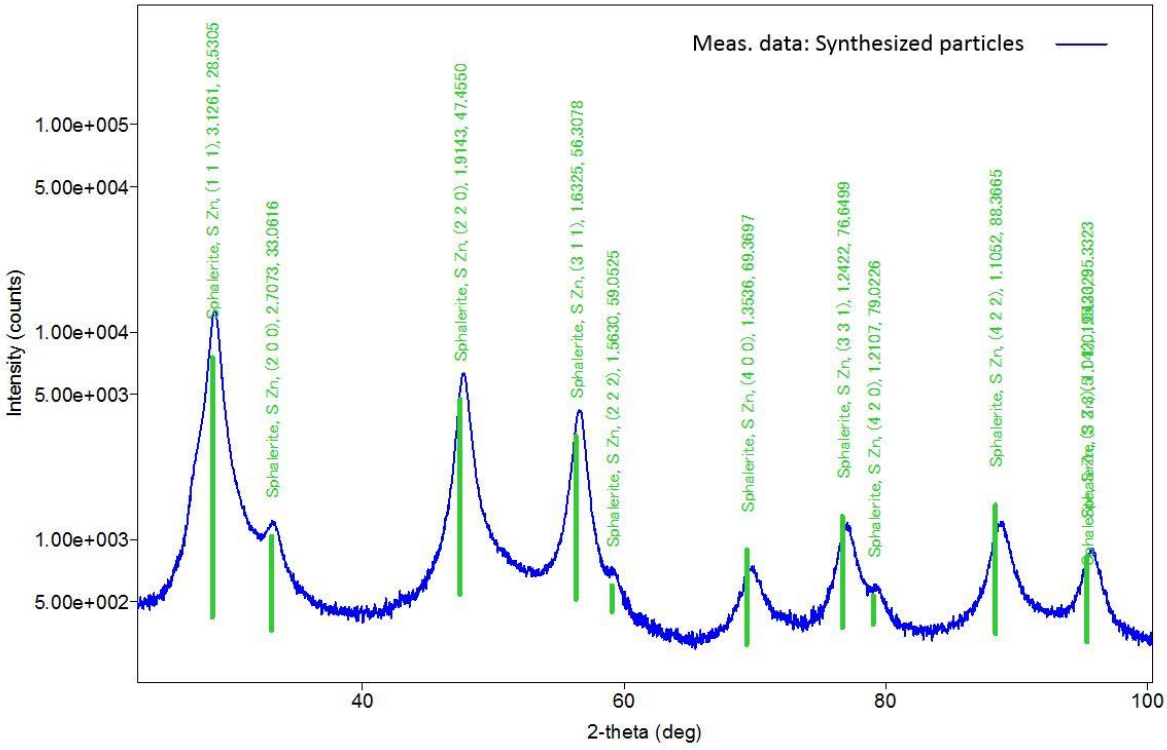

Figure 4.8: XRD profile of the synthesized ZnS particles (Comp A)

The results showed that Sulfate Reducing Bacteria successfully produced ZnS particles with a sphalerite crystal structure. Cryomilling as post synthesis process decreased the particle size as well as changed the shape of the ZnS particles.

4.4.3 ZOI Assay

Figure 4.4 showed the ZOI assay result for 50 mg Comp A treatment on *S. aureus* AH133 bacteria lawn, the treatment created the ZOI of average of 11.5 mm with standard deviation of 0.656 mm in diameter. Meanwhile, Figure 4.5 showed the ZOI result for 50 mg Comp B ZnS treatment, the treatment created a ZOI of average of 18.87 mm with standard deviation of 0.902 mm in diameter. The results showed that both types of the ZnS particles have antibacterial effectiveness on *S. aureus*, however, whether the desired level of effectiveness was achieved was not yet determined and this is to be tested in the CFU analyses.

Statistical analyses (see Appendix A.1) showed that the ZOI diameter data collected followed normal distributions and the two groups of data had equal variance, thus the corresponding Student's *t* test was employed to test the difference in means of ZOI diameters between Comp A and Comp B treatment group. Test results showed that there was significant difference between the two treated groups and Comp B had better antibacterial properties than Comp A based on ZOI assays.

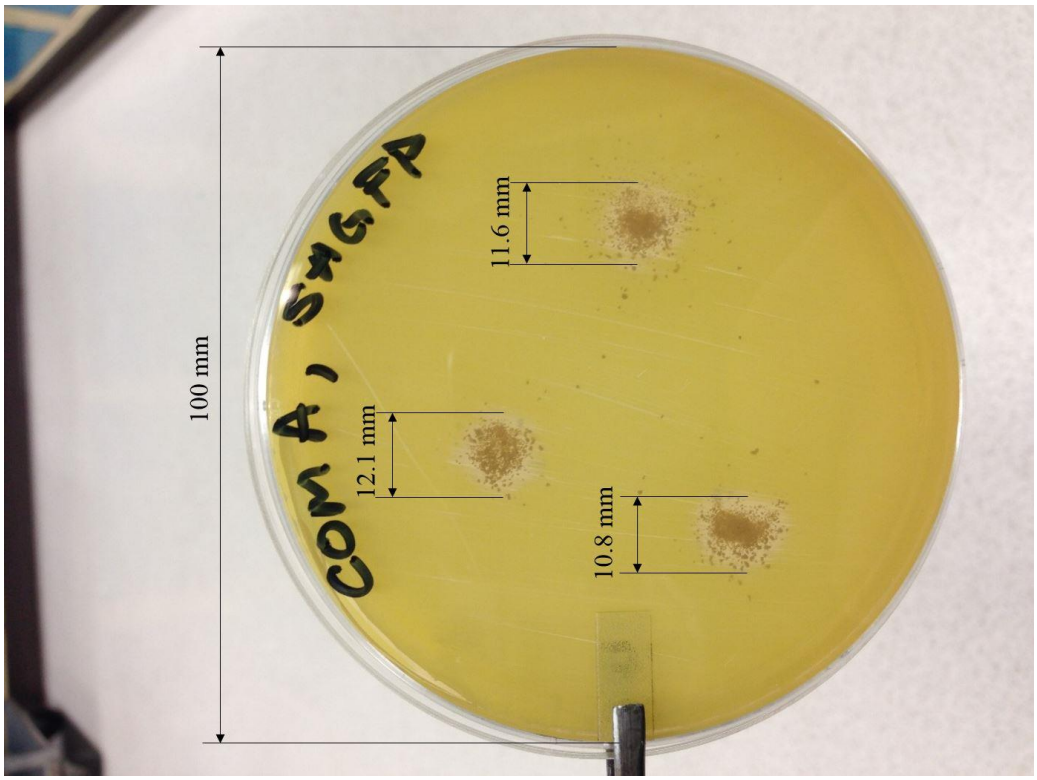

Figure 4.9: ZOI results for 50 mg ZnS Comp A treatments

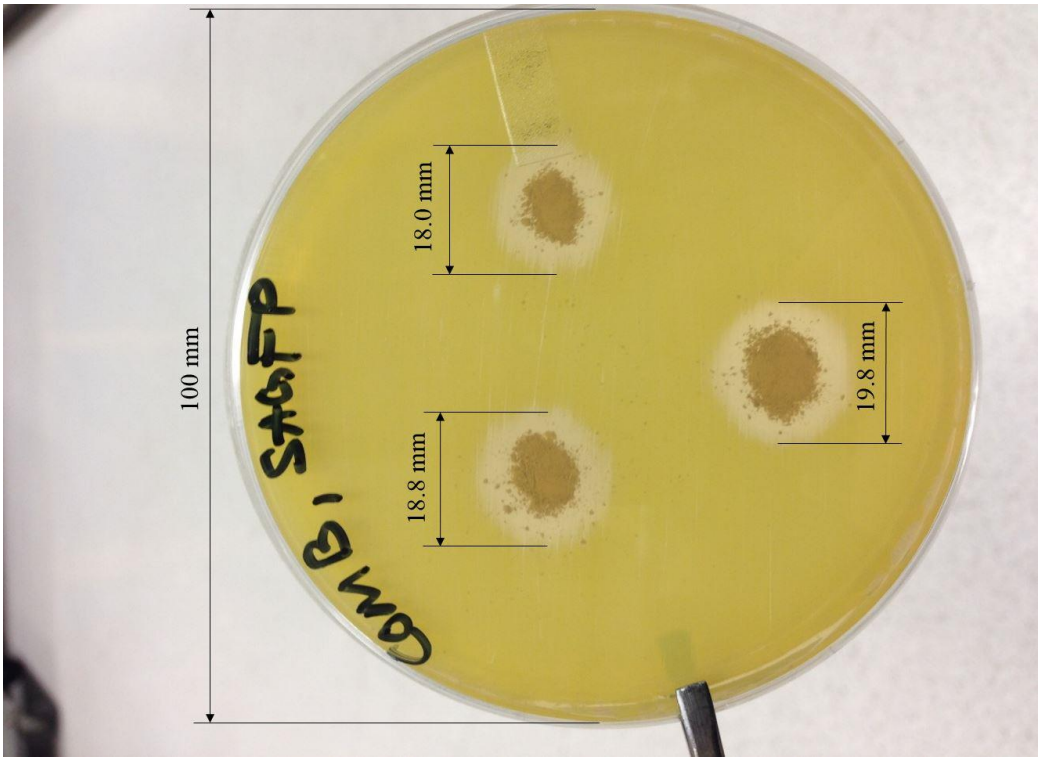

Figure 4.10: ZOI results for 50 mg ZnS Comp B treatments

4.4.4 *In Vitro* Biofilm Model CFU Analyses

Based on the in vitro biofilm CFU assays, Figure 4.6 showed statistics of residual bacteria that were left on the biofilm based on 50, 25, 15 and 10 mg of ZnS Comp A treatments on an disk with area of diameter of 6 mm, and Figure 4.7 showed the statistics tested under the same condition for Comp B. Figure 4.6 and 4.7 also showed results for Untreated control disks and PEG disks, the statistics used were the same for these two groups. There were three samples under each treatment group. As the bacteria grow exponentially, all data were plotted in log 10 scale. A minimum of 99.9% inhibition (3 log bacteria reduction) is usually required to prove the effectiveness of the antibacterial agents [45].

Statistical analyses (see Appendix A.2) showed that the original data collected through repeated measurements did not follow normal distribution, and a reduced model of linear mix-effect model was used to analyze the data as shown in Appendix A.2. In the new model, repeatedly measured data were averaged to represent the observation of each specific sample. Based on normality assumption and equal variance assumption, corresponding one-way ANOVA test was used to test difference in means between groups, the conclusions showed that: 1) both Comp A and Comp B when mixed with PEG can completely inhibit bacterial biofilm formation at 15 mg or higher level of treatment. 2) at 10 mg level of treatment, both Comp A and Comp B when mixed with PEG could reach 3 log reduction of bacteria counts, which met requirements desired level of antibacterial effectiveness. 3) Comp B showed better antibacterial effectiveness than Comp A. 4) PEG has no antibacterial effect.

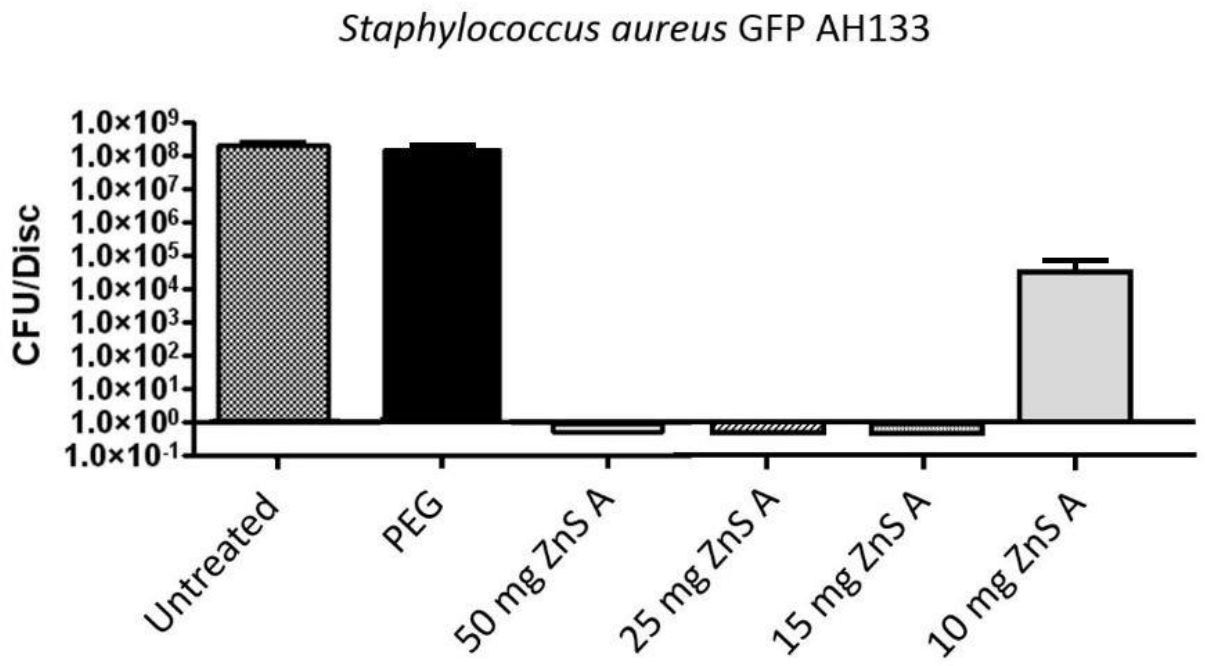

Figure 4.11: Log transformed CFU statistics for control and Comp A treatments

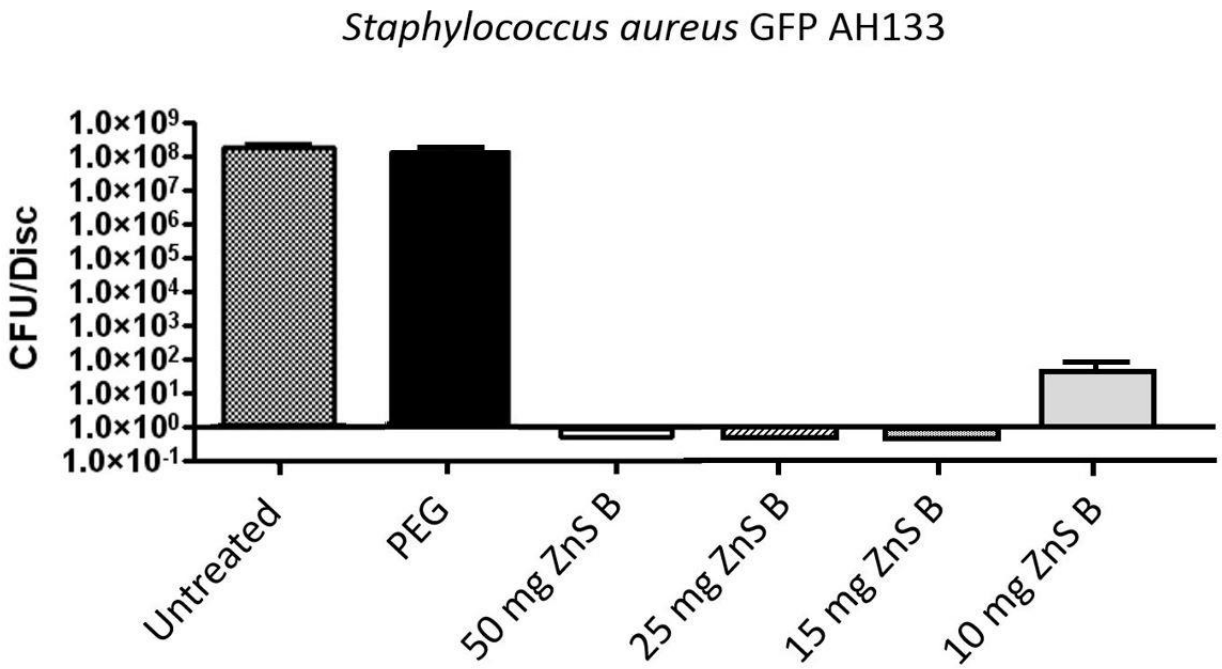

Figure 4.12: Log transformed CFU statistics for control and Comp B treatments

4.4.5 CLSM Analysis

CLSM analysis is the qualitative result of antibacterial effectiveness for different compounds. Figure 4.8 showed the results of CLSM analysis of bacteria on the biofilms after being treated with ZnS Comp A. Complying with the statistics from i*n vitro* biofilm model analysis, the untreated disks and disks with PEG controls showed that the biofilms had well developed. Due to higher concentration of ZnS, the disks with levels of 50, 25 and 15 mg ZnS treatments showed good antibacterial effectiveness, as there was no green fluorescence left under these treatment levels, indicating the biofilm forming bacteria strains were all eradicated. However, at the 10 mg level, there were obvious bacteria strains left, which indicated that the bacteria were not completely eradicated due to lower concentration of ZnS. The CLSM results aligned with the *in vitro* biofilm model quantitative analyses.

Figure 4.9 showed the results of CLSM for biofilms treated with ZnS Comp B. In this case, the results were the same under higher dosages as 50, 25 and 15 mg treatments with Comp A, all biofilms were eradicated. However, the result under dosage of 10 mg Comp B showed different result with same amount of dosage of Comp A, this difference in antibacterial properties was due to the dosage differences between treatments, which is also confirmed by other studies using ZnO or Ag [16, 46]. In the meantime, due to effect of cryomilling, Comp B showed better eradication of biofilms than Comp A under 10 mg level.

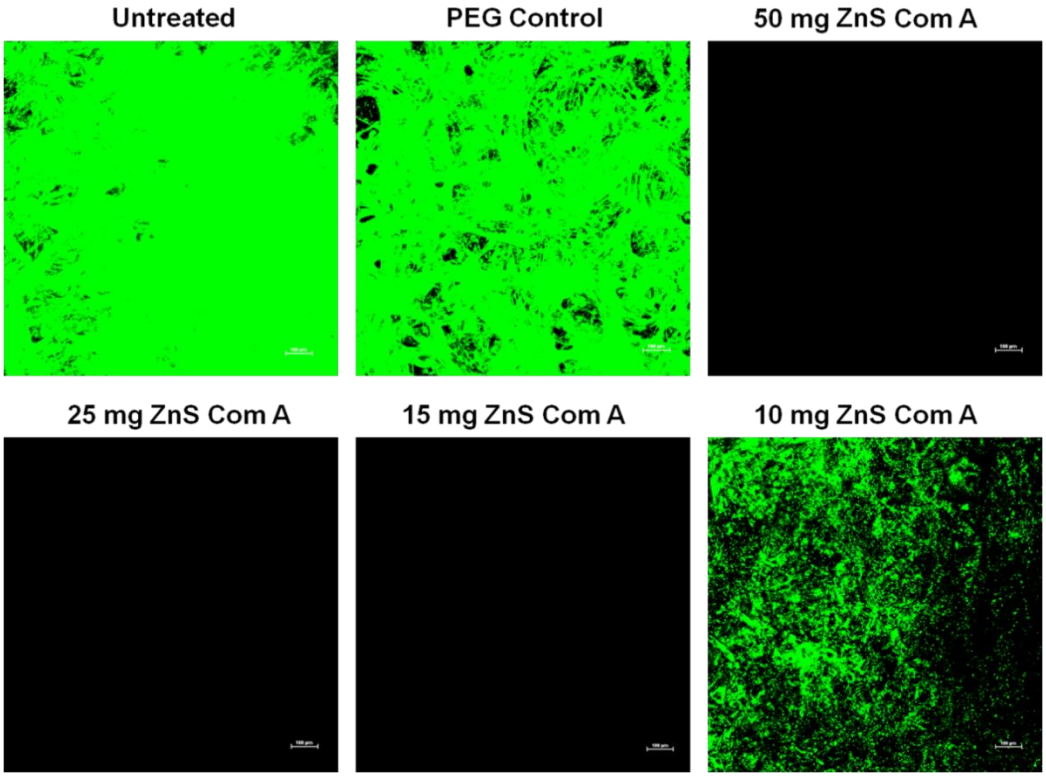

Figure 4.13: CLSM results of controls and treatments of Comp A

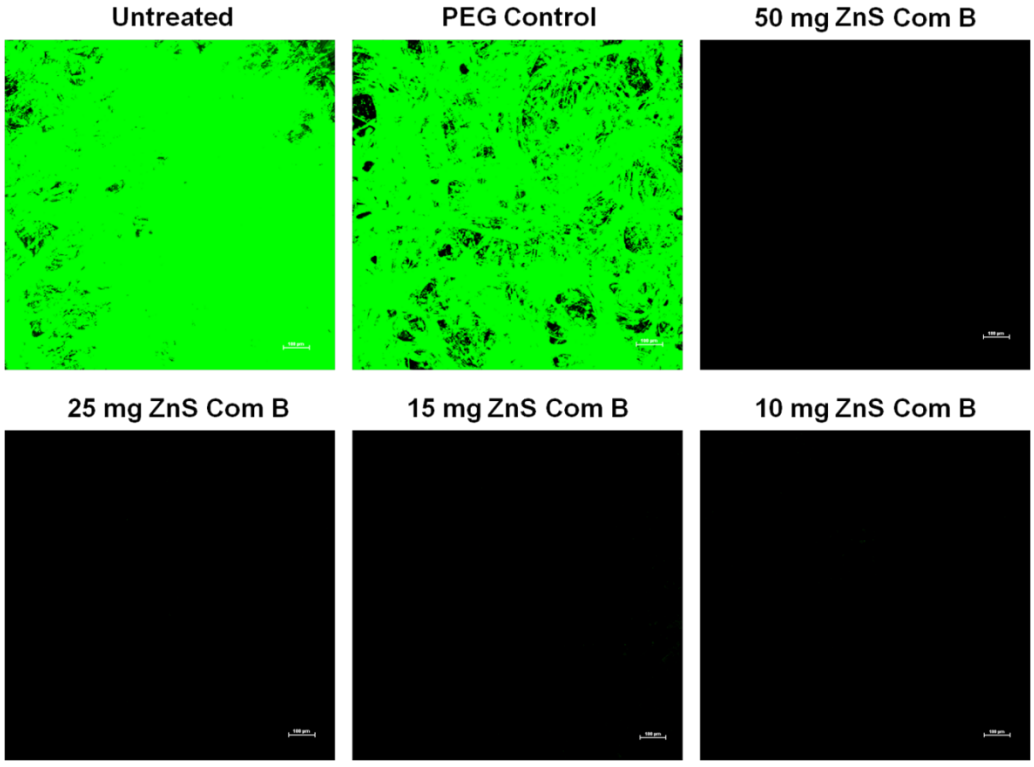

Figure 4.14: CLSM results of controls and treatments of Comp B

4.5 Discussion

The results showed that the ZnS particles possess antibacterial properties both before and after cryomilling. The antibacterial properties may be due to two different mechanisms: first is the release of zinc ions, which plays a major roles in killing the bacteria, and secondly, the direct deposition of the nanoparticles may also have an impact on cell death [47-49]. However, we see that the Comp B, which was the cryomilled sample, showed better antibacterial effectiveness than Comp A, as the decrease in particle size, which resulted in increase in surface to volume ratio, has increased the ZnS antibacterial effectiveness. It has been proven that the smaller the particle size, the better antibacterial properties the particles have due to more soluble zinc ions released from the particles [47].

Besides particle size changes, cryomilling might have introduced difference in terms of lattice constant. As sphalerite has cubic crystal structure with lattice constant *c* of 0.5404 nm [50], mechanical milling will result in a change in the crystal structure. Past research has shown that milling will result in slightly higher *c* values [51], and a lattice relaxation occurred along the axis for zinc oxide [52]. The increased *c* value has significant effect on the amount of H_2O_2 generated from the surface of the particles, which in turn helps the inhibition of bacterial growth [26, 53]. This is another possible reason that explains the better antibacterial activity of Comp B.

One possible reason for the difference between chemically synthesized and biosynthesized ZnS in terms of antibacterial properties, was the chemical composition. The chemical synthesis produced ZnS particles with white color, while the biosynthesis ZnS possessed a deep purple color. Although XRD profiles showed that the bulk compositions of both types of particles were ZnS, the XRD technique has the limitation that the presence of other phases in very low concentration and/or amorphous phases cannot be detected [54]. Studies

showed that the biosynthesized ZnS nanoparticles are usually bound to proteins [24, 55]. Other studies also showed similar results for biosynthesized silver nanoparticles [56, 57]. These proteins are either released by dead cells or generated by live cells [55], the antibacterial properties of these proteins are unknown. However, for chemically synthesized ZnS, the particles might be encapsulated by non-toxic white polymer PVP [58] based on one-pot colloidal synthesis [22]. So the properties of proteins and their organization might be the reason that caused difference in color and the difference in antibacterial properties between the chemical and biological synthesis of ZnS. However, the concentration of proteins is low [55], and the identification of the actual types of proteins attached to the ZnS needs further investigation.

The ZnS in this study was mixed with PEG ointment, which served as delivery method, however, different ways of drug delivery may also be taken into consideration for future direction of this project. As 10 mg of ZnS was mixed in 100 mg of PEG, the concentration is 9.09% wt%. One study used Sidr and Manuka honey as topical antibacterial agent to treat *S. aureus* biofilm, the concentration had to be 50% in order to be effective [59], another study used Next Science Gel mixed with PEG to treat *S. aureus* biofilm, which had concentration of 0.36% [31], one study used silver containing nanocomposites $AgNO_3$ mixed with gelatin which contained 2.5% of the materials to apply on *S. aureus* biofilm [60]. Commercially available silver nitrate cream for wound healing contains 10% of silver nitrate, hydrogen peroxide cream has 1% of H_2O_2, silver sulfadiazine cream contains 1% active ingredient, nitrofurazone cream contains 0.2% of the material [61]. By comparing with other topical antibacterial agents, the ZnS treatment in this study showed relatively high concentration, which requires more study for decreasing the concentration while retaining the antibacterial properties.

4.6 Conclusions

A novel approach of antibacterial agent for burn wound treatment has been introduced. The ZnS particles were biologically, reproducibly and economically synthesized with anaerobic sulfate reducing bacteria *Thermoanaerobacter* species. Smaller sized ZnS particles were produced by grinding original biologically synthesized ZnS under cryogenic environment for 56 min. Both types of ZnS have been proven to be statistically significant demonstrating ZnS effectiveness against common burn wound infection bacteria *Staphylococcus aureus* and its biofilm. Cryomilling decreased the original particle sizes, thus increased the surface to volume ratio. ZOI results also showed that plates treated with cryomilled ZnS samples have larger inhibition areas. Both types of ZnS, when mixed with PEG ointment showed 8 log reduction on bacteria strains left on the biofilm at level of 50, 25 and 15 mg. However, at 10 mg level, original ZnS particles mixed with PEG ointment showed approximately 3 log reduction on bacteria strains, while an approximately 7 log reduction on bacteria strains for cryomilled ZnS. Overall ZnS particles have been proven to possess antibacterial effectiveness against *Staphylococcus aureus* and cryomilling imposes a positive effect on ZnS antibacterial effectiveness.

REFERENCES

[1] J. W. ALEXANDER, "Mechanism of immunologic suppression in burn injury," *Journal of Trauma and Acute Care Surgery,* vol. 30, pp. 70-74, 1990.

[2] J. F. Hansbrough, T. O. Field Jr, M. A. Gadd, and C. Soderberg, "Immune response modulation after burn injury: T cells and antibodies," *Journal of Burn Care & Research,* vol. 8, p. 509&hyhen, 1987.

[3] N. Moss, D. Gough, A. Jordan, J. Grbic, J. Wood, M. Rodrick, *et al.*, "Temporal correlation of impaired immune response after thermal injury with susceptibility to infection in a murine model," *Surgery,* vol. 104, pp. 882-887, 1988.

[4] K. Markley, "The role of bacteria in burn mortality," *Annals of the New York Academy of Sciences,* vol. 150, pp. 922-930, 1968.

[5] S. Guo and L. A. DiPietro, "Factors affecting wound healing," *Journal of dental research,* vol. 89, pp. 219-229, 2010.

[6] R. Edwards and K. G. Harding, "Bacteria and wound healing," *Current opinion in infectious diseases,* vol. 17, pp. 91-96, 2004.

[7] B. A. Pruitt Jr, A. T. McManus, S. H. Kim, and C. W. Goodwin, "Burn wound infections: current status," *World journal of surgery,* vol. 22, pp. 135-145, 1998.

[8] J. P. Barret and D. N. Herndon, "Effects of burn wound excision on bacterial colonization and invasion," *Plastic and reconstructive surgery,* vol. 111, pp. 744-50; discussion 751-2, 2003.

[9] D. Church, S. Elsayed, O. Reid, B. Winston, and R. Lindsay, "Burn wound infections," *Clinical microbiology reviews,* vol. 19, pp. 403-434, 2006.

[10] A. A. Hammond, K. G. Miller, C. J. Kruczek, J. Dertien, J. A. Colmer-Hamood, J. A. Griswold, *et al.*, "An in vitro biofilm model to examine the effect of antibiotic ointments on biofilms produced by burn wound bacterial isolates," *Burns,* vol. 37, pp. 312-321, 2011.

[11] P. S. Stewart, "Mechanisms of antibiotic resistance in bacterial biofilms," *International Journal of Medical Microbiology,* vol. 292, pp. 107-113, 2002.

[12] P. Kennedy, S. Brammah, and E. Wills, "Burns, biofilm and a new appraisal of burn wound sepsis," *Burns,* vol. 36, pp. 49-56, 2010.

[13] S. L. Percival, K. E. Hill, S. Malic, D. W. Thomas, and D. W. Williams, "Antimicrobial tolerance and the significance of persister cells in recalcitrant chronic wound biofilms," *Wound repair and regeneration,* vol. 19, pp. 1-9, 2011.

[14] P. Stoodley, K. Sauer, D. Davies, and J. W. Costerton, "Biofilms as complex differentiated communities," *Annual Reviews in Microbiology,* vol. 56, pp. 187-209, 2002.

[15] K. E. Jones, N. G. Patel, M. A. Levy, A. Storeygard, D. Balk, J. L. Gittleman, *et al.*, "Global trends in emerging infectious diseases," *Nature,* vol. 451, pp. 990-993, 2008.

[16] J. B. Wright, K. Lam, and R. E. Burrell, "Wound management in an era of increasing bacterial antibiotic resistance: a role for topical silver treatment," *American journal of infection control*, vol. 26, pp. 572-577, 1998.

[17] H. K. Estahbanati, P. P. Kashani, and F. Ghanaatpisheh, "Frequency of Pseudomonas aeruginosa serotypes in burn wound infections and their resistance to antibiotics," *Burns*, vol. 28, pp. 340-348, 2002.

[18] J. Fong and F. Wood, "Nanocrystalline silver dressings in wound management: a review," *international Journal of Nanomedicine,* vol. 1, p. 441, 2006.

[19] L. H. Taylor, S. M. Latham, and E. Mark, "Risk factors for human disease emergence," *Philosophical Transactions of the Royal Society of London B: Biological Sciences,* vol. 356, pp. 983-989, 2001.

[20] M. E. Woolhouse and S. Gowtage-Sequeria, "Host range and emerging and reemerging pathogens," in *Ending the War Metaphor:: The Changing Agenda for Unraveling the Host-Microbe Relationship-Workshop Summary*, 2006.

[21] S. Cleaveland, M. Laurenson, and L. Taylor, "Diseases of humans and their domestic mammals: pathogen characteristics, host range and the risk of emergence," *Philosophical Transactions of the Royal Society B: Biological Sciences,* vol. 356, pp. 991-999, 2001.

[22] G. Li, J. Zhai, D. Li, X. Fang, H. Jiang, Q. Dong, *et al.*, "One-pot synthesis of monodispersed ZnS nanospheres with high antibacterial activity," *Journal of Materials Chemistry,* vol. 20, pp. 9215-9219, 2010.

[23] G. Amir, S. Fatahian, and N. Kianpour, "Investigation of ZnS Nanoparticle Antibacterial Effect," *Current Nanoscience,* vol. 10, pp. 796-800, 2014.

[24] J.-W. Moon, I. N. Ivanov, P. C. Joshi, B. L. Armstrong, W. Wang, H. Jung, *et al.*, "Scalable production of microbially mediated zinc sulfide nanoparticles and application to functional thin films," *Acta biomaterialia*, vol. 10, pp. 4474-4483, 2014.

[25] D. Witkin and E. J. Lavernia, "Synthesis and mechanical behavior of nanostructured materials via cryomilling," *Progress in Materials Science*, vol. 51, pp. 1-60, 2006.

[26] N. Salah, S. S. Habib, Z. H. Khan, A. Memic, A. Azam, E. Alarfaj, *et al.*, "High-energy ball milling technique for ZnO nanoparticles as antibacterial material," *International journal of nanomedicine*, vol. 6, p. 863, 2011.

[27] Y. Roh, S. V. Liu, G. Li, H. Huang, T. J. Phelps, and J. Zhou, "Isolation and characterization of metal-reducing Thermoanaerobacter strains from deep subsurface environments of the Piceance Basin, Colorado," *Applied and Environmental Microbiology*, vol. 68, pp. 6013-6020, 2002.

[28] T. Phelps, E. Raione, D. White, and C. Fliermans, "Microbial activities in deep subsurface environments," *Geomicrobiology Journal*, vol. 7, pp. 79-91, 1989.

[29] P. L. Tran, S. Patel, A. N. Hamood, T. Enos, T. Mosley, C. Jarvis, *et al.*, "A Novel Organo-Selenium Bandage that Inhibits Biofilm Development in a Wound by Gram-Positive and Gram-Negative Wound Pathogens," *Antibiotics*, vol. 3, pp. 435-449, 2014.

[30] C. L. Malone, B. R. Boles, K. J. Lauderdale, M. Thoendel, J. S. Kavanaugh, and A. R. Horswill, "Fluorescent reporters for Staphylococcus aureus," *Journal of microbiological methods*, vol. 77, pp. 251-260, 2009.

[31] K. G. Miller, P. L. Tran, C. L. Haley, C. Kruzek, J. A. Colmer-Hamood, M. Myntti, *et al.*, "Next science wound gel technology, a novel agent that inhibits biofilm development by gram-positive and gram-negative wound pathogens," *Antimicrobial agents and chemotherapy*, vol. 58, pp. 3060-3072, 2014.

[32] J. Hudzicki, "Kirby-Bauer disk diffusion susceptibility test protocol," *Am Soc Microbiol*, 2009.

[33] P. L. Tran, A. A. Hammond, T. Mosley, J. Cortez, T. Gray, J. A. Colmer-Hamood, *et al.*, "Organoselenium coating on cellulose inhibits the formation of biofilms by Pseudomonas aeruginosa and Staphylococcus aureus," *Applied and environmental microbiology*, vol. 75, pp. 3586-3592, 2009.

[34] P. L. Tran, N. Lowry, T. Campbell, T. W. Reid, D. R. Webster, E. Tobin, *et al.*, "An organoselenium compound inhibits Staphylococcus aureus biofilms on hemodialysis catheters in vivo," *Antimicrobial agents and chemotherapy*, vol. 56, pp. 972-978, 2012.

[35] S. Malhotra-Kumar, C. Lammens, S. Coenen, K. Van Herck, and H. Goossens, "Effect of azithromycin and clarithromycin therapy on pharyngeal carriage of macrolide-resistant streptococci in healthy volunteers: a randomised, double-blind, placebo-controlled study," *The Lancet*, vol. 369, pp. 482-490, 2007.

[36] M. Bergman, S. Huikko, M. Pihlajamäki, P. Laippala, E. Palva, P. Huovinen, *et al.*, "Effect of macrolide consumption on erythromycin resistance in Streptococcus pyogenes in Finland in 1997–2001," *Clinical Infectious Diseases*, vol. 38, pp. 1251-1256, 2004.

[37] N. M. Razali and Y. B. Wah, "Power comparisons of shapiro-wilk, kolmogorov-smirnov, lilliefors and anderson-darling tests," *Journal of Statistical Modeling and Analytics,* vol. 2, pp. 21-33, 2011.

[38] D. S. Moore and G. P. McCabe, *Introduction to the Practice of Statistics*: WH Freeman/Times Books/Henry Holt & Co, 1989.

[39] R. Peck, C. Olsen, and J. Devore, *Introduction to statistics and data analysis*: Cengage Learning, 2015.

[40] B. D. Mapstone, "Scalable decision rules for environmental impact studies: effect size, Type I, and Type II errors," *Ecological applications,* pp. 401-410, 1995.

[41] B. Leverentz, W. J. Janisiewicz, W. S. Conway, R. A. Saftner, Y. Fuchs, C. E. Sams, *et al.*, "Combining yeasts or a bacterial biocontrol agent and heat treatment to reduce postharvest decay of 'Gala'apples," *Postharvest biology and technology,* vol. 21, pp. 87-94, 2000.

[42] K. Nanda, A. Maisels, F. Kruis, H. Fissan, and S. Stappert, "Higher surface energy of free nanoparticles," *Physical review letters,* vol. 91, p. 106102, 2003.

[43] W. Bremser, "Buchbesprechung: Organic Coatings–Science and Technology–Third Edition. Von ZW Wicks Jr., FN Jones, SP Pappas, DA Wicks," *Chemie Ingenieur Technik,* vol. 80, pp. 236-236, 2008.

[44] J. Jiang, G. Oberdörster, and P. Biswas, "Characterization of size, surface charge, and agglomeration state of nanoparticle dispersions for toxicological studies," *Journal of Nanoparticle Research,* vol. 11, pp. 77-89, 2009.

[45] S. Bloomfield, R. Baird, R. Leak, and R. Leech, "Microbial Quality Assurance in Pharmaceuticals," *Cosmetics and Toiletries, Ellis Horwood Ltd,* 1988.

[46] Z. Emami-Karvani and P. Chehrazi, "Antibacterial activity of ZnO nanoparticle on gram-positive and gram-negative bacteria," *Afr J Microbiol Res,* vol. 5, pp. 1368-1373, 2011.

[47] K. R. Raghupathi, R. T. Koodali, and A. C. Manna, "Size-dependent bacterial growth inhibition and mechanism of antibacterial activity of zinc oxide nanoparticles," *Langmuir,* vol. 27, pp. 4020-4028, 2011.

[48] N. M. Franklin, N. J. Rogers, S. C. Apte, G. E. Batley, G. E. Gadd, and P. S. Casey, "Comparative toxicity of nanoparticulate ZnO, bulk ZnO, and ZnCl2 to a freshwater microalga (Pseudokirchneriella subcapitata): the importance of particle solubility," *Environmental Science & Technology,* vol. 41, pp. 8484-8490, 2007.

[49] A. Lipovsky, Z. Tzitrinovich, H. Friedmann, G. Applerot, A. Gedanken, and R. Lubart, "EPR study of visible light-induced ROS generation by nanoparticles of ZnO," *The Journal of Physical Chemistry C,* vol. 113, pp. 15997-16001, 2009.

[50] G. Engel and R. Needs, "Calculations of the structural properties of cubic zinc sulfide," *Physical Review B,* vol. 41, p. 7876, 1990.

[51] D. Bao, H. Gu, and A. Kuang, "Sol-gel-derived c-axis oriented ZnO thin films," *Thin solid films,* vol. 312, pp. 37-39, 1998.

[52] H. Maki, N. Ichinose, N. Ohashi, H. Haneda, and J. Tanaka, "The lattice relaxation of ZnO single crystal (0001) surface," *Surface science,* vol. 457, pp. 377-382, 2000.

[53] O. Yamamoto, M. Komatsu, J. Sawai, and Z.-e. Nakagawa, "Effect of lattice constant of zinc oxide on antibacterial characteristics," *Journal of materials science: materials in medicine,* vol. 15, pp. 847-851, 2004.

[54] B. P. Barbero, J. A. Gamboa, and L. E. Cadús, "Synthesis and characterisation of La 1− x Ca x FeO 3 perovskite-type oxide catalysts for total oxidation of volatile organic compounds," *Applied Catalysis B: Environmental,* vol. 65, pp. 21-30, 2006.

[55] J. W. Moreau, P. K. Weber, M. C. Martin, B. Gilbert, I. D. Hutcheon, and J. F. Banfield, "Extracellular proteins limit the dispersal of biogenic nanoparticles," *Science,* vol. 316, pp. 1600-1603, 2007.

[56] A. M. Fayaz, K. Balaji, M. Girilal, R. Yadav, P. T. Kalaichelvan, and R. Venketesan, "Biogenic synthesis of silver nanoparticles and their synergistic effect with antibiotics: a study against gram-positive and gram-negative bacteria," *Nanomedicine: Nanotechnology, Biology and Medicine,* vol. 6, pp. 103-109, 2010.

[57] N. Durán, P. D. Marcato, M. Durán, A. Yadav, A. Gade, and M. Rai, "Mechanistic aspects in the biogenic synthesis of extracellular metal nanoparticles by peptides, bacteria, fungi, and plants," *Applied microbiology and biotechnology,* vol. 90, pp. 1609-1624, 2011.

[58] G. Ghosh, M. K. Naskar, A. Patra, and M. Chatterjee, "Synthesis and characterization of PVP-encapsulated ZnS nanoparticles," *Optical Materials,* vol. 28, pp. 1047-1053, 2006.

[59] T. Alandejani, J. Marsan, W. Ferris, R. Slinger, and F. Chan, "Effectiveness of honey on Staphylococcus aureus and Pseudomonas aeruginosa biofilms," *Otolaryngology--Head and Neck Surgery,* vol. 141, pp. 114-118, 2009.

[60] V. Rattanaruengsrikul, N. Pimpha, and P. Supaphol, "In vitro efficacy and toxicology evaluation of silver nanoparticle-loaded gelatin hydrogel pads as antibacterial wound dressings," *Journal of Applied Polymer Science,* vol. 124, pp. 1668-1682, 2012.

[61] B. A. Lipsky and C. Hoey, "Topical antimicrobial therapy for treating chronic wounds," *Clinical infectious diseases,* vol. 49, pp. 1541-1549, 2009.

CHAPTER 5.

GENERAL CONCLUSIONS

5.1 Conclusions

This thesis has summarized literature on burn wound healing and treatments, as well as information on ZnS properties and its synthesis. The major part of this thesis demonstrates the study of ZnS effectiveness as antibacterial substance for burn wound healing. Based on this study, a novel approach of antibacterial agent for burn wound treatment has been introduced. The ZnS particles (Comp A) were biologically, reproducibly and economically synthesized with anaerobic metal-reducing *Thermoanaerobacter* species. Cryomilled ZnS particles (Comp B) were successfully produced by grinding original biologically synthesized ZnS particles under cryogenic environment for 56 min. The conventional chemical one-pot colloidal synthesis was also conducted, both as-synthesized ZnS (Comp C) and further cryomilled ZnS (Comp D) were evaluated. In comparison, Comp C did not show antibacterial properties against *S. aureus*, but cryomilled sample Comp D showed very good antibacterial properties. Both Comp A and Comp B have been proven to have significant effectiveness against common burn wound infection bacteria *S. aureus*. Cryomilling decreased the original particle sizes by order of about 3000, which has significantly increased the surface to volume ratio. ZOI results have also proved that Comp B has larger inhibition areas than Comp A. Both Comp A and B, when mixed with PEG ointment showed 8 log reduction on bacteria strains left on the biofilm at level of 50, 25 and 15 mg when applied on area of diameter of 6 mm. However, the ZnS particles mixed with PEG ointment showed approximately 3.5 log reduction on bacteria strains at level of 10 mg for Comp A, while a 7 log reduction on bacteria strains for Comp B. Overall ZnS particles have been

proven to possess antibacterial effectiveness and cryomilling imposes an positive effect on ZnS antibacterial effectiveness.

5.2 Review of Contributions

ZnS possess antibacterial properties against *S. aureus* and cryomilling as a fabrication process has improved the ZnS antibacterial effectiveness. In a world of infections with more drug resistance, the new drug of ZnS can have high potential of application.

5.3 Future Perspectives

In order to further understand the characteristics antibacterial properties of the material: 1) *In vivo* studies are necessary to examine the effectiveness of ZnS on animals and humans with *S. aureus* infections. 2) As this study has proven the effectiveness of ZnS only on gram-positive bacteria *S. aureus*, more studies on other microorganisms like gram-negative bacteria and fungi are in order. 3) Further investigation on cryomilling is also necessary to study ZnS antibacterial effectiveness based on gradually increased cryomilling time. 4) Lastly, a study identifying how surface composition could make a difference in terms of antibacterial properties needs to be developed.

APPENDIX A.

STATISTICAL ANALYSES OF ZNS ANTIBACTERIAL TESTS

Appendix A summarizes all the details of statistical analyses for section 4.4.3 and 4.4.4 in terms of derivations, assumptions, validations and tests. A.1 provides detailed explanation of statistical analyses for ZOI assay, and A.2 provides detailed explanation of statistical analyses for *in vitro* biofilm model CFU analyses.

A.1 Statistical analyses for ZOI assay

There were three samples in each treatment group, they were all tested under the same condition within each group, so the diameters of ZOI in each treatment group were expected to have the same distribution. By following the ZOI assay protocol, the ZnS treatments were placed on the bacterial lawn at least 24 mm (center to center) away from each other [185]. Also, according to Figures 4.4 and 4.5, there was no overlap between each of the two inhibition zones, so that each sample was expected to be independent from the other, and the assumption was made that the observed diameters of the inhibition zones under each treatment were independent and identically distributed random variables, they were denoted as Y_{Ai} and Y_{Bi} (i = 1, 2, 3). Figure A.1 showed the distributions of the data points, and their corresponding normal quantile plots of the two treatment groups. For small sample size, Shapiro-Wilk W test has higher power by comparison to other normality test [192], thus is usually used to test normality of the data, and the corresponding null hypothesis was that the samples were from normally distributed population. The test using JMP software revealed p values of 0.7470 and 0.8777 for Comp A and Comp B ZOI assay data respectively (See Appendix B.1 for calculation procedure for Shapiro-Wilk W test), which failed to reject the null hypothesis.

In this test, the sample size was very small (n = 3), the power was very low, usually not higher than 0.2 given the sample size [192, 193]. However, according to the data collected in database of European Society of Clinical Microbiology and Infectious Diseases, the distributions of ZOI diameters from antibacterial tests on S. aureus using antibiotics are basically normal [194], thus researchers usually assume that the distributions of ZOI diameters are normal [195-197]. Given that the Shapiro-Wilk W tests revealed the same results, the corresponding Student's *t* tests can be used to statistically evaluate the difference in means as Student's *t* test assumes normality of the data.

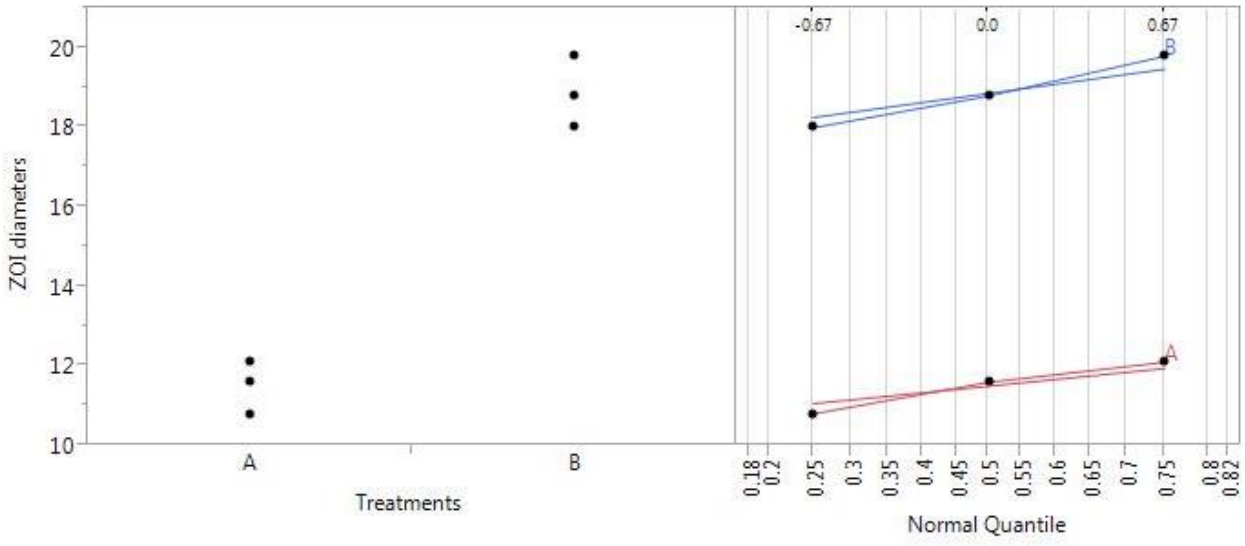

Figure A.1: ZOI statistics and normal quantile plots

In order to compare difference between ZOI results under two different treatments, assumption of equal variances is needed to perform a Student's *t* test. A two-sided *F*-test at 0.95 confidence level was performed to check the equal variance of the two sample groups with the null hypothesis being that the variances of the two groups were equal. The test showed the *p* value 0.6917 (See Appendix B.2 for calculation procedures for two-sided *F* test). As *p* value was

larger than the designated Type I error rate 0.05, the null hypothesis was not rejected, thus conclusion was made that the variances were equal between the two groups. Still, the sample size was very small, there might not be enough power for the test, however, equal variance is usually assumed and the Student's *t*-test is used [195, 198].

In order to test the difference between the means of ZOI diameters under Comp A and Comp B treatments, a right-tail Student's *t*-test assuming equal variance was performed at 0.95 confidence level with pooled variance. Let μ_A and μ_B denote the true means of diameter of ZOI under 50 mg treatment of Comp A and Comp B respectively. In antibacterial ZOI test, the larger ZOI diameter indicates better antibacterial properties [185]. Thus the test was based on the following null and alternative hypotheses:

$$H_0: \mu_A = \mu_B \tag{A.1}$$

$$H_a: \mu_A < \mu_B \tag{A.2}$$

The result showed a p value of 0.0002 (See appendix B.3 for calculation procedures of Student's t test), which was smaller than the designated Type I error rate 0.05, thus the null hypothesis was rejected and this concluded that 50 mg Comp B treatment had significantly better antibacterial properties than 50 mg Comp A treatment based on ZOI assays.

In conclusion, based on the assumptions of normal distribution and equal variance, the Student's *t*-test showed that there was significant difference between the two treated groups and Comp B had better antibacterial properties than Comp A based on ZOI assays.

A.2 Statistical analyses for In vitro biofilm model CFU analyses

As stated in Section 4.4.4, requirement of minimum of 99.9% of bacteria reduction needs to be reached in order to be considered as effective [199], which can be expressed in Equation A.3, where μ_{before} denotes true mean CFU value left on the disk before treatment and μ_{after}

denotes true mean CFU value left on the disk after treatment. Equations A.4 and A.5 were the arithmetic derivations from Equation A.3.

$$\mu_{before}/\mu_{after} > 1000 \quad (A.3)$$

$$\lg(\mu_{before}/\mu_{after}) > \lg(1000) \quad (A.4)$$

$$\lg(\mu_{before}) - \lg(\mu_{after}) > 3 \quad (A.5)$$

Equation A.3 and Equation A.5 are mathematically equivalent, in the 10 log transformed data, requirement of a minimum of 99.9% reduction (3 log reduction) is equivalent to the difference of true means being larger than 3 between before and after treatment groups. Based on the calculations, the log transformed raw data can be used instead of raw data. For the convenience of analyses and notation, the transformed data were referred as original data here and after while the non-transformed data were referred as raw data here and after.

All groups were tested independently, and due to the nature of the experiment each disk was washed and biofilm destroyed in order to count the CFU. There was no paring between each two groups. PEG was used as carrier material to immobilize the ZnS particles on the disks. PEG had nonmeasureable effectiveness [182]. Also, as ZnS is not soluble in nature, while PEG is hydrophilic with low melting point (4 – 8 °C) [200], mixing ZnS with PEG promoted an even diffusion of metal ions [182, 201]. However, studies have reported that PEG as a carrier material, when mixed with ZnO or Ag nanoparticles, does not show enhancement of antibacterial properties than testing the nanoparticles alone in suspension state, due to the reason that when these particles are in suspension, the antibacterial substances, like metal ions, can diffuse evenly without promotion of PEG [202-204]. As ZnS mixed with PEG as a whole was considered as the treatment, in this experiment, the antibacterial properties were reported on ZnS mixed with PEG,

but the discussion of mechanisms that cause the difference in antibacterial properties was based on differences between Comp A and Comp B.

Under 15 mg to 50 mg levels of Comp A and Comp B treatments, all bacteria were completely eradicated. The raw data of CFU values for these samples were all 0, and there were no variances associated with these groups. This showed that 15 mg to 50 mg of ZnS Comp A and Comp B were able to completely inhibit biofilm formation due to higher drug concentrations [205]. However, the 10 mg treatment groups for both Comp A and Comp B, untreated groups and PEG treated groups had bacteria strains left on the disks due to insufficient ZnS concentration, statistical analyses were needed to evaluate the differences between these groups.

For the convenience of analyses, the untreated group was referred as the "Control" group, the PEG group as Treatment 1, the 10 mg Comp A group as Treatment 2, and the 10 mg Comp B group as Treatment 3 here and after.

Each treatment group had three samples, there was variance associated between samples. Each CFU measurement from each sample was repeated three times to get more accurate data, there was also variance associated between readings. Considering variance between samples and variance within measurements, linear mixed effect model is appropriate to fit this situation as it allows combination of regression methods while accounting for the repeated measures of the data [206, 207]. A linear mixed effect model can be expressed using the equation A.6 [208]:

$$\boldsymbol{y} = \boldsymbol{X\beta} + \boldsymbol{Zu} + \boldsymbol{\epsilon} \tag{A.6}$$

In equation A.6, $\boldsymbol{y}$ is a known vector of observations, with $E(\boldsymbol{y}) = \boldsymbol{X\beta}$, $\boldsymbol{\beta}$ is an unknown vector of fixed effects. As each treatment has only one level, thus $\boldsymbol{\beta}$ contains only main effects of different treatments, and statistical inferences were made through comparing contrasts of main effects. $\boldsymbol{u}$ is an unknown vector of random effects, with mean $E(\boldsymbol{u}) = \mathbf{0}$ and

variance-covariance matrix var($\boldsymbol{u}$) = $\boldsymbol{G}$. In this experiment, there was only one random variable for each observation in vector $\boldsymbol{u}$ which denotes the variance between samples in the same treatment, so that there was no covariance in this matrix. $\boldsymbol{\epsilon}$ is unknown vector of random errors, with mean $E(\boldsymbol{\epsilon})$ = $\mathbf{0}$ and variance var($\boldsymbol{\epsilon}$) = $\boldsymbol{R}$. Assumption was made that cov($\boldsymbol{u}$, $\boldsymbol{\epsilon}$) = $\mathbf{0}$, as variance between samples and variance within measurements are usually assumed to be independent from each other [208]. This equation can be expressed as equation A.7 to address this experiment design for each single observation:

$$y_{ijk} = \mu + \alpha_i + u_{ij} + e_{ijk} \tag{A.7}$$

where i = 1 … 4 (4 groups), j = 1 … 3 (3 samples in each group), k = 1 … 3 (3 repeated measurements for each sample). Initially assumptions associated with this model are made that u_{ij} are i.i.d. and follow $D_1(0, \sigma_u^2)$ distribution. Also e_{ijk} are i.i.d. and follow $D_2(0, \sigma_e^2)$ distribution, u_{ij} and e_{ijk} are independent from each other, thus y_{ijk} are i.i.d. and follow $D_3(\mu + \alpha_i, \sigma_u^2 + \sigma_e^2)$ distribution. D_i stands for a certain distribution (normal or otherwise).

To apply ANOVA analyses requires normality of the data, so that u_{ij} and e_{ijk} need to follow normal distributions, it true, y_{ijk} should also follow normal distribution. In order to test whether assumption $y_{ijk} \sim N(\mu + \alpha_i, \sigma_u^2 + \sigma_e^2)$ could be used, Shapiro-Wilk W test at 0.95 confidence level was employed to test the normality of the data. The null hypothesis for this test was that the data were sampled from normally distributed population. As α_i are fixed effect, and are different between treatments, the normality was tested separately for data collected under each treatment group. Figure A.2 summarized the distributions of all observations and their corresponding box plots and normal quantile plots. Based on JMP analysis results, Table A.1 summarized the p values for each group:

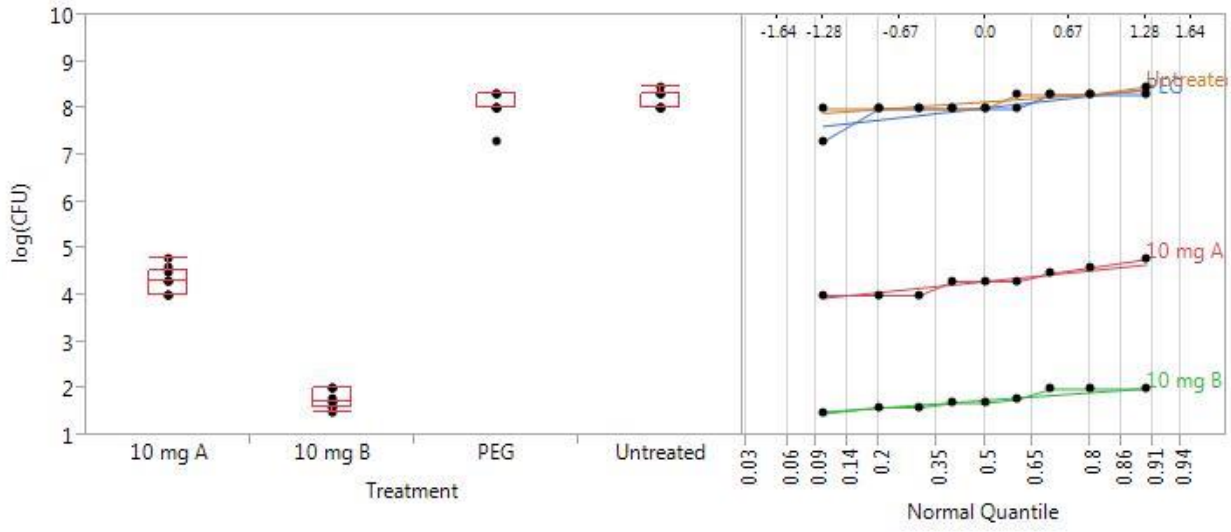

Figure A.2: Observed CFU statistics for different treatments with normal quantile plots and box plots

Table A.1: Normality tests results for all observations in different treatment groups

Groups	Control	Treatment 1	Treatment 2	Treatment 3
p value	0.0065	0.0038	0.2570	0.1642

As *p* values for Control and Treatment 1 groups were smaller than the designated Type I error rate 0.05, the null hypotheses that data from Control and Treatment 1 groups were sampled from normally distributed populations were rejected. However, for Treatment 2 and 3 groups, they had *p* values higher than the designated Type I error rate 0.05, the null hypotheses were not rejected.

The typical methods of dealing with non-normal data for the convenience of analysis is applying transformations [209]. Different transformations were used in attempt to obtain normal distribution for Control and Treatment 1 groups, and the normality of the transformed data were also evaluated using Shapiro-Wilk W tests at 0.95 confidence level. Based on the results, the common transformations were unable to transform the data of Control and Treatment 1 into

normally distributed data as their corresponding *p* values were all still below the designated Type I error rate 0.05, and the null hypotheses were rejected. Table A.2 summarized the *p* values for each group after transformations. As a result, the transformations were not employed and the analyses would still be based on original data.

Table A.2: Normality tests results for different transformation methods

Transformation	Groups	Control	Treatment 1	Treatment 2	Treatment 3
Log	*p* value	0.0063	0.0028	0.2509	0.2162
Square Root	*p* value	0.0064	0.0032	0.2549	0.1901
Reciprocal	*p* value	0.0061	0.0020	0.2375	0.2635
Box-Cox	*P* value	0.0060	0.0050	0.2183	0.2264

As the test results indicated, the assumption that $y_{ijk} \sim N(\mu + \alpha_i, \sigma_u^2 + \sigma_e^2)$ could not be used as normality was not proven. Hence derivations from equation A.7 were shown below to reduce the original model (*K* stands for number of repetition and is equal to 3):

$$\overline{y}_{ij\cdot} = \frac{1}{K}\sum_{k=1}^{K} y_{ijk} = \frac{1}{K}\sum_{k=1}^{K}\left(\mu + \alpha_i + u_{ij} + e_{ijk}\right) = \mu + \alpha_i + u_{ij} + \frac{1}{K}\sum_{k=1}^{K} e_{ijk} \qquad (A.8)$$

Let $\theta_{ij} = u_{ij} + \frac{1}{K}\sum_{k=1}^{K} e_{ijk}$, the equation A.8 can be rewritten as:

$$\overline{y}_{ij\cdot} = \mu + \alpha_i + \theta_{ij} \qquad (A.9)$$

As u_{ij} are i.i.d. and follow $D_1(0, \sigma_u^2)$ distribution, also e_{ijk} are i.i.d. and follow $D_2(0, \sigma_e^2)$ distribution, u_{ij} and e_{ijk} were independent, so that:

$$\mathrm{var}\left(\overline{y}_{ij\cdot}\right) = \mathrm{var}(\theta_{ij}) = \mathrm{var}(u_{ij}) + \mathrm{var}\left(\frac{1}{K}\sum_{k=1}^{K} e_{ijk}\right) = \sigma_u^2 + \frac{1}{K^2}\cdot K\sigma_e^2 = \sigma_u^2 + \sigma_e^2/K \quad (A.10)$$

So $\overline{y}_{ij\cdot}$ were also i.i.d. and follow $D_4(\mu + \alpha_i, \sigma_u^2 + \sigma_e^2/K)$ distribution. In this case, the linear mixed-effect model has been reduced to a simple linear model, and the new observations became the averaged repeated measurements in each sample. As ANOVA analysis based on this model also requires normality of the data, the Shapiro-Wilk W tests were performed to check normality of averaged observations of each sample.

Figure A.3 showed the distributions of the original data for the reduced model and their corresponding normal quantile plots.

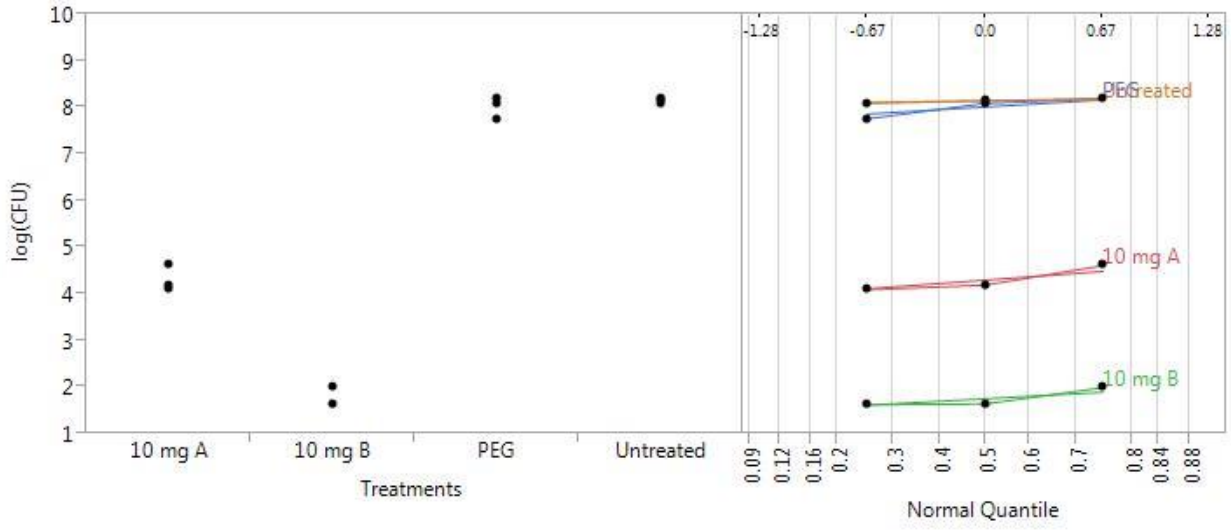

Figure A.3: Averaged CFU statistics for different treatments and normal quantile plots

Based on the normal quantile plots, log(CFU) data for all 4 groups all scattered approximately on a straight line. In order to statistically test the normality of the data, the Shapiro-Wilk W test for each treatment group at 0.95 confidence level was performed. The null hypothesis for this test was that the data were sampled from normally distributed population. Based on JMP analysis results, Table A.3 summarized the *p* values of normality test for each group:

Table A.3: Normality tests results for averaged statistics for different treatment groups

Groups	Control	Treatment 1	Treatment 2	Treatment 3
p value	0.8877	0.4256	0.3502	0.0789

Based on the test results, all *p* values were greater than the designated Type I error rate 0.05, so the null hypotheses that these data were sampled from normally distributed populations were not rejected. But it is important to see that in this experiment, the sample size was very small, which might not give enough power for the test, in another word, the Type II error rate might be very high. Type II error by definition means the failure to reject a false null hypothesis [209], which in this Shapiro-Wilk W test means the original data actually did not follow normal distribution. However, many researchers have studied the distribution of CFU data for microorganisms, as bacteria grow and die exponentially, when logarithms are used, a log-normal distribution of micro-organisms is assumed to be approximately correct, and the logarithms of data can be used to obtain mean log count and standard deviation to describe the distribution [210-213]. Thus the null hypotheses were accepted and the assumptions that the four different groups were sampled from normally distributed populations were used here and after. Thus $\overline{y}_{ij\cdot} \sim N(\mu + \alpha_i, \sigma_u^2 + \sigma_e^2/K)$ were assumed, and the reduced model shown in equation A.9 could be used for further analysis.

First the test of equal variance needs to be conducted for the ANOVA analysis. In order to test among four groups, Levene's test, Hartley's test or Bartlett's test can be employed. However, among them, Levene's test is robust and less sensitive to departure from normality [214], and was chosen to test equal variance with the null hypothesis that the four sample groups had equal variance. Using JMP software, the test revealed a *p* value of 0.1072 (See Appendix B.4

for calculation procedures for Levene's test), which is higher than the designated Type I error rate 0.05, so the null hypothesis was not rejected, and conclusion could be made that the four groups had equal variance.

As stated above, the data collected in each group followed normal distribution, and equal variance was proven across the groups. One-way ANOVA could be performed to check if there was significant difference between the treatment groups with null hypothesis being that there was no difference between the means of each group (See Appendix B.5 for calculation procedures for ANOVA). Table A.4 showed the results for ANOVA.

Table A.4: ANOVA analysis table

Source	d.f.	Sum of Squares	Mean Squares	*F*	*p*
Treatment	3	86.341466	28.7805	667.9085	< 0.0001
Error	8	0.344724	0.0431		
Total	11	86.686190			

The result revealed a *p* value of < 0.0001, which is smaller than the designated Type I error rate 0.05, so the null hypothesis was rejected, thus there were significant differences between groups.

PEG was used to carry the ZnS for burn wound healing, whether PEG has antibacterial properties needed to be confirmed, thus contrast between Control and Treatment 1 was tested. To check if Comp A and Comp B could reach desired antibacterial effectiveness (3 log reduction), comparisons needed to be made between Control group and Treatment 2 and 3 groups respectively. Lastly, comparison needed to be made between Treatment 2 and 3 groups to determine if cryomilling had impact on antibacterial effectiveness. So altogether there were four multiple comparisons needed to be made to establish the antibacterial effectiveness of ZnS mixed with PEG. However, multiple comparisons will increase the Type I error rate if we

maintain 0.05 Type I error rate for each individual test, thus the Bonferroni correction could be used to control the family wise error rate to at most 0.05 [209, 215]. There were 4 different comparisons, thus the individual error rate is 0.0125 as calculated in equation A.11 and this corrected Type I error rate would be used for the four multiple comparisons mentioned above.

$$\alpha_I = \frac{\alpha_E}{m} = \frac{0.05}{4} = 0.0125 \tag{A.11}$$

First the difference between Control group and Treatment 1 group was compared. The null hypothesis was that the two groups had no difference in terms of group means, which can be shown in the following form (Let $\mu_{control}$ and μ_{PEG} denote the true means of log(CFU) values under Untreated and PEG groups respectively):

$$H_0: \mu_{control} = \mu_{PEG} \tag{A.12}$$

$$H_a: \mu_{control} \neq \mu_{PEG} \tag{A.13}$$

Using two-sided Student's *t* test, it revealed a *p* value of 0.3892, which was larger than the corrected Type I error rate, so the null hypothesis was not rejected, thus conclusion could be made that the PEG had no antibacterial properties.

Secondly the difference between Control group and Treatment 2 groups was compared. In order to test if 10 Comp A with PEG has reached desired antibacterial level (3 log reduction), the null hypothesis can be expressed as follows (Let μ_{PEG} and μ_A denote the true means of log(CFU) values under Control and 10 mg Comp A groups respectively):

$$H_0: \mu_{control} - \mu_A = 3 \tag{A.14}$$

$$H_a: \mu_{control} - \mu_A > 3 \tag{A.15}$$

Using right-tailed Student's *t* test, it revealed a *p* value of 0.0032, which is smaller than the corrected Type I error rate 0.0125, so the null hypothesis was rejected, thus conclusion could

be made that 10 mg Comp A with PEG has reached desired antibacterial effectiveness of 3 log reduction.

Using the same procedure, the difference between Control and Treatment 3 groups was tested. The right-tailed Student's *t* test revealed a *p* value of < 0.0001, which is also smaller than the corrected Type I error rate 0.0125, so the null hypothesis was rejected. Thus the conclusion could be made that 10 mg Comp B with PEG has also reached desired antibacterial effectiveness of 3 log reduction.

In order to approximately determine the actual antibacterial effectiveness, the subtraction of means between groups is usually used to measure the log reduction [216-218]. For Control group, the mean value for the original data was 8.1522, while the Treatment 2 group had an average value of 4.3067. The subtraction of these two value yielded a value of 3.8455 log reduction, which is equivalent to 99.98573% reduction of bacteria.

Treatment 3 group had an average value of 1.7619. The subtraction between this value and Control group yielded a value of 6.3903 log reduction, which is equivalent to 99.99996% reduction of bacteria.

So far the statistical analyses have proven that 10 mg of treatments of both Comp A and Comp B could both reach a desired level of antibacterial effectiveness, and then difference in antibacterial effectiveness of Comp A and Comp B themselves needed to be evaluated. Let μ_A and μ_B denote the true means of log(CFU) values under Treatment 2 and 3 respectively, as fewer CFU counts mean better antibacterial effectiveness, the test was based on the following null and alternative hypotheses:

$$H_0: \mu_A = \mu_B \tag{A.16}$$

$$H_a: \mu_A > \mu_B \tag{A.17}$$

Using right-tailed Student's *t* test, the analysis revealed a *p* value of 0.0001, which was smaller than the corrected Type I error rate 0.0125, thus the null hypothesis was rejected and this concluded that Comp B had significantly better antibacterial properties than Comp A. This result also matched with the ZOI result as stated in section 4.4.3.

Based on the analyses above, the following conclusions could be drawn: 1) both Comp A and Comp B when mixed with PEG can completely inhibit bacterial biofilm formation at 15 mg or higher level of treatment. 2) at 10 mg level of treatment, both Comp A and Comp B when mixed with PEG could reach desired level of antibacterial effectiveness. 3) Comp B showed better antibacterial effectiveness than Comp A. 4) PEG has no antibacterial effect.

APPENDIX B.

ALGORITHMS FOR RELATED STATISTICAL TESTS

This appendix is used to provide support information of calculation procedures for all statistical tests involved in Appendix A.

B.1 Shapiro-Wilk *W* Normality Test Calculations

Shapiro-Wilk W test is used for test normality of the data set with null hypothesis being that the observed data follow normal distribution. The test statistic is calculated using equation B.1 [219].

$$W_t = \frac{\left(\sum_{i=1}^{n} a_i x_{(i)}\right)^2}{\sum_{i=1}^{n}(x_i - \bar{x})^2} \tag{B.1}$$

First we sort the data in ascending order, in this equation, $x_{(i)}$ is the i^{th} ordered statistic of the entire data set, $\bar{x}$ is the mean of all statistics. a_i comes from a data set as shown in equation B.2:

$$(a_1, \cdots, a_n) = \frac{\boldsymbol{m}^{\mathrm{T}}\boldsymbol{V}^{-1}}{\sqrt{\boldsymbol{m}^{\mathrm{T}}\boldsymbol{V}^{-1}\boldsymbol{V}^{-1}\boldsymbol{m}}} \tag{B.2}$$

In B.2, $\boldsymbol{m}$ is defined as B.3:

$$\boldsymbol{m} = (m_1, \cdots, m_n)^{\mathrm{T}} \tag{B.3}$$

In B.3, m_i are the expected values of the ordered statistics of i.i.d. random variables sampled from the standard normal distribution, and $\boldsymbol{V}$ from equation B.2 is the covariance matrix of the ordered statistics.

Test statistic W_t as well as sample size will be used to look up Shapiro-Wilk tables to find the matching *W* value, and the corresponding *p* value is used to compare with predefined Type I error rate 0.05.

B.2 Two-sided *F* Test Calculations

Assuming normality of the data set, two-sided *F* test can be used to test equal variance of two data sets with null hypothesis being there is no difference in variance between two groups. The test statistic is shown as equation B.4 (null hypothesis being variances are equal, thus $\sigma_1^2 = \sigma_2^2$) [209]:

$$F_t = \frac{s_1^2/\sigma_1^2}{s_2^2/\sigma_2^2} = \frac{s_1^2}{s_2^2} \tag{B.4}$$

Test statistic F_t follows *F* distribution with $df_1 = n_1 - 1$, and $df_2 = n_2 - 1$, where n_1 and n_2 are the sample sizes for two data sets. The more F_t statistic deviates from 1, the stronger evidence that the variances are not equal. The test statistic F_t and two df's are used to look up in *F* distribution table to find matching *F* value, and the corresponding *p* value is the possibility of *F* value greater than F_t, this value is used to compare with predefined Type I error rate 0.05.

B.3 Student's *t* Test Calculations

Assuming normality and equal variance, the Student's *t* test can be used to test the difference in means for two data sets with null hypothesis being there is no difference in means between two groups. The test statistic is shown as equation B.5 [209]:

$$t_t = \frac{Z}{s/\sqrt{n}} = \frac{\bar{X}_1 - \bar{X}_2}{s_{X_1X_2}/\sqrt{n}} \quad \text{(B. 5)}$$

In equation B.5, $\bar{X}_1$ and $\bar{X}_2$ are the means of the two data sets, $s_{X_1X_2}$ is the pooled standard deviation as shown in equation B.6:

$$s_{X_1X_2} = \sqrt{s_1^2 + s_2^2} \quad \text{(B. 6)}$$

In equation B.6, s_1^2 and s_2^2 are the variances of the two data sets.

Test statistic t_t follows *t* distribution with $df = n_1 + n_2 - 2$. For left sided Student's *t* test, $-t_t$ and df are used to look up in the *t* distribution table to find matching *t* value, and the corresponding *p* value is the possibility of absolute value of actual difference can be larger than $-t_t$, this value is used to compare with predefined Type I error rate 0.05. For right sided Student's *t* test, t_t and df are used to look up in the *t* distribution table to find matching *t* value, and the corresponding *p* value is the possibility of actual difference can be larger than t_t, this is used to compare with predefined Type I error rate 0.05. For two sided Student's *t* test, the absolute value of t_t and df are used to look up in the *t* distribution table to find matching *t* value, and the corresponding *p* value is the two times of possibility of actual difference being larger than absolute value of t_t, this value is compare with predefined Type I error rate 0.05.

B.4 Levene's *F* Test Calculations

Levene's test is an inferential statistic used to assess the equality of variances for two or more groups [220], with null hypothesis being there is no difference in variances between groups. The test statistic is shown as in equation B.7:

$$W_t = \frac{(N-k)}{(k-1)} \frac{\sum_{i=1}^{k} N_i (Z_{i\cdot} - Z_{\cdot\cdot})^2}{\sum_{i=1}^{k} \sum_{j=1}^{N_i} (Z_{ij} - Z_{i\cdot})^2} \quad \text{(B.7)}$$

In equation B.7, k is the number of groups, N is the total number of samples, N_i is the number of samples in i^{th} group, $Z_{ij} = |Y_{ij} - \bar{Y}_{i\cdot}|$, Y_{ij} is the specific observation of that sample, and $\bar{Y}_{i\cdot}$ is the mean of all samples in i^{th} group. $Z_{\cdot\cdot}$ and $Z_{i\cdot}$ are shown in equations B.8 and B.9:

$$Z_{\cdot\cdot} = \frac{1}{N} \sum_{i=1}^{k} \sum_{j=1}^{N_i} Z_{ij} \quad \text{(B.8)}$$

$$Z_{i\cdot} = \frac{1}{N_i} \sum_{j=1}^{N_i} Z_{ij} \quad \text{(B.9)}$$

According to equations B.8 and B.9, $Z_{\cdot\cdot}$ is the mean of all Z_{ij}, and $Z_{i\cdot}$ is the mean for all Z_{ij} for i^{th} group.

Test statistic W_t follows F distribution with $df_1 = k - 1$ and $df_2 = N - k$, these parameters are used to look up F distribution table to find matching F value, and the corresponding p value is the possibility of F value greater than W_t, this value is used to compare with predefined Type I error rate 0.05.

B.5 One way ANOVA Calculations

One way ANOVA is used to compare differences in means between two or more groups, with null hypothesis being there is no difference between means for all groups. The test statistic is shown in equation B.10:

$$F_t = \frac{MS_{treatment}}{MS_{error}} = \frac{SS_{treatment}/(k-1)}{SS_{error}/(N-k)} \quad \text{(B.10)}$$

In equation B.10, $MS_{treatment}$ is the mean square error resulted from treatments, $SS_{treatment}$ is its corresponding sum of error. MS_{error} is the mean square error due to sampling error, SS_{error} is its corresponding sum of error. N is the total number of samples in the experiment, k is the total number of treatments. $SS_{treatment}$ and SS_{error} can be expressed as equations B.11 and B.12:

$$SS_{treatment} = \sum_{i=1}^{k} n_i(\bar{Y}_{i\cdot} - \bar{Y}_{\cdot\cdot})^2 \quad \text{(B.11)}$$

$$SS_{error} = \sum_{i=1}^{k} (n_i - 1)s_i^2 \quad \text{(B.12)}$$

In equations B.11 and B.12, $\bar{Y}_{\cdot\cdot}$ is the grand mean for all observations, $\bar{Y}_{i\cdot}$ is the mean of all observations in i^{th} group, n_i is the number of observations in i^{th} group, s_i^2 is the variance of all samples in i^{th} group.

Test statistic F_t follows F distribution with $df_1 = k - 1$ and $df_2 = N - k$, these parameters are used to look up F distribution table to find matching F value, and the corresponding p value is the possibility of F value greater than F_t, this value is used to compare with predefined Type I error rate 0.05.

APPENDIX C.

IMMUNE REACTIONS OF ZNS TREATMENT

This Appendix is used to discuss the immune reactions when ZnS is applied on the wound and possible danger of reducing the particle size to nanoscale.

Burn results in open wounds, and ZnS particles, as foreign bodies, can trigger immune reactions by body's immune system. Studies have shown that nanoparticles are able to penetrate the stratum corneum of the skin, typically through hair follicles [221], flexed [222] and broken skin [223], the broken skin will facilitate the penetration with large particles, followed by translocation of nanoparticles from skin into the lymphatic system [224] and eventually moved to lymphatic nodes [225]. Particles that are not able to be killed by macrophages will be translocated to the liver, spleen or kidneys. Renal clearance of nanoparticles has been reported, and the clearance time is positively related to particle size left in the kidneys, the larger the size, the longer the clearance takes [226, 227]. In the meantime, hepatic clearance represents another primary route of excretion for particles that do not undergo renal clearance, the liver provides critical function of catabolism and biliary excretion of blood-borne particles as well as serve as important site for eliminating foreign substances through phagocytosis [228].

However, decreasing the particle size may result in toxication, especially for particles within nanometer range [229], as nanoparticles have much higher surface to volume ratio, therefore more chemical molecules may attach to the surface, which would enhance its reactivity and result in increase of toxic effects [230, 231], and the smaller the particles, the higher toxic effect they may have [225]. Thus even if decreasing the particle size may result in better

antibacterial properties, it is important to note that the possible toxicity associated with the particle size.

APPENDIX D.

HYDROGEN PEROXIDE QUANTIFICATION METHODS

This appendix discusses the methods of quantifying amount of H_2O_2 generated by material processed through cryomilling as discussed in Section 4.5, which results in different lattice constants.

The amount of H_2O_2 can be measured using UV-Visible Spectroscopy as H_2O_2 has an absorbance peak of 240 nm, and the concentration of H_2O_2 is positively correlated with intensity of the peak [232]. However, this is not a very sensitive method. Another frequently used method to measure the amount of H_2O_2 with higher sensitivity is through oxidation of ferric iron to its ferrous state, which will form a complex with the dye xylenol orange, resulting in an increase in absorbance of the solution at 550 nm [233]. This method is more sensitive and selective.

REFERENCES

[1] J. W. ALEXANDER, "Mechanism of immunologic suppression in burn injury," *Journal of Trauma and Acute Care Surgery,* vol. 30, pp. 70-74, 1990.

[2] J. F. Hansbrough, T. O. Field Jr, M. A. Gadd, and C. Soderberg, "Immune response modulation after burn injury: T cells and antibodies," *Journal of Burn Care & Research,* vol. 8, p. 509&hyhen, 1987.

[3] N. Moss, D. Gough, A. Jordan, J. Grbic, J. Wood, M. Rodrick, *et al.*, "Temporal correlation of impaired immune response after thermal injury with susceptibility to infection in a murine model," *Surgery,* vol. 104, pp. 882-887, 1988.

[4] D. Church, S. Elsayed, O. Reid, B. Winston, and R. Lindsay, "Burn wound infections," *Clinical microbiology reviews,* vol. 19, pp. 403-434, 2006.

[5] S. Guo and L. A. DiPietro, "Factors affecting wound healing," *Journal of dental research,* vol. 89, pp. 219-229, 2010.

[6] I. W. Sutherland, "The biofilm matrix–an immobilized but dynamic microbial environment," *Trends in microbiology,* vol. 9, pp. 222-227, 2001.

[7] L. H. Taylor, S. M. Latham, and E. Mark, "Risk factors for human disease emergence," *Philosophical Transactions of the Royal Society of London B: Biological Sciences,* vol. 356, pp. 983-989, 2001.

[8] A. Russell, U. Tattawasart, J.-Y. Maillard, and J. Furr, "Possible link between bacterial resistance and use of antibiotics and biocides," *Antimicrobial Agents and Chemotherapy,* vol. 42, pp. 2151-2151, 1998.

[9] S. Percival, P. Bowler, and D. Russell, "Bacterial resistance to silver in wound care," *Journal of hospital infection,* vol. 60, pp. 1-7, 2005.

[10] S. Silver, L. T. Phung, and G. Silver, "Silver as biocides in burn and wound dressings and bacterial resistance to silver compounds," *Journal of Industrial Microbiology and Biotechnology,* vol. 33, pp. 627-634, 2006.

[11] H.-J. Bai, Z.-M. Zhang, and J. Gong, "Biological synthesis of semiconductor zinc sulfide nanoparticles by immobilized Rhodobacter sphaeroides," *Biotechnology letters,* vol. 28, pp. 1135-1139, 2006.

[12] G. Li, J. Zhai, D. Li, X. Fang, H. Jiang, Q. Dong, *et al.*, "One-pot synthesis of monodispersed ZnS nanospheres with high antibacterial activity," *Journal of Materials Chemistry,* vol. 20, pp. 9215-9219, 2010.

[13] Y. Suito, S. Yokoyama, H. Takahashi, K. Suto, C. Inoue, and K. Tohji, "Bactericidal mechanisms of stratified ZnS photocatalysts and ZnO nanoparticles," in *Meeting Abstracts*, 2013, pp. 21-21.

[14] G. Amir, S. Fatahian, and N. Kianpour, "Investigation of ZnS Nanoparticle Antibacterial Effect," *Current Nanoscience*, vol. 10, pp. 796-800, 2014.

[15] N. Salah, S. S. Habib, Z. H. Khan, A. Memic, A. Azam, E. Alarfaj, *et al.*, "High-energy ball milling technique for ZnO nanoparticles as antibacterial material," *International journal of nanomedicine*, vol. 6, p. 863, 2011.

[16] J.-W. Moon, I. N. Ivanov, P. C. Joshi, B. L. Armstrong, W. Wang, H. Jung, *et al.*, "Scalable production of microbially mediated zinc sulfide nanoparticles and application to functional thin films," *Acta biomaterialia*, vol. 10, pp. 4474-4483, 2014.

[17] R. Mohil, "Classification of wounds," *Principles and practice of wound care*, vol. 1, pp. 42-52, 2012.

[18] D. J. Leaper, "ABC of wound healing: Traumatic and surgical wounds," *BMJ: British Medical Journal*, vol. 332, p. 532, 2006.

[19] V. Maida, M. Ennis, C. Kuziemsky, and J. Corban, "Wounds and survival in cancer patients," *European Journal of Cancer*, vol. 45, pp. 3237-3244, 2009.

[20] R. A. Bryant, "Acute and chronic wounds," *Nursing Management Second Edition. Mosby*, pp. 88-90, 2000.

[21] W. T. Lawrence, "Physiology of the acute wound," *Clinics in plastic surgery*, vol. 25, pp. 321-340, 1998.

[22] P. Sridhar, "What are the Causes of Gastric Problems?," 2012.

[23] R. Krishnamoorthy and G. Karthikeyan, "Degloving injuries of the hand," *Indian journal of plastic surgery: official publication of the Association of Plastic Surgeons of India*, vol. 44, p. 227, 2011.

[24] S. Erol, U. Altoparlak, M. N. Akcay, F. Celebi, and M. Parlak, "Changes of microbial flora and wound colonization in burned patients," *Burns*, vol. 30, pp. 357-361, 2004.

[25] P. Appelgren, V. Björnhagen, K. Bragderyd, C. E. Jonsson, and U. Ransjö, "A prospective study of infections in burn patients," *Burns*, vol. 28, pp. 39-46, 2002.

[26] J. P. Barret and D. N. Herndon, "Effects of burn wound excision on bacterial colonization and invasion," *Plastic and reconstructive surgery*, vol. 111, pp. 744-50; discussion 751-2, 2003.

[27] S. Nasser, A. Mabrouk, and A. Maher, "Colonization of burn wounds in Ain Shams University burn unit," *Burns,* vol. 29, pp. 229-233, 2003.

[28] A. A. Hammond, K. G. Miller, C. J. Kruczek, J. Dertien, J. A. Colmer-Hamood, J. A. Griswold, *et al.*, "An in vitro biofilm model to examine the effect of antibiotic ointments on biofilms produced by burn wound bacterial isolates," *Burns,* vol. 37, pp. 312-321, 2011.

[29] P. Kennedy, S. Brammah, and E. Wills, "Burns, biofilm and a new appraisal of burn wound sepsis," *Burns,* vol. 36, pp. 49-56, 2010.

[30] S. L. Percival, K. E. Hill, S. Malic, D. W. Thomas, and D. W. Williams, "Antimicrobial tolerance and the significance of persister cells in recalcitrant chronic wound biofilms," *Wound repair and regeneration,* vol. 19, pp. 1-9, 2011.

[31] P. Stoodley, K. Sauer, D. Davies, and J. W. Costerton, "Biofilms as complex differentiated communities," *Annual Reviews in Microbiology,* vol. 56, pp. 187-209, 2002.

[32] C. Harrison‐Balestra, A. L. Cazzaniga, S. C. Davis, and P. M. Mertz, "A Wound‐Isolated Pseudomonas aeruginosa Grows a Biofilm In Vitro Within 10 Hours and Is Visualized by Light Microscopy," *Dermatologic surgery,* vol. 29, pp. 631-635, 2003.

[33] S. R. Karukonda, T. C. Flynn, E. E. Boh, E. I. McBurney, G. G. Russo, and L. E. Millikan, "The effects of drugs on wound healing: part 1," *International journal of dermatology,* vol. 39, pp. 250-257, 2000.

[34] R. A. Clark, "Cutaneous tissue repair: basic biologic considerations. I," *Journal of the American Academy of Dermatology,* vol. 13, pp. 701-725, 1985.

[35] P. G. Rodriguez, F. N. Felix, D. T. Woodley, and E. K. Shim, "The role of oxygen in wound healing: a review of the literature," *Dermatologic surgery,* vol. 34, pp. 1159-1169, 2008.

[36] P. Martin, "Wound healing--aiming for perfect skin regeneration," *Science,* vol. 276, pp. 75-81, 1997.

[37] G. Broughton 2nd, J. E. Janis, and C. E. Attinger, "The basic science of wound healing," *Plastic and reconstructive surgery,* vol. 117, pp. 12S-34S, 2006.

[38] J. S. Boateng, K. H. Matthews, H. N. Stevens, and G. M. Eccleston, "Wound healing dressings and drug delivery systems: a review," *Journal of pharmaceutical sciences,* vol. 97, pp. 2892-2923, 2008.

[39] G. Schultz, "Molecular regulation of wound healing," *Acute and chronic wounds: Nursing management. 2nd edition. St. Louis, MO: Mosby,* pp. 413-429, 1999.

[40] M. Rothe and V. Falanga, "Growth factors: their biology and promise in dermatologic diseases and tissue repair," *Archives of dermatology,* vol. 125, pp. 1390-1398, 1989.

[41] P. Shakespeare, "Burn wound healing and skin substitutes," *Burns,* vol. 27, pp. 517-522, 2001.

[42] R. Ross, "Platelet-derived growth factor," *Annual review of medicine,* vol. 38, pp. 71-79, 1987.

[43] G. F. Pierce, T. A. Mustoe, B. W. Altrock, T. F. Deuel, and A. Thomason, "Role of platelet ‐ derived growth factor in wound healing," *Journal of cellular biochemistry,* vol. 45, pp. 319-326, 1991.

[44] S. E. Lynch, J. C. Nixon, R. B. Colvin, and H. N. Antoniades, "Role of platelet-derived growth factor in wound healing: synergistic effects with other growth factors," *Proceedings of the National Academy of Sciences,* vol. 84, pp. 7696-7700, 1987.

[45] R. Montesano and L. Orci, "Transforming growth factor beta stimulates collagen-matrix contraction by fibroblasts: implications for wound healing," *Proceedings of the National Academy of Sciences,* vol. 85, pp. 4894-4897, 1988.

[46] S. O'Kane and M. W. Ferguson, "Transforming growth factor βs and wound healing," *The international journal of biochemistry & cell biology,* vol. 29, pp. 63-78, 1997.

[47] T. M. Krummel, B. A. Michna, B. L. Thomas, M. B. Sporn, J. M. Nelson, A. M. Salzberg, *et al.*, "Transforming growth factor beta (TGF-β) induces fibrosis in a fetal wound model," *Journal of pediatric surgery,* vol. 23, pp. 647-652, 1988.

[48] C. K. Sen, S. Khanna, G. Gordillo, D. Bagchi, M. Bagchi, and S. Roy, "Oxygen, oxidants, and antioxidants in wound healing," *Annals of the New York Academy of Sciences,* vol. 957, pp. 239-249, 2002.

[49] G. S. Schultz, M. White, R. Mitchell, G. Brown, J. Lynch, D. R. Twardzik, *et al.*, "Epithelial wound healing enhanced by transforming growth factor-alpha and vaccinia growth factor," *Science,* vol. 235, pp. 350-352, 1987.

[50] R. Todd, B. Donoff, T. Chiang, M. Y. Chou, A. Elovic, G. Gallagher, *et al.*, "The eosinophil as a cellular source of transforming growth factor alpha in healing cutaneous wounds," *The American journal of pathology,* vol. 138, p. 1307, 1991.

[51] S. A. Eming, T. Krieg, and J. M. Davidson, "Inflammation in wound repair: molecular and cellular mechanisms," *Journal of Investigative Dermatology,* vol. 127, pp. 514-525, 2007.

[52] K. Shimokado, E. W. Raines, D. K. Madtes, T. B. Barrett, E. P. Benditt, and R. Ross, "A significant part of macrophage-derived growth factor consists of at least two forms of PDGF," *Cell*, vol. 43, pp. 277-286, 1985.

[53] A. Baird, P. Mormède, and P. Bőhlen, "Immunoreactive fibroblast growth factor in cells of peritoneal exudate suggests its identity with macrophage-derived growth factor," *Biochemical and biophysical research communications*, vol. 126, pp. 358-364, 1985.

[54] M. Braddock, "Euroconference on tissue repair and ulcer/wound healing: molecular mechanisms, therapeutic targets and future directions: Paris, France, March 17-18, 2005," 2005.

[55] T. A. Mustoe, K. O'Shaughnessy, and O. Kloeters, "Chronic wound pathogenesis and current treatment strategies: a unifying hypothesis," *Plastic and reconstructive surgery*, vol. 117, pp. 35S-41S, 2006.

[56] P. G. Bowler, "Wound pathophysiology, infection and therapeutic options," *Annals of medicine*, vol. 34, pp. 419-427, 2002.

[57] M. C. Robson, "Wound infection: a failure of wound healing caused by an imbalance of bacteria," *Surgical Clinics of North America*, vol. 77, pp. 637-650, 1997.

[58] K. Markley, "The role of bacteria in burn mortality," *Annals of the New York Academy of Sciences*, vol. 150, pp. 922-930, 1968.

[59] R. Edwards and K. G. Harding, "Bacteria and wound healing," *Current opinion in infectious diseases*, vol. 17, pp. 91-96, 2004.

[60] J. M. Martinko and M. Madigan, "Brock biology of microorganisms," ed: Englewood Cliffs, NJ: Prentice Hall. ISBN 0-13-144329-1, 2005.

[61] M. Simões, L. C. Simões, and M. J. Vieira, "A review of current and emergent biofilm control strategies," *LWT-Food Science and Technology*, vol. 43, pp. 573-583, 2010.

[62] S. C. Davis, C. Ricotti, A. Cazzaniga, E. Welsh, W. H. Eaglstein, and P. M. Mertz, "Microscopic and physiologic evidence for biofilm - associated wound colonization in vivo," *Wound repair and Regeneration*, vol. 16, pp. 23-29, 2008.

[63] T.-F. C. Mah and G. A. O'Toole, "Mechanisms of biofilm resistance to antimicrobial agents," *Trends in microbiology*, vol. 9, pp. 34-39, 2001.

[64] D. Korber, G. James, and J. Costerton, "Evaluation of fleroxacin activity against established Pseudomonas fluorescens biofilms," *Applied and environmental microbiology*, vol. 60, pp. 1663-1669, 1994.

[65] P. S. Stewart, "Mechanisms of antibiotic resistance in bacterial biofilms," *International Journal of Medical Microbiology*, vol. 292, pp. 107-113, 2002.

[66] G. Midelet and B. Carpentier, "Impact of cleaning and disinfection agents on biofilm structure and on microbial transfer to a solid model food*," *Journal of applied microbiology,* vol. 97, pp. 262-270, 2004.

[67] M. Simões, L. C. Simões, I. Machado, M. O. Pereira, and M. J. Vieira, "Control of flow-generated biofilms with surfactants: evidence of resistance and recovery," *Food and Bioproducts Processing,* vol. 84, pp. 338-345, 2006.

[68] A. Pereira, J. Mendes, and L. F. Melo, "Using nanovibrations to monitor biofouling," *Biotechnology and bioengineering,* vol. 99, pp. 1407-1415, 2008.

[69] A. Pereira, J. Mendes, and L. Melo, "Monitoring cleaning-in-place of shampoo films using nanovibration technology," *Sensors and Actuators B: Chemical,* vol. 136, pp. 376-382, 2009.

[70] A. Smith, F. J. Buchinsky, and J. C. Post, "Eradicating Chronic Ear, Nose, and Throat Infections A Systematically Conducted Literature Review of Advances in Biofilm Treatment," *Otolaryngology--Head and Neck Surgery,* vol. 144, pp. 338-347, 2011.

[71] K. R. Ha, A. J. Psaltis, A. R. Butcher, P. J. Wormald, and L. W. Tan, "In vitro activity of mupirocin on clinical isolates of Staphylococcus aureus and its potential implications in chronic rhinosinusitis," *The Laryngoscope,* vol. 118, pp. 535-540, 2008.

[72] E. W. Wang, G. Agostini, O. Olomu, D. Runco, J. Y. Jung, and R. A. Chole, "Gentian violet and ferric ammonium citrate disrupt Pseudomonas aeruginosa biofilms," *The Laryngoscope,* vol. 118, pp. 2050-2056, 2008.

[73] A. Serra, G. Schito, G. Nicoletti, and G. Fadda, "A therapeutic approach in the treatment of infections of the upper airways: thiamphenicol glycinate acetylcysteinate in sequential treatment (systemic-inhalatory route)," *International journal of immunopathology and pharmacology,* vol. 20, pp. 607-617, 2007.

[74] M. E. Davey, N. C. Caiazza, and G. A. O'Toole, "Rhamnolipid surfactant production affects biofilm architecture in Pseudomonas aeruginosa PAO1," *Journal of bacteriology,* vol. 185, pp. 1027-1036, 2003.

[75] U. Klueh, V. Wagner, S. Kelly, A. Johnson, and J. Bryers, "Efficacy of silver‐coated fabric to prevent bacterial colonization and subsequent device‐based biofilm formation," *Journal of biomedical materials research,* vol. 53, pp. 621-631, 2000.

[76] G. Applerot, J. Lellouche, N. Perkas, Y. Nitzan, A. Gedanken, and E. Banin, "ZnO nanoparticle-coated surfaces inhibit bacterial biofilm formation and increase antibiotic susceptibility," *Rsc Advances,* vol. 2, pp. 2314-2321, 2012.

[77] M. E. Woolhouse and S. Gowtage-Sequeria, "Host range and emerging and reemerging pathogens," in *Ending the War Metaphor:: The Changing Agenda for Unraveling the Host-Microbe Relationship-Workshop Summary*, 2006.

[78] S. Cleaveland, M. Laurenson, and L. Taylor, "Diseases of humans and their domestic mammals: pathogen characteristics, host range and the risk of emergence," *Philosophical Transactions of the Royal Society B: Biological Sciences,* vol. 356, pp. 991-999, 2001.

[79] K. E. Jones, N. G. Patel, M. A. Levy, A. Storeygard, D. Balk, J. L. Gittleman, *et al.*, "Global trends in emerging infectious diseases," *Nature,* vol. 451, pp. 990-993, 2008.

[80] M. E. Mulligan, K. A. Murray-Leisure, B. S. Ribner, H. C. Standiford, J. F. John, J. A. Korvick, *et al.*, "Methicillin-resistant Staphylococcus aureus: a consensus review of the microbiology, pathogenesis, and epidemiology with implications for prevention and management," *The American journal of medicine,* vol. 94, pp. 313-328, 1993.

[81] D. M. Livermore, "Antibiotic resistance in staphylococci," *International Journal of Antimicrobial Agents,* vol. 16, pp. 3-10, 2000.

[82] M. B. Loeb, C. Main, A. Eady, and C. Walkers‐Dilks, "Antimicrobial drugs for treating methicillin‐resistant Staphylococcus aureus colonization," *The Cochrane Library,* 2003.

[83] L. A. Selvey, M. Whitby, and B. Johnson, "Nosocomial methicillin-resistant Staphylococcus aureus bacteremia: is it any worse than nosocomial methicillin-sensitive Staphylococcus aureus bacteremia?," *Infection Control,* vol. 21, pp. 645-648, 2000.

[84] C. Griffiths, T. L. Lamagni, N. Crowcroft, G. Duckworth, and C. Rooney, "Trends in MRSA in England and Wales: analysis of morbidity and mortality data for 1993-2002," *Health Statistics Quarterly,* pp. 15-22, 2004.

[85] R. M. Klevens, M. A. Morrison, J. Nadle, S. Petit, K. Gershman, S. Ray, *et al.*, "Invasive methicillin-resistant Staphylococcus aureus infections in the United States," *Jama,* vol. 298, pp. 1763-1771, 2007.

[86] A. Tomasz and S. Waks, "Mechanism of action of penicillin: triggering of the pneumococcal autolytic enzyme by inhibitors of cell wall synthesis," *Proceedings of the National Academy of Sciences,* vol. 72, pp. 4162-4166, 1975.

[87] B. Colombo, L. Felicetti, and C. Baglioni, "Inhibition of protein synthesis in reticulocytes by antibiotics: I. Effects on polysomes," *Biochimica et Biophysica Acta (BBA)-Nucleic Acids and Protein Synthesis,* vol. 119, pp. 109-119, 1966.

[88] K. A. Brogden, "Antimicrobial peptides: pore formers or metabolic inhibitors in bacteria?," *Nature Reviews Microbiology,* vol. 3, pp. 238-250, 2005.

[89] F. C. Tenover, "Mechanisms of antimicrobial resistance in bacteria," *The American journal of medicine*, vol. 119, pp. S3-S10, 2006.

[90] H.-L. Su, C.-C. Chou, D.-J. Hung, S.-H. Lin, I.-C. Pao, J.-H. Lin, *et al.*, "The disruption of bacterial membrane integrity through ROS generation induced by nanohybrids of silver and clay," *Biomaterials*, vol. 30, pp. 5979-5987, 2009.

[91] G. M. Gordillo and C. K. Sen, "Revisiting the essential role of oxygen in wound healing," *The American journal of surgery*, vol. 186, pp. 259-263, 2003.

[92] A. Bishop, "Role of oxygen in wound healing," *Journal of wound care*, vol. 17, p. 399, 2008.

[93] A. A. Tandara and T. A. Mustoe, "Oxygen in wound healing—more than a nutrient," *World journal of surgery*, vol. 28, pp. 294-300, 2004.

[94] I. Chapple, "Reactive oxygen species and antioxidants in inflammatory diseases," *Journal of clinical periodontology*, vol. 24, pp. 287-296, 1997.

[95] C. Marambio-Jones and E. M. Hoek, "A review of the antibacterial effects of silver nanomaterials and potential implications for human health and the environment," *Journal of Nanoparticle Research*, vol. 12, pp. 1531-1551, 2010.

[96] W. Song, J. Zhang, J. Guo, J. Zhang, F. Ding, L. Li, *et al.*, "Role of the dissolved zinc ion and reactive oxygen species in cytotoxicity of ZnO nanoparticles," *Toxicology letters*, vol. 199, pp. 389-397, 2010.

[97] H. Yin, P. S. Casey, M. J. McCall, and M. Fenech, "Effects of surface chemistry on cytotoxicity, genotoxicity, and the generation of reactive oxygen species induced by ZnO nanoparticles," *Langmuir*, vol. 26, pp. 15399-15408, 2010.

[98] C. Carlson, S. M. Hussain, A. M. Schrand, L. K. Braydich-Stolle, K. L. Hess, R. L. Jones, *et al.*, "Unique cellular interaction of silver nanoparticles: size-dependent generation of reactive oxygen species," *The journal of physical chemistry B*, vol. 112, pp. 13608-13619, 2008.

[99] P. Singleton, *Bacteria in biology, biotechnology and medicine*: John Wiley & Sons, 2004.

[100]F. M. Harold, "Antimicrobial agents and membrane function," *Adv. Microb. Physiol*, vol. 4, pp. 45-104, 1970.

[101]L. Qi, Z. Xu, X. Jiang, C. Hu, and X. Zou, "Preparation and antibacterial activity of chitosan nanoparticles," *Carbohydrate Research*, vol. 339, pp. 2693-2700, 2004.

[102] Y.-C. Chung and C.-Y. Chen, "Antibacterial characteristics and activity of acid-soluble chitosan," *Bioresource Technology,* vol. 99, pp. 2806-2814, 2008.

[103]W. Hamilton, "Membrane-active antibacterial compounds," *Biochem. J,* vol. 118, pp. 46P-47P, 1970.

[104] M. A. Kohanski, D. J. Dwyer, and J. J. Collins, "How antibiotics kill bacteria: from targets to networks," *Nature Reviews Microbiology,* vol. 8, pp. 423-435, 2010.

[105] B. A. Pruitt Jr, A. T. McManus, S. H. Kim, and C. W. Goodwin, "Burn wound infections: current status," *World journal of surgery,* vol. 22, pp. 135-145, 1998.

[106] O. Cope, J. L. Langohr, F. D. Moore, and R. C. Webster Jr, "Expeditious care of full-thickness burn wounds by surgical excision and grafting," *Annals of surgery,* vol. 125, p. 1, 1947.

[107] J. A. MONCRIEF, W. E. SWITZER, S. E. ORDER, W. MILLS Jr, and R. B. LINDBERG, "The successful control of burn wound sepsis," *Journal of Trauma and Acute Care Surgery,* vol. 5, pp. 601-616, 1965.

[108] G. M. Silver, R. L. Gamelli, and M. O'Reilly, "The beneficial effect of granulocyte colony-stimulating factor (G-CSF) in combination with gentamicin on survival after Pseudomonas burn wound infection," *Surgery,* vol. 106, pp. 452-5; discussion 455-6, 1989.

[109] D. E. ZASKE, R. J. SAWCHUK, D. N. GERDING, and R. G. STRATE, "Increased dosage requirements of gentamicin in burn patients," *Journal of Trauma and Acute Care Surgery,* vol. 16, pp. 824-828, 1976.

[110] R. A. Weinstein and C. G. Mayhall, "The epidemiology of burn wound infections: then and now," *Clinical Infectious Diseases,* vol. 37, pp. 543-550, 2003.

[111] S. T. Boyce, M. J. Goretsky, D. G. Greenhalgh, R. J. Kagan, M. T. Rieman, and G. D. Warden, "Comparative assessment of cultured skin substitutes and native skin autograft for treatment of full-thickness burns," *Annals of surgery,* vol. 222, p. 743, 1995.

[112] J. B. Wright, K. Lam, and R. E. Burrell, "Wound management in an era of increasing bacterial antibiotic resistance: a role for topical silver treatment," *American journal of infection control,* vol. 26, pp. 572-577, 1998.

[113] H. K. Estahbanati, P. P. Kashani, and F. Ghanaatpisheh, "Frequency of Pseudomonas aeruginosa serotypes in burn wound infections and their resistance to antibiotics," *Burns,* vol. 28, pp. 340-348, 2002.

[114] R. Wise, T. Hart, O. Cars, M. Streulens, R. Helmuth, P. Huovinen, *et al.*, "Antimicrobial resistance: is a major threat to public health," *BMJ: British Medical Journal,* vol. 317, p. 609, 1998.

[115] G. French, "Bactericidal agents in the treatment of MRSA infections—the potential role of daptomycin," *Journal of Antimicrobial Chemotherapy,* vol. 58, pp. 1107-1117, 2006.

[116] E. Tacconelli, G. De Angelis, M. A. Cataldo, E. Pozzi, and R. Cauda, "Does antibiotic exposure increase the risk of methicillin-resistant Staphylococcus aureus (MRSA) isolation? A systematic review and meta-analysis," *Journal of Antimicrobial Chemotherapy,* vol. 61, pp. 26-38, 2008.

[117] B. S. Atiyeh, M. Costagliola, S. N. Hayek, and S. A. Dibo, "Effect of silver on burn wound infection control and healing: review of the literature," *burns,* vol. 33, pp. 139-148, 2007.

[118] H. Klasen, "Historical review of the use of silver in the treatment of burns. I. Early uses," *Burns,* vol. 26, pp. 117-130, 2000.

[119] J. Fong and F. Wood, "Nanocrystalline silver dressings in wound management: a review," *international Journal of Nanomedicine,* vol. 1, p. 441, 2006.

[120] M. Rai, A. Yadav, and A. Gade, "Silver nanoparticles as a new generation of antimicrobials," *Biotechnology advances,* vol. 27, pp. 76-83, 2009.

[121] N. V. Ayala-Núñez, H. H. L. Villegas, L. d. C. I. Turrent, and C. R. Padilla, "Silver nanoparticles toxicity and bactericidal effect against methicillin-resistant Staphylococcus aureus: nanoscale does matter," *Nanobiotechnology,* vol. 5, pp. 2-9, 2009.

[122] M. Rai, S. Deshmukh, A. Ingle, and A. Gade, "Silver nanoparticles: the powerful nanoweapon against multidrug ‐ resistant bacteria," *Journal of applied microbiology,* vol. 112, pp. 841-852, 2012.

[123] J. Tian, K. K. Wong, C. M. Ho, C. N. Lok, W. Y. Yu, C. M. Che, *et al.*, "Topical delivery of silver nanoparticles promotes wound healing," *ChemMedChem,* vol. 2, pp. 129-136, 2007.

[124] P. Asharani, M. P. Hande, and S. Valiyaveettil, "Anti-proliferative activity of silver nanoparticles," *BMC Cell Biology,* vol. 10, p. 65, 2009.

[125] A. J. Kora and J. Arunachalam, "Assessment of antibacterial activity of silver nanoparticles on Pseudomonas aeruginosa and its mechanism of action," *World Journal of Microbiology and Biotechnology,* vol. 27, pp. 1209-1216, 2011.

[126] O. Choi, K. K. Deng, N.-J. Kim, L. Ross, R. Y. Surampalli, and Z. Hu, "The inhibitory effects of silver nanoparticles, silver ions, and silver chloride colloids on microbial growth," *Water research,* vol. 42, pp. 3066-3074, 2008.

[127] C. L. Fox, "Silver sulfadiazine—a new topical therapy for pseudomonas in burns: therapy of pseudomonas infection in burns," *Archives of Surgery,* vol. 96, pp. 184-188, 1968.

[128] S. Hoffmann, "Silver sulfadiazine: an antibacterial agent for topical use in burns," *Scandinavian Journal of Plastic and Reconstructive Surgery and Hand Surgery,* vol. 18, pp. 119-126, 1984.

[129] J. Wasiak, H. Cleland, F. Campbell, and A. Spinks, "Dressings for superficial and partial thickness burns," *The Cochrane Library,* 2013.

[130] M. Trop, M. Novak, S. Rodl, B. Hellbom, W. Kroell, and W. Goessler, "Silver-coated dressing acticoat caused raised liver enzymes and argyria-like symptoms in burn patient," *Journal of Trauma and Acute Care Surgery,* vol. 60, pp. 648-652, 2006.

[131] E. E. Tredget, H. A. Shankowsky, A. Groeneveld, and R. Burrell, "A Matched-Pair, Randomized Study Evaluating the Efficacy and Safety of Acticoat* Silver-Coated Dressing for the Treatment of Burn Wounds," *Journal of Burn Care & Research,* vol. 19, pp. 531-537, 1998.

[132] J. Wright, K. Lam, D. Hansen, and R. Burrell, "Efficacy of topical silver against fungal burn wound pathogens," *American journal of infection control,* vol. 27, pp. 344-350, 1999.

[133] R. H. Demling and M. L. DeSanti, "The rate of re-epithelialization across meshed skin grafts is increased with exposure to silver," *Burns,* vol. 28, pp. 264-266, 2002.

[134] L. K. Limbach, P. Wick, P. Manser, R. N. Grass, A. Bruinink, and W. J. Stark, "Exposure of engineered nanoparticles to human lung epithelial cells: influence of chemical composition and catalytic activity on oxidative stress," *Environmental science & technology,* vol. 41, pp. 4158-4163, 2007.

[135] S. Silver, "Bacterial resistances to toxic metal ions-a review," *Gene,* vol. 179, pp. 9-19, 1996.

[136] M. S. Ågren, M. Chvapil, and L. Franzén, "Enhancement of re-epithelialization with topical zinc oxide in porcine partial-thickness wounds," *Journal of Surgical Research,* vol. 50, pp. 101-105, 1991.

[137] A. B. Lansdown, U. Mirastschijski, N. Stubbs, E. Scanlon, and M. S. Ågren, "Zinc in wound healing: theoretical, experimental, and clinical aspects," *Wound Repair and Regeneration,* vol. 15, pp. 2-16, 2007.

[138] M. S. Agren, "Studies on zinc in wound healing," *Acta dermato-venereologica. Supplementum,* vol. 154, pp. 1-36, 1989.

[139] C. Fox Jr, S. M. Modak, and J. Stanford, "Zinc sulfadiazine for topical therapy of pseudomonas infection in burns," *Surgery, gynecology & obstetrics,* vol. 142, pp. 553-559, 1976.

[140] M. S. Ågren, L. Franzén, and M. Chvapil, "Effects on wound healing of zinc oxide in a hydrocolloid dressing," *Journal of the American Academy of Dermatology,* vol. 29, pp. 221-227, 1993.

[141] K. R. Raghupathi, R. T. Koodali, and A. C. Manna, "Size-dependent bacterial growth inhibition and mechanism of antibacterial activity of zinc oxide nanoparticles," *Langmuir,* vol. 27, pp. 4020-4028, 2011.

[142] O. Yamamoto, "Influence of particle size on the antibacterial activity of zinc oxide," *International Journal of Inorganic Materials,* vol. 3, pp. 643-646, 2001.

[143] W. Pories, J. Henzel, C. Rob, and W. Strain, "Acceleration of wound healing in man with zinc sulphate given by mouth," *The Lancet,* vol. 289, pp. 121-124, 1967.

[144] W. J. Pories, J. H. Henzel, C. G. Rob, and W. H. Strain, "Acceleration of healing with zinc sulfate," *Annals of Surgery,* vol. 165, p. 432, 1967.

[145] T. H. Sollmann, *A manual of pharmacology and its applications to therapeutics and toxicology*: WB Saunders, 1922.

[146] C. F. Walker and R. E. Black, "Zinc and the risk for infectious disease," *Annu. Rev. Nutr.,* vol. 24, pp. 255-275, 2004.

[147] N. M. Franklin, N. J. Rogers, S. C. Apte, G. E. Batley, G. E. Gadd, and P. S. Casey, "Comparative toxicity of nanoparticulate ZnO, bulk ZnO, and ZnCl2 to a freshwater microalga (Pseudokirchneriella subcapitata): the importance of particle solubility," *Environmental Science & Technology,* vol. 41, pp. 8484-8490, 2007.

[148] A. Lipovsky, Z. Tzitrinovich, H. Friedmann, G. Applerot, A. Gedanken, and R. Lubart, "EPR study of visible light-induced ROS generation by nanoparticles of ZnO," *The Journal of Physical Chemistry C,* vol. 113, pp. 15997-16001, 2009.

[149] O. Yamamoto, M. Komatsu, J. Sawai, and Z.-e. Nakagawa, "Effect of lattice constant of zinc oxide on antibacterial characteristics," *Journal of materials science: materials in medicine,* vol. 15, pp. 847-851, 2004.

[150] L. M. Plum, L. Rink, and H. Haase, "The essential toxin: impact of zinc on human health," *International journal of environmental research and public health,* vol. 7, pp. 1342-1365, 2010.

[151] J. Barret, P. Ramzy, J. Heggers, C. Villareal, D. Herndon, and M. Desai, "Topical nystatin powder in severe burns: a new treatment for angioinvasive fungal infections refractory to other topical and systemic agents," *Burns,* vol. 25, pp. 505-508, 1999.

[152] S. A. Kramer, "Effect of povidone-iodine on wound healing: a review," *Journal of Vascular Nursing,* vol. 17, pp. 17-23, 1999.

[153] J. L. HUNT, R. SATO, E. L. HECK, and C. R. BAXTER, "A critical evaluation of povidone-iodine absorption in thermally injured patients," *Journal of Trauma and Acute Care Surgery*, vol. 20, pp. 127-129, 1980.

[154] C. T. Spann, W. D. Tutrone, J. M. Weinberg, N. Scheinfeld, and B. Ross, "Topical antibacterial agents for wound care: a primer," *Dermatologic surgery*, vol. 29, pp. 620-626, 2003.

[155] K. Dunn and V. Edwards-Jones, "The role of Acticoat™ with nanocrystalline silver in the management of burns," *Burns*, vol. 30, pp. S1-S9, 2004.

[156] J. P. HEGGERS, V. VELANOVICH, M. C. ROBSON, S. M. ZOELLNER, R. SCHILERU, and J. BOERTMAN, "Control of burn wound sepsis: a comparison of in vitro topical antimicrobial assays," *Journal of Trauma and Acute Care Surgery*, vol. 27, pp. 176-179, 1987.

[157] R. J. Inman, C. F. Snelling, F. J. Roberts, K. Shaw, and J. C. Boyle, "Prospective comparison of silver sulfadiazine 1 per cent plus chlorhexidine digluconate 0· 2 per cent (Silvazine) and silver sulfadiazine 1 per cent (Flamazine) as prophylaxis against burn wound infection," *Burns*, vol. 11, pp. 35-40, 1984.

[158] J. Heggers, J. Sazy, B. Stenberg, L. Strock, R. McCauley, D. Herndon, *et al.*, "Bactericidal and wound-healing properties of sodium hypochlorite solutions: the 1991 Lindberg Award," *Journal of Burn Care & Research*, vol. 12, pp. 420-424, 1991.

[159] 山本修, 澤井淳, 石村真聖, 小島博光, and 笹本忠, "Change of Antibacterial Activity with Oxidation of ZnS Powder," *Journal of the Ceramic Society of Japan (日本セラミックス協会学術論文誌)*, vol. 107, pp. 853-856, 1999.

[160] J. Joo, H. B. Na, T. Yu, J. H. Yu, Y. W. Kim, F. Wu, *et al.*, "Generalized and facile synthesis of semiconducting metal sulfide nanocrystals," *Journal of the American Chemical Society*, vol. 125, pp. 11100-11105, 2003.

[161] J. Nanda, S. Sapra, D. Sarma, N. Chandrasekharan, and G. Hodes, "Size-selected zinc sulfide nanocrystallites: synthesis, structure, and optical studies," *Chemistry of Materials*, vol. 12, pp. 1018-1024, 2000.

[162] N. A. Dhas, A. Zaban, and A. Gedanken, "Surface synthesis of zinc sulfide nanoparticles on silica microspheres: sonochemical preparation, characterization, and optical properties," *Chemistry of materials*, vol. 11, pp. 806-813, 1999.

[163] S. Biswas, S. Kar, and S. Chaudhuri, "Optical and magnetic properties of manganese-incorporated zinc sulfide nanorods synthesized by a solvothermal process," *The Journal of Physical Chemistry B*, vol. 109, pp. 17526-17530, 2005.

[164] X. Yu, J. Yu, B. Cheng, and B. Huang, "One‐Pot Template‐Free Synthesis of Monodisperse Zinc Sulfide Hollow Spheres and Their Photocatalytic Properties," *Chemistry-A European Journal,* vol. 15, pp. 6731-6739, 2009.

[165] K. P. Velikov and A. van Blaaderen, "Synthesis and characterization of monodisperse core-shell colloidal spheres of zinc sulfide and silica," *Langmuir,* vol. 17, pp. 4779-4786, 2001.

[166] S. K. Panda, A. Datta, and S. Chaudhuri, "Nearly monodispersed ZnS nanospheres: synthesis and optical properties," *Chemical Physics Letters*, vol. 440, pp. 235-238, 2007.

[167] D. Denzler, M. Olschewski, and K. Sattler, "Luminescence studies of localized gap states in colloidal ZnS nanocrystals," *Journal of applied physics,* vol. 84, pp. 2841-2845, 1998.

[168] M. Labrenz, G. K. Druschel, T. Thomsen-Ebert, B. Gilbert, S. A. Welch, K. M. Kemner, *et al.*, "Formation of sphalerite (ZnS) deposits in natural biofilms of sulfate-reducing bacteria," *Science,* vol. 290, pp. 1744-1747, 2000.

[169] V. P. Utgikar, S. M. Harmon, N. Chaudhary, H. H. Tabak, R. Govind, and J. R. Haines, "Inhibition of sulfate‐reducing bacteria by metal sulfide formation in bioremediation of acid mine drainage," *Environmental toxicology,* vol. 17, pp. 40-48, 2002.

[170] J. W. Moreau, P. K. Weber, M. C. Martin, B. Gilbert, I. D. Hutcheon, and J. F. Banfield, "Extracellular proteins limit the dispersal of biogenic nanoparticles," *Science,* vol. 316, pp. 1600-1603, 2007.

[171] B. P. Rosen, "Bacterial resistance to heavy metals and metalloids," *JBIC Journal of Biological Inorganic Chemistry,* vol. 1, pp. 273-277, 1996.

[172] R. M. Maier, I. L. Pepper, and C. P. Gerba, *Environmental microbiology* vol. 397: Academic press, 2009.

[173] A. J. Nair, *Introduction to biotechnology and genetic engineering*: Laxmi Publications, Ltd., 2008.

[174] W. J. Ravensberg, *A roadmap to the successful development and commercialization of microbial pest control products for control of arthropods* vol. 10: Springer Science & Business Media, 2011.

[175] E. Lavernia, B. Han, and J. Schoenung, "Cryomilled nanostructured materials: processing and properties," *Materials Science and Engineering: A,* vol. 493, pp. 207-214, 2008.

[176] D. Witkin and E. J. Lavernia, "Synthesis and mechanical behavior of nanostructured materials via cryomilling," *Progress in Materials Science,* vol. 51, pp. 1-60, 2006.

[177] C. Suryanarayana, *Mechanical alloying and milling*: CRC Press, 2004.

[178] D. Witkin, P. Newbery, B. Q. Han, and E. J. Lavernia, "Nanostructured Alloys: Cryomilling Synthesis and Behavior," in *Dekker Encyclopedia of Nanoscience and Nanotechnology, Second Edition*, ed, 2009, pp. 2958-2966.

[179] M. Fabián, G. Tyuliev, A. Feldhoff, N. Kostova, P. Kollár, S. Suzuki, *et al.*, "One-step synthesis of nanocrystalline ZnO via cryomilling," *Powder Technology,* vol. 235, pp. 395-399, 2013.

[180] H. Fecht, E. Hellstern, Z. Fu, and W. Johnson, "Nanocrystalline metals prepared by high-energy ball milling," *Metallurgical Transactions A,* vol. 21, pp. 2333-2337, 1990.

[181] M. Raffi, F. Hussain, T. Bhatti, J. Akhter, A. Hameed, and M. Hasan, "Antibacterial characterization of silver nanoparticles against E. coli ATCC-15224," *Journal of Materials Science and Technology,* vol. 24, pp. 192-196, 2008.

[182] L. Zhang, Y. Jiang, Y. Ding, M. Povey, and D. York, "Investigation into the antibacterial behaviour of suspensions of ZnO nanoparticles (ZnO nanofluids)," *Journal of Nanoparticle Research,* vol. 9, pp. 479-489, 2007.

[183] M. E. Samberg, P. E. Orndorff, and N. A. Monteiro-Riviere, "Antibacterial efficacy of silver nanoparticles of different sizes, surface conditions and synthesis methods," *Nanotoxicology,* vol. 5, pp. 244-253, 2011.

[184] C. L. Malone, B. R. Boles, K. J. Lauderdale, M. Thoendel, J. S. Kavanaugh, and A. R. Horswill, "Fluorescent reporters for Staphylococcus aureus," *Journal of microbiological methods,* vol. 77, pp. 251-260, 2009.

[185] J. Hudzicki, "Kirby-Bauer disk diffusion susceptibility test protocol," *Am Soc Microbiol,* 2009.

[186] Y. Zhu, Z. Li, D. Zhang, and T. Tanimoto, "Abs/iron nanocomposites prepared by cryomilling," *Journal of applied polymer science,* vol. 99, pp. 501-505, 2006.

[187] J. Ye, B. Han, and J. Schoenung, "Mechanical behaviour of an Al–matrix composite reinforced with nanocrystalline Al-coated B4C particulates," *Philosophical magazine letters,* vol. 86, pp. 721-732, 2006.

[188] J. Jiang, G. Oberdörster, and P. Biswas, "Characterization of size, surface charge, and agglomeration state of nanoparticle dispersions for toxicological studies," *Journal of Nanoparticle Research,* vol. 11, pp. 77-89, 2009.

[189] D. Walter, "Primary Particles–Agglomerates–Aggregates," *Nanomaterials,* pp. 9-24, 2012.

[190] G. Ghosh, M. K. Naskar, A. Patra, and M. Chatterjee, "Synthesis and characterization of PVP-encapsulated ZnS nanoparticles," *Optical Materials*, vol. 28, pp. 1047-1053, 2006.

[191] C. Beer, R. Foldbjerg, Y. Hayashi, D. S. Sutherland, and H. Autrup, "Toxicity of silver nanoparticles—nanoparticle or silver ion?," *Toxicology letters*, vol. 208, pp. 286-292, 2012.

[192] N. M. Razali and Y. B. Wah, "Power comparisons of shapiro-wilk, kolmogorov-smirnov, lilliefors and anderson-darling tests," *Journal of Statistical Modeling and Analytics*, vol. 2, pp. 21-33, 2011.

[193] E. H. Chen, "The power of the Shapiro-Wilk W test for normality in samples from contaminated normal distributions," *Journal of the American Statistical Association*, vol. 66, pp. 760-762, 1971.

[194] E. C. o. A. S. Testing, "Data from the EUCAST MIC distribution website," ed, 2015.

[195] G. J. Kaur and D. S. Arora, "Antibacterial and phytochemical screening of Anethum graveolens, Foeniculum vulgare and Trachyspermum ammi," *BMC complementary and alternative medicine*, vol. 9, p. 30, 2009.

[196] W. Lorowitz, E. Saxton, M. Sondossi, and K. Nakaoka, "Integrating Statistics with a Microbiology Laboratory Activity," *Microbiology Education*, vol. 6, p. 14, 2005.

[197] J. Kim, M. R. Marshall, and C.-i. Wei, "Antibacterial activity of some essential oil components against five foodborne pathogens," *Journal of Agricultural and Food Chemistry*, vol. 43, pp. 2839-2845, 1995.

[198] M. A. De Groote, T. Testerman, Y. Xu, G. Stauffer, and F. C. Fang, "Homocysteine antagonism of nitric oxide-related cytostasis in Salmonella typhimurium," *Science*, vol. 272, pp. 414-417, 1996.

[199] S. Bloomfield, R. Baird, R. Leak, and R. Leech, "Microbial Quality Assurance in Pharmaceuticals," *Cosmetics and Toiletries, Ellis Horwood Ltd*, 1988.

[200] V. Toncheva, M. A. Wolfert, P. R. Dash, D. Oupicky, K. Ulbrich, L. W. Seymour, *et al.*, "Novel vectors for gene delivery formed by self-assembly of DNA with poly (L-lysine) grafted with hydrophilic polymers," *Biochimica et Biophysica Acta (BBA)-General Subjects*, vol. 1380, pp. 354-368, 1998.

[201] S. J. Bryant, R. J. Bender, K. L. Durand, and K. S. Anseth, "Encapsulating chondrocytes in degrading PEG hydrogels with high modulus: engineering gel structural changes to facilitate cartilaginous tissue production," *Biotechnology and bioengineering*, vol. 86, pp. 747-755, 2004.

[202] L. Zhang, Y. Jiang, Y. Ding, N. Daskalakis, L. Jeuken, M. Povey, *et al.*, "Mechanistic investigation into antibacterial behaviour of suspensions of ZnO nanoparticles against E. coli," *Journal of Nanoparticle Research*, vol. 12, pp. 1625-1636, 2010.

[203] S. Nair, A. Sasidharan, V. D. Rani, D. Menon, S. Nair, K. Manzoor, *et al.*, "Role of size scale of ZnO nanoparticles and microparticles on toxicity toward bacteria and osteoblast cancer cells," *Journal of Materials Science: Materials in Medicine*, vol. 20, pp. 235-241, 2009.

[204] A. Mandal, V. Meda, W. Zhang, K. Farhan, and A. Gnanamani, "Synthesis, characterization and comparison of antimicrobial activity of PEG/TritonX-100 capped silver nanoparticles on collagen scaffold," *Colloids and Surfaces B: Biointerfaces*, vol. 90, pp. 191-196, 2012.

[205] Z. Emami-Karvani and P. Chehrazi, "Antibacterial activity of ZnO nanoparticle on gram-positive and gram-negative bacteria," *Afr J Microbiol Res*, vol. 5, pp. 1368-1373, 2011.

[206] S. Malhotra-Kumar, C. Lammens, S. Coenen, K. Van Herck, and H. Goossens, "Effect of azithromycin and clarithromycin therapy on pharyngeal carriage of macrolide-resistant streptococci in healthy volunteers: a randomised, double-blind, placebo-controlled study," *The Lancet*, vol. 369, pp. 482-490, 2007.

[207] M. Bergman, S. Huikko, M. Pihlajamäki, P. Laippala, E. Palva, P. Huovinen, *et al.*, "Effect of macrolide consumption on erythromycin resistance in Streptococcus pyogenes in Finland in 1997–2001," *Clinical Infectious Diseases*, vol. 38, pp. 1251-1256, 2004.

[208] F. Ramsey and D. Schafer, *The statistical sleuth: a course in methods of data analysis*: Cengage Learning, 2012.

[209] R. Peck, C. Olsen, and J. Devore, *Introduction to statistics and data analysis*: Cengage Learning, 2015.

[210] D. Kilsby and M. Pugh, "The Relevance of the Distribution of Micro ‐ organisms Within Batches of Food to the Control of Microbiological Hazards from Foods," *Journal of Applied Bacteriology*, vol. 51, pp. 345-354, 1981.

[211] A. Landrin, A. Bissery, and G. Kac, "Monitoring air sampling in operating theatres: can particle counting replace microbiological sampling?," *Journal of Hospital infection*, vol. 61, pp. 27-29, 2005.

[212] Z. Fang, Z. Ouyang, L. Hu, X. Wang, H. Zheng, and X. Lin, "Culturable airborne fungi in outdoor environments in Beijing, China," *Science of the Total Environment*, vol. 350, pp. 47-58, 2005.

[213] C. E. Wainwright, M. W. France, P. O'Rourke, S. Anuj, T. J. Kidd, M. D. Nissen, *et al.*, "Cough-generated aerosols of Pseudomonas aeruginosa and other Gram-negative bacteria from patients with cystic fibrosis," *Thorax,* vol. 64, pp. 926-931, 2009.

[214] A. Sayago and A. G. Asuero, "Fitting straight lines with replicated observations by linear regression: Part II. Testing for homogeneity of variances," *Critical reviews in analytical chemistry,* vol. 34, pp. 133-146, 2004.

[215] E. L. Nuermberger, T. Yoshimatsu, S. Tyagi, K. Williams, I. Rosenthal, R. J. O'Brien, *et al.*, "Moxifloxacin-containing regimens of reduced duration produce a stable cure in murine tuberculosis," *American journal of respiratory and critical care medicine,* vol. 170, pp. 1131-1134, 2004.

[216] G. Mulberrry, A. T. Snyder, J. Heilman, J. Pyrek, and J. Stahl, "Evaluation of a waterless, scrubless chlorhexidine gluconate/ethanol surgical scrub for antimicrobial efficacy," *American Journal of Infection Control,* vol. 29, pp. 377-382, 2001.

[217] A. Castillo, L. Lucia, K. Goodson, J. Savell, and G. Acuff, "Comparison of water wash, trimming, and combined hot water and lactic acid treatments for reducing bacteria of fecal origin on beef carcasses," *Journal of Food Protection®,* vol. 61, pp. 823-828, 1998.

[218] P. H. Ruane, R. Edrich, D. Gampp, S. D. Keil, R. L. Leonard, and R. P. Goodrich, "Photochemical inactivation of selected viruses and bacteria in platelet concentrates using riboflavin and light," *Transfusion,* vol. 44, pp. 877-885, 2004.

[219] S. S. Shapiro and M. B. Wilk, "An analysis of variance test for normality (complete samples)," *Biometrika,* pp. 591-611, 1965.

[220] H. Levene, "Robust tests for equality of variances," *Contributions to probability and statistics. Essays in honor of Harold Hotelling,* pp. 279-292, 1961.

[221] R. Toll, U. Jacobi, H. Richter, J. Lademann, H. Schaefer, and U. Blume-Peytavi, "Penetration profile of microspheres in follicular targeting of terminal hair follicles," *Journal of Investigative Dermatology,* vol. 123, pp. 168-176, 2004.

[222] S. S. Tinkle, J. M. Antonini, B. A. Rich, J. R. Roberts, R. Salmen, K. DePree, *et al.*, "Skin as a route of exposure and sensitization in chronic beryllium disease," *Environmental Health Perspectives,* vol. 111, p. 1202, 2003.

[223] G. Oberdörster, E. Oberdörster, and J. Oberdörster, "Nanotoxicology: an emerging discipline evolving from studies of ultrafine particles. Environ Health Perspect 113: 823–839," 2005.

[224] A. M. Dar, S. Naseem, M. A. Gatoo, M. Y. Arfat, and K. Qasim, "IN VIVO TOXICITY OF NANOPARTICLES: MODALITIES AND TREATMENT," *European Chemical Bulletin,* vol. 3, pp. 992-1000, 2014.

[225] J. Ai, E. Biazar, M. Jafarpour, M. Montazeri, A. Majdi, S. Aminifard, *et al.*, "Nanotoxicology and nanoparticle safety in biomedical designs," *Int J Nanomedicine,* vol. 6, pp. 1117-1127, 2011.

[226] H. S. Choi, W. Liu, P. Misra, E. Tanaka, J. P. Zimmer, B. I. Ipe, *et al.*, "Renal clearance of quantum dots," *Nature biotechnology,* vol. 25, pp. 1165-1170, 2007.

[227] M. Longmire, P. L. Choyke, and H. Kobayashi, "Clearance properties of nano-sized particles and molecules as imaging agents: considerations and caveats," 2008.

[228] E. Kuntz and H.-D. Kuntz, *Hepatology, Principles and practice: history, morphology, biochemistry, diagnostics, clinic, therapy*: Springer Science & Business Media, 2006.

[229] S. F. Hansen, E. S. Michelson, A. Kamper, P. Borling, F. Stuer-Lauridsen, and A. Baun, "Categorization framework to aid exposure assessment of nanomaterials in consumer products," *Ecotoxicology,* vol. 17, pp. 438-447, 2008.

[230] I. Linkov, F. K. Satterstrom, and L. M. Corey, "Nanotoxicology and nanomedicine: making hard decisions," *Nanomedicine: Nanotechnology, Biology and Medicine,* vol. 4, pp. 167-171, 2008.

[231] W. H. Suh, K. S. Suslick, G. D. Stucky, and Y.-H. Suh, "Nanotechnology, nanotoxicology, and neuroscience," *Progress in neurobiology,* vol. 87, pp. 133-170, 2009.

[232] S. L. Hazen, A. d'Avignon, M. M. Anderson, F. F. Hsu, and J. W. Heinecke, "Human neutrophils employ the myeloperoxidase-hydrogen peroxide-chloride system to oxidize α-amino acids to a family of reactive aldehydes mechanistic studies identifying labile intermediates along the reaction pathway," *Journal of Biological Chemistry,* vol. 273, pp. 4997-5005, 1998.

[233] K. Cheng, "Determination of zirconium and hafnium with xylenol orange and methylthymol blue," *Analytica Chimica Acta,* vol. 28, pp. 41-53, 1963.